

Appendices to

“Report on field tests with the PEM-system at the West Coast of Jutland 2005-2008” by Jørgen Fredsøe.

1: Field test (Written by SIC).

2: Evaluation of the field tests (Written by Peter Engesgaard)

3: Numerical modeling of the ground water flow (Written by Peter Engesgaard)

4: Undulations alongshore (Written by JF)

**Appendix 1 Field test
(Written by SIC).**

Evaluation of the function of the PEM system

By Eng. Poul Jakobsen og Eng. Claus Brøgger, SIC

Abstract

The PEM system is used for beach erosion control and involves the well known principle of vertical draining.

Scientists generally agree that a well drained beach is robust and often accrete whereas beaches with a high water pressure will erode (Li and Berry).

The theory is confirmed by a number of tests with the PEM system around the world. In Denmark tests at on the West Coast in Old Skagen, Lønstrup and Holmsland Klit near Skodbjerg show that the PEM system is capable of reducing erosion and building a beach.

Scientists generally agree that a wide/high beach provides the best protection of the hinterland and of special focus in the Skodbjerg test is the mean height of the beach, measured from the foot of the dune and 100 m seawards.

The mean height of the beach prior to the test was 1,14. After 12 months the mean height of the PEM test areas were 1.46 m and 2.17 m while the controls had been reduced to 0,95 m and 0.81m.

At the test at Old Skagen the mean height of the beach with PEM installed was 0.63 m and 0.47 m higher than the two controls after 5 years.

We believe the results demonstrate a significant effect of the PEM system.



The PEM modules create a groin that catches long shore sand transport.

The effect of the PEM system is documented in several parts of the world under different weather and wave conditions.

Water pressure in the beach.

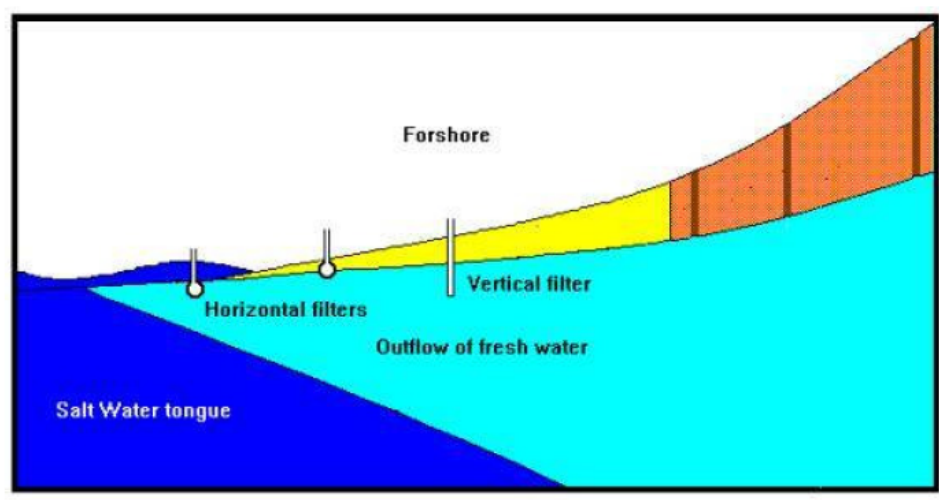


Fig. 2

Fig. 2 illustrates the water pressure at beach face and the seepage area for the fresh water outside the swash zone, which varies depending on the tides. The tides at Hvide Sande near Skodbjerg is 0.75m and highest tide is 3.0 over DVR 90 (normal level).

Vertical drains

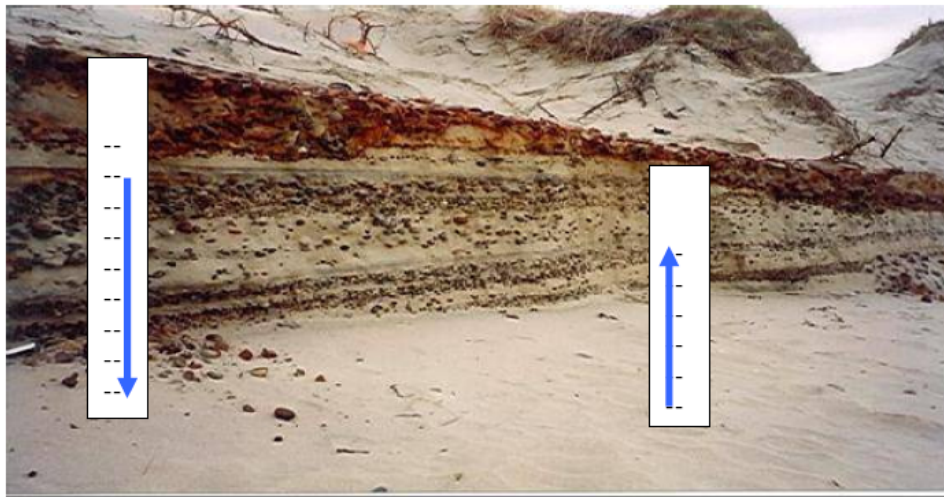


Fig. 3

The vertical drains connect the different layers in the beach and drain the beach. The water may move up or down inside the tubes depending on the water pressure in the beach and the swash zone.

Test Area 2 Skodbjerge.



fig. 4

During the first 12 months of the test period test area 2 added up to 65 m in width and in average 34 m. Mean height of the beach recorded over 1000 m has been raised from 1.25 m to 2.17 m. The volumetric change is plus 92 cubic m per m beach.

Pressure Equalization Skodbjerge

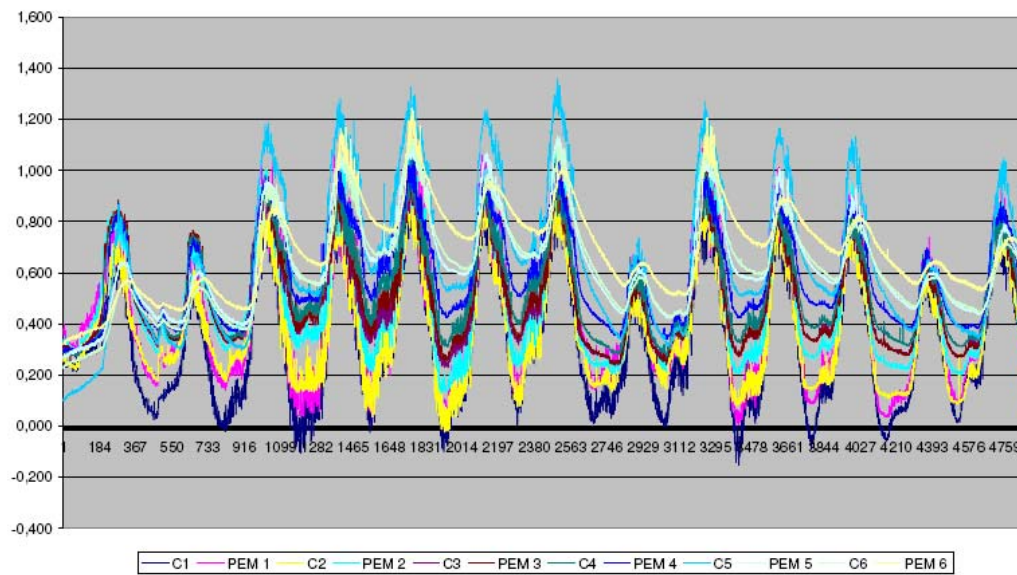


fig. 5

Based on the physical effects of the PEM tubes on the beach described above a separate test was made with water level sensors (Diver), to determine the effect of PEM on the water table in the beach. The test was carried out in the northern part of the Skodbjerge test area in control area 1.

Project description.

The test was initiated on March 20, 2006; a description of the test plan can be seen on page 5.

17 water level sensors (Diver) were placed in 3 rows 50 m apart starting from level 0 and every 10 m towards the dunes to record the pressure-gradient (water level) in the beach.

The sensors were installed in a plastic tube, 1,75 m long and a diameter of 60 mm with a screen 10 cm above the bottom to ensure free hydraulic flow. The tubes were installed in the beach and closed at the top.

The sensors inside plastic tubes are marked with a red dot 

Measurements were taken every 2 minutes.

On March 26, 2006 the beach was drained with 6 PEM modules  placed in the centre row (C) and 5 PEM modules placed in the southern row (S). The distance to the neighboring sensor tubes was 5 m.

PEM modules is vertical drain tubes as allow water to drain in the beach.

In each PEM module a water level sensor was placed. The sensors were preinstalled in the PEM module which allowed recording to take place from the start of the installation the 26 March. .

The sensors are illustrated in Appendix 2.

The water level during the test period is illustrated in Fig. 7.

Beach profile.

Station	C1	C2	C3	C4	C5	C6
Ground level	3 cm	35 cm	59 cm	63 cm	92 cm	121 cm.

Dynamic area



Weather conditions

The weather shifted during the test period with high tide up to 1.0 m during week 2 and wind speeds up to 14 m/sec. The beach was over-washed up to 40 m into the beach for several days.

Because of the high tide, it was possible to measure the out flow of fresh water from the hinterland to the submerged PEM tubes closest to the sea.

Method

The draining effect is illustrated by comparing the water level inside the PEM modules with the water level in the beach as recorded of the sensors inside plastic pipes. $(C1+C2)/2$, $(C2+C3)/2$, $(C3+C4)/2$, $(C4+C5)/2$, $(C5+C6)/2$

Holmsland Klit – water level in beach measured with DIVER

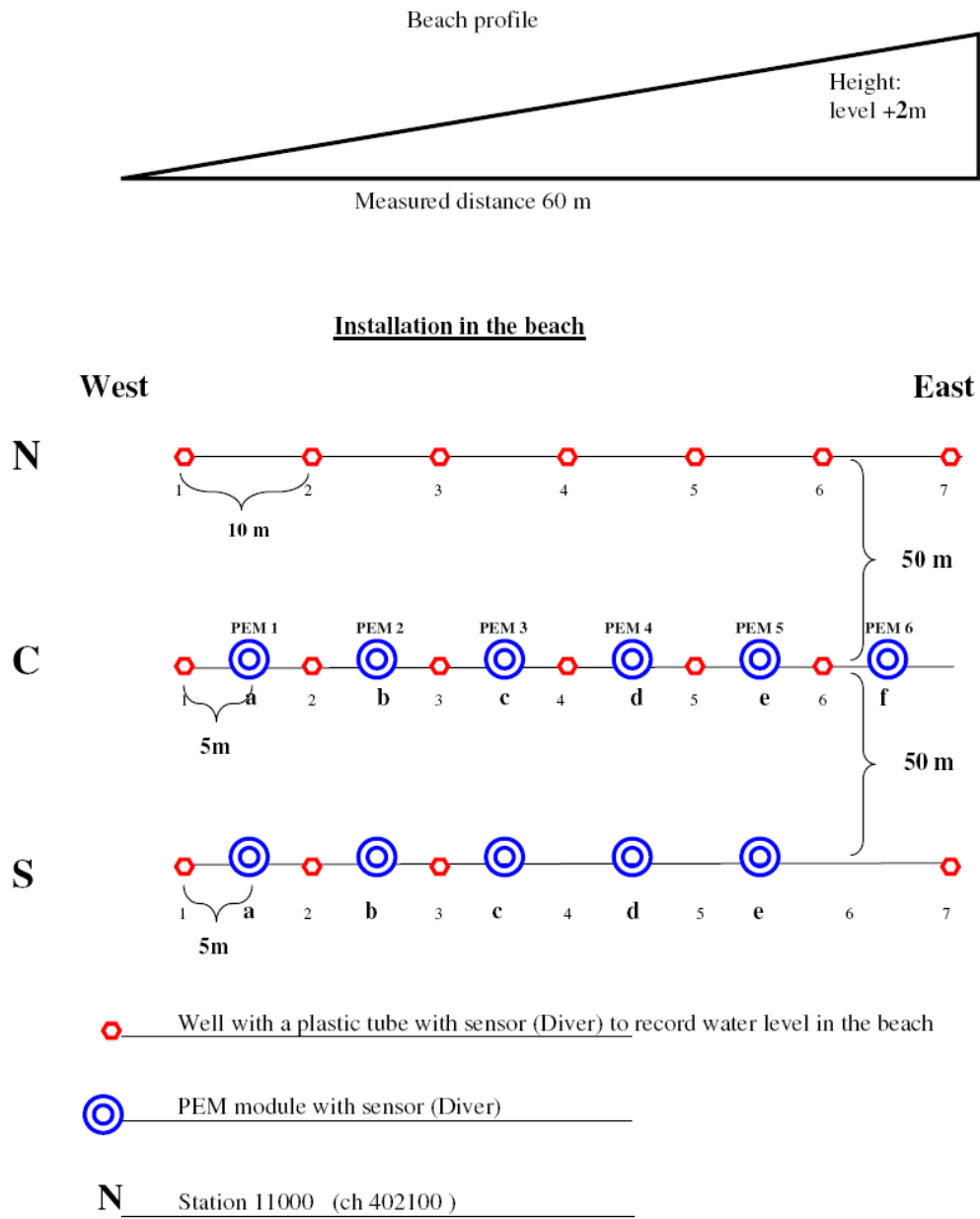


Fig. 6

Water level C1

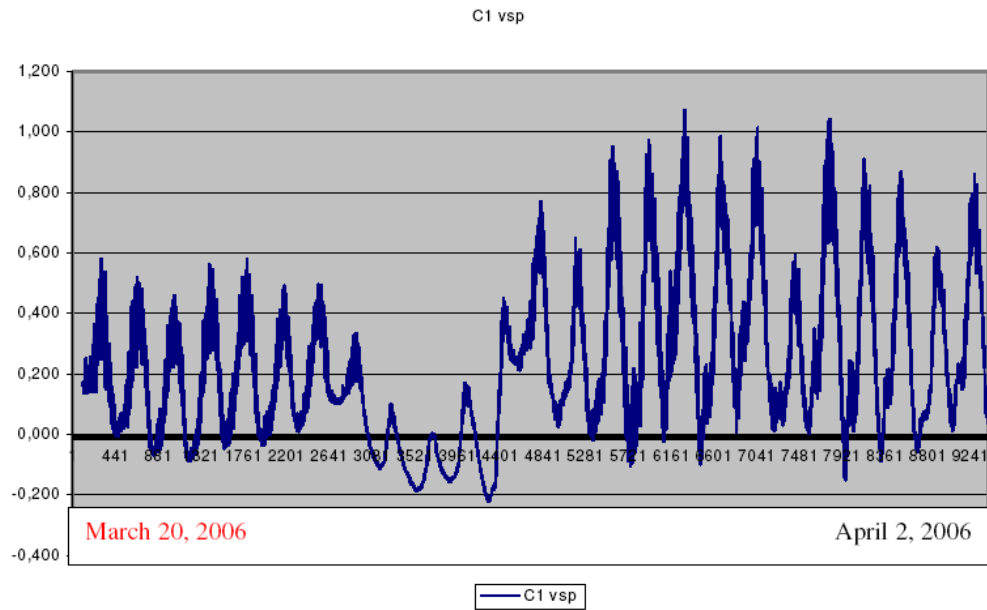


fig. 7

A comparison of the water level C1 with the sea level at the near by Hvide Sande Habor has shown good correlation and C1 is considered the sea level.

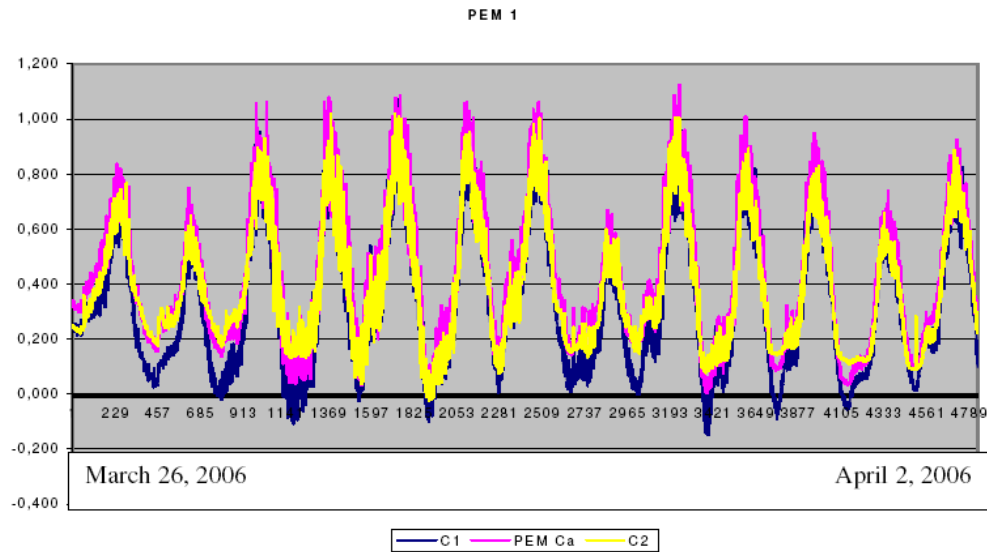
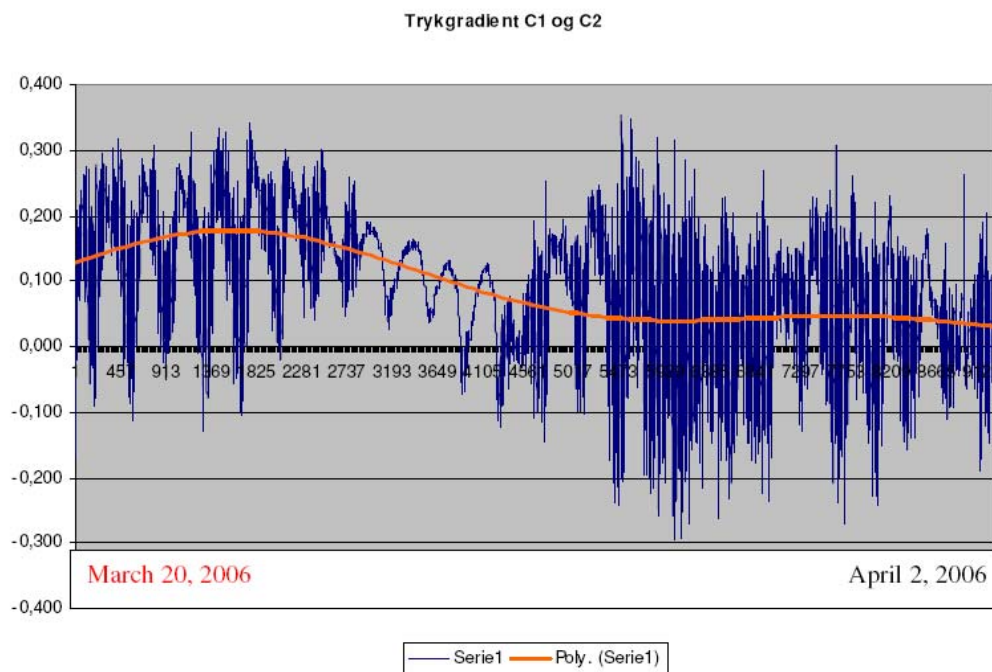
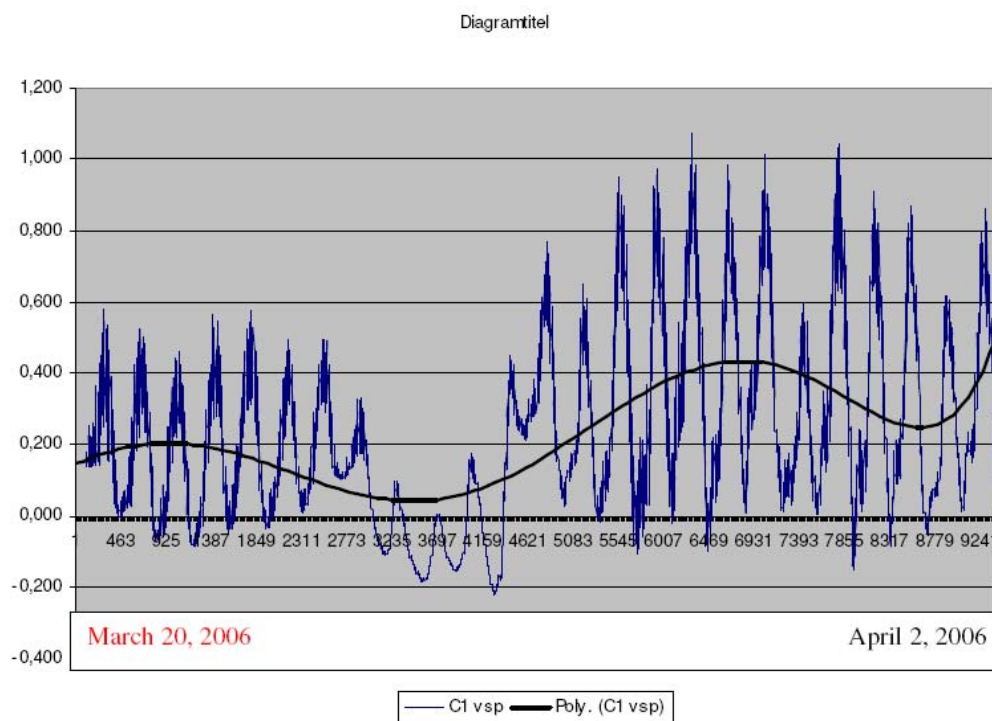


fig. 8

The above graph illustrates that the water level inside the PEM tubes is often higher than the neighboring C1 and C2 sensor tubes while the area is under water in the swash zone.

Water level in the beach.



The difference in water level in C1 and C2 is reduced to 5 – 6 cm after the draining with PEM has started (after measurement 4541). Without draining the level difference is 14 – 19 cm.

PEM 2

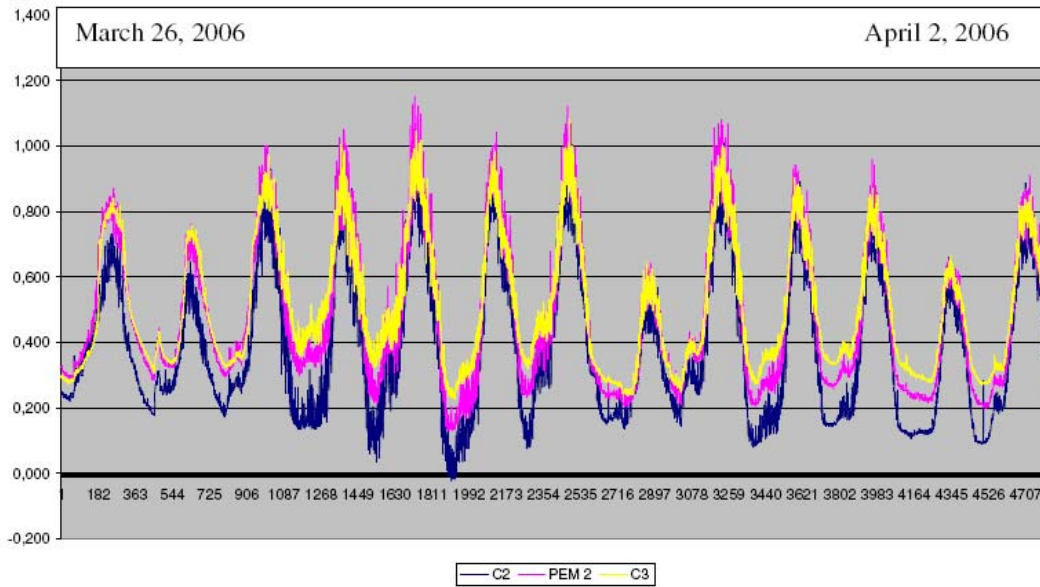


fig. 11

PEM 3

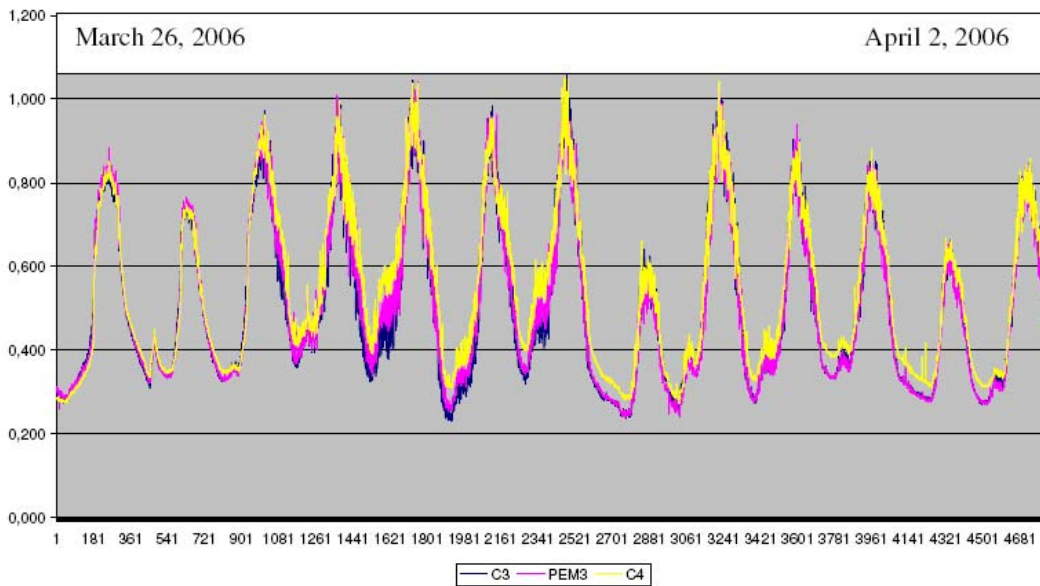
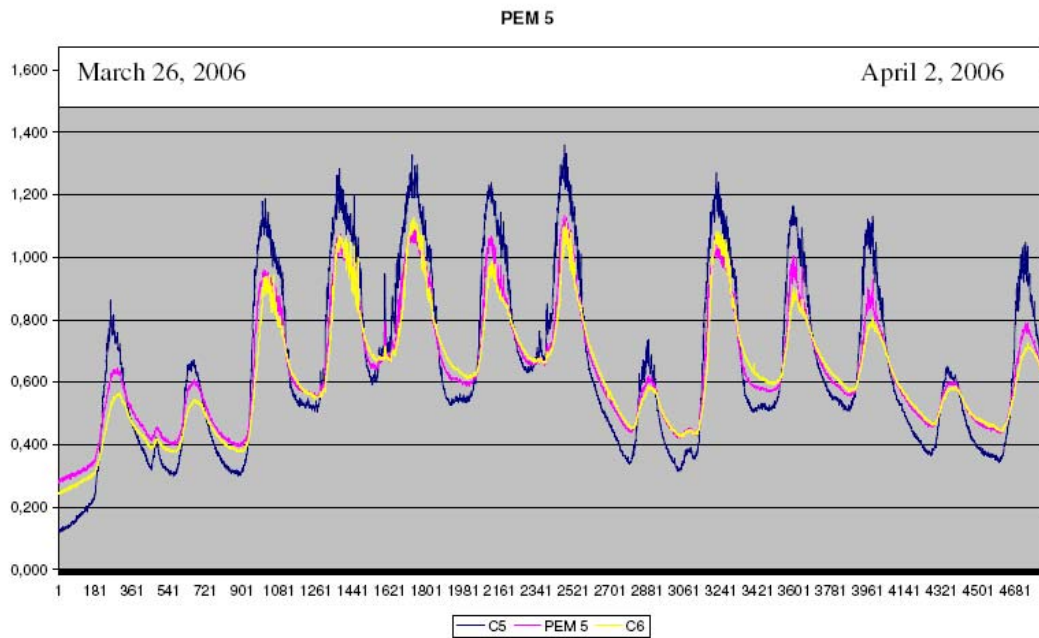
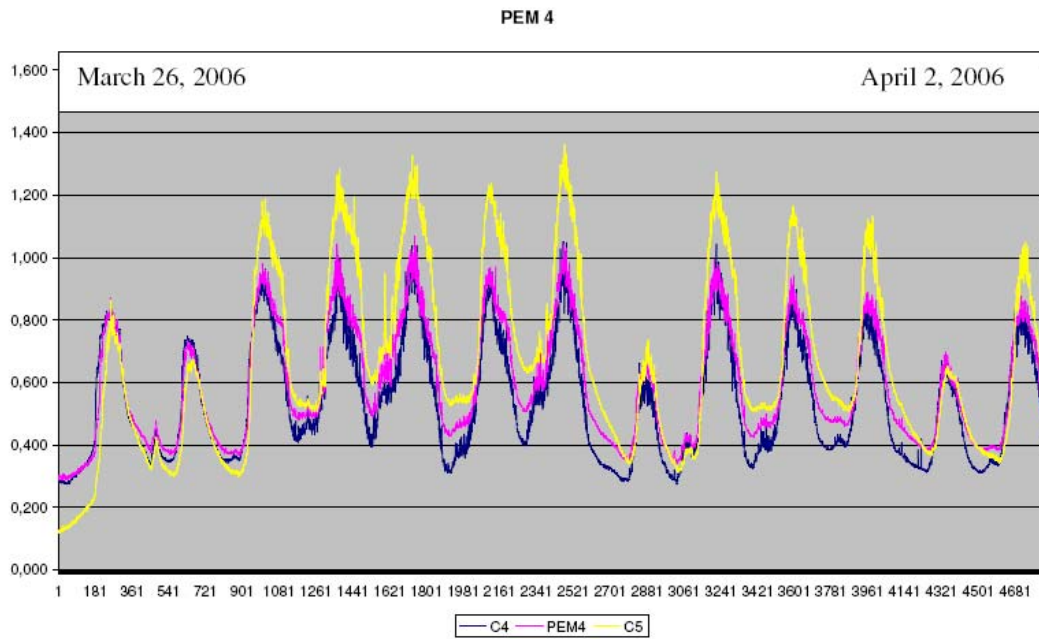


fig. 12



The effect of PEM draining modules can be seen in the graphs below where the water level in a PEM module is compared to the average water level in the neighboring sensor tubes.

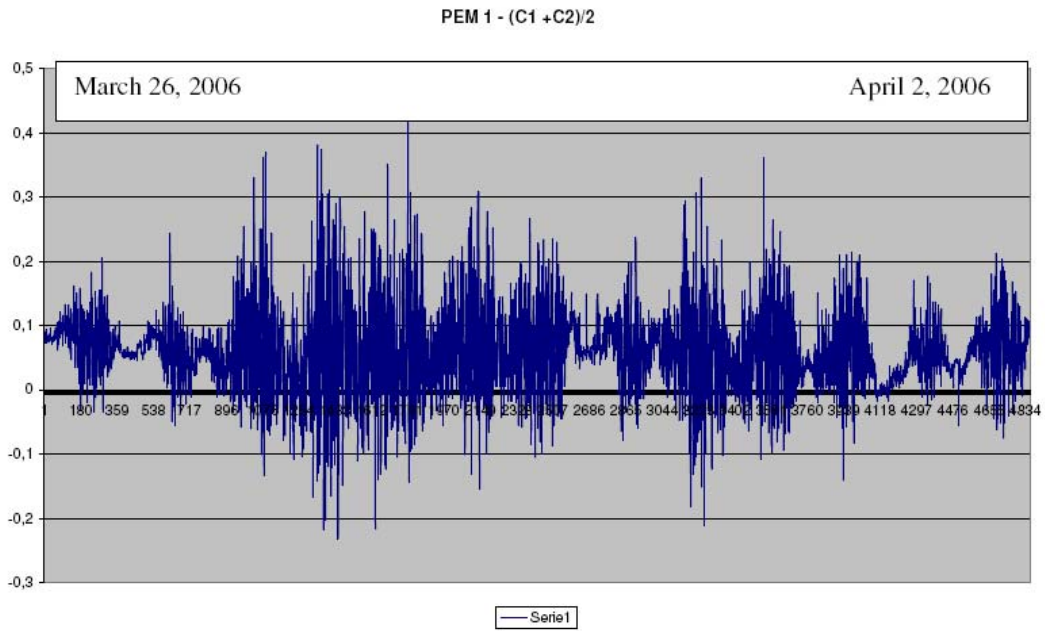


fig. 15

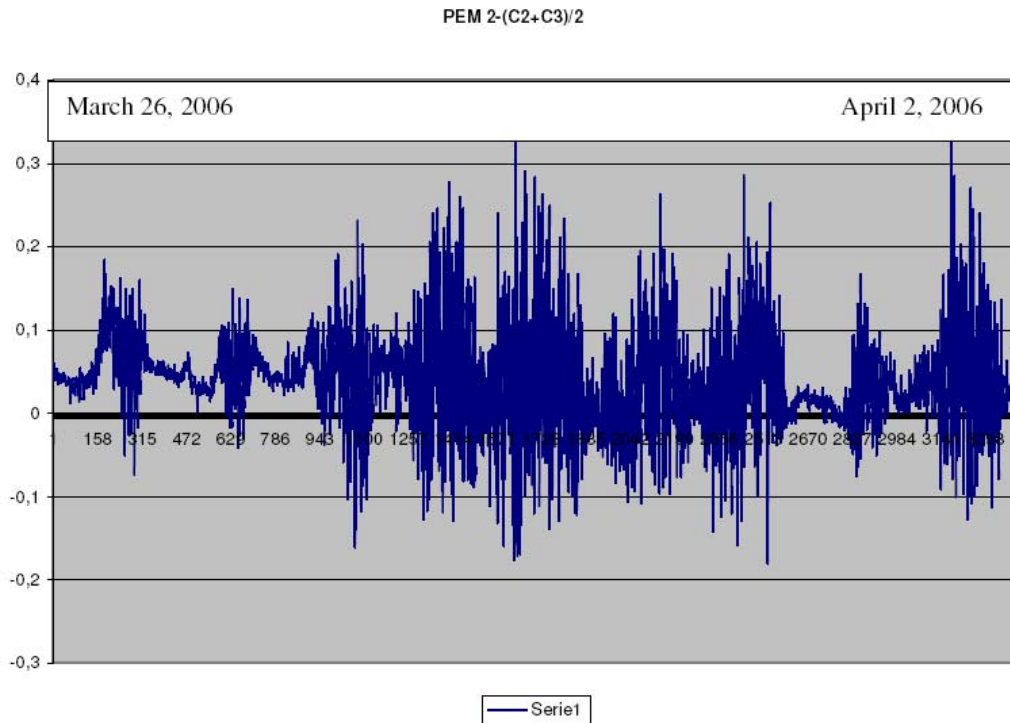


fig. 16

In fig 15 and 16 the PEM modules are under water due to high tide. The water level is higher in the PEM modules than the neighboring sensor tubes indicating that the pressure in the outflow zone is released via the PEM modules.

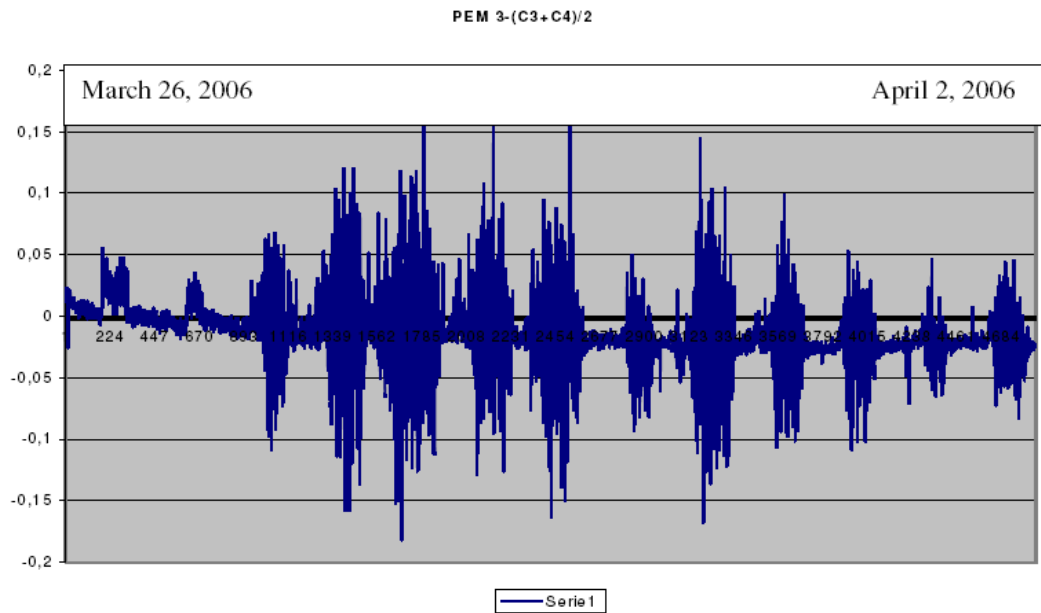


Fig 17

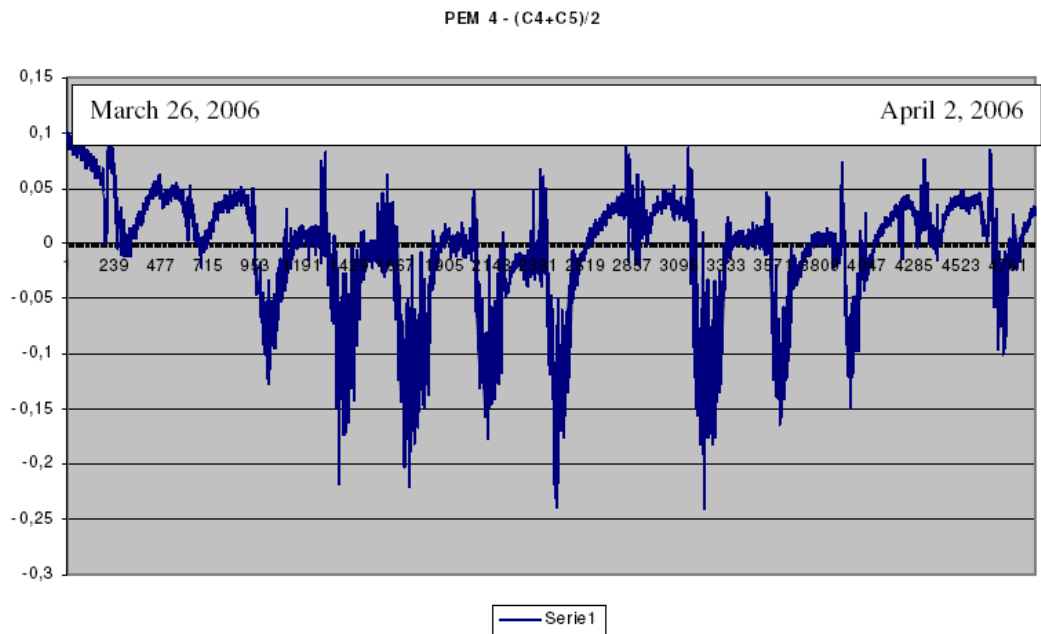


Fig 18

In fig 17, 18, and 19 the PEM modules were on the dry beach. The water level is significantly lower in the PEM tubes than the neighboring sensor tubes indicating downward draining of the beach.

PEM 5-(C5+C6)/2

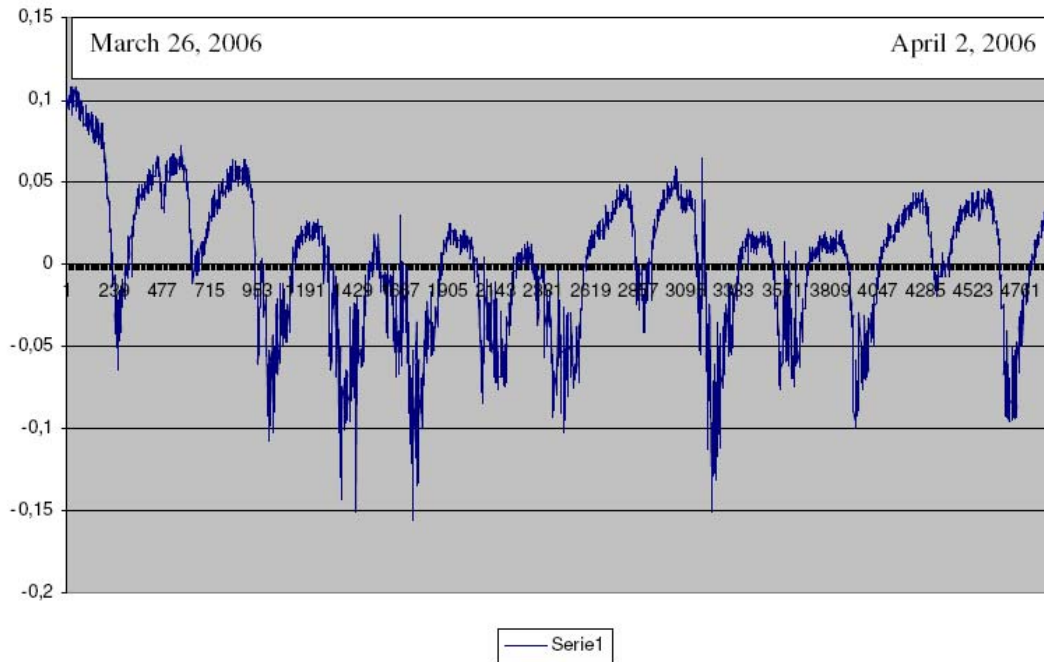


Fig 19

Conclusion

The hydraulic effect of installing pressure equalizing modules (PEM) in a beach was investigated. The test showed that on a dry beach the water level inside the PEM modules was up to 15 cm lower than in the neighboring wells, indicating effective downward draining of the beach. PEM modules in the swash zones that were submerged due to high tide, showed a higher water level than the neighboring wells. This indicates that the outflow of water is increased by PEM.

Effective draining of a beach will increase the beach's capacity to absorb the incoming waves and the sediment they contain will be deposited on the shore. Gradually a sand groin will develop that pick up the long shore sediment and thus builds a beach.



Skagen April 15, 2006.

Poul Jakobsen/Claus Brøgger.

Appendix 2: Evaluation of the field test (written by Peter Engesgaard, KU)

Effect of Vertical Drains on Tidal Dynamics in Beaches

Peter Engesgaard
Geological Institute
University of Copenhagen

FINAL REPORT - JUNE 2006

1 Introduction

A low water table in beaches will generally favour infiltration and onshore sediment transport [Horn, 2006]. The location of the water table in beaches is primarily controlled by tidal dynamics. Controlled laboratory experiments have recently demonstrated how a single harmonic tide can generate tidal responses with higher harmonics due to different physical phenomena [Cartwright et al., 2003, 2004]. These may include the non-linear filtering effect of a sloping beach, which also leads to a water table over height [Nielsen, 1990], the effects of the development of a seepage face, and the effects of the presence of a (truncated) capillary fringe near the beach surface. Observations in the field by Raubenheimer et al. [1999] confirm these findings.

The effects of so-called vertical drains on the tidal response in beaches are investigated in this report. The drains are also called Pressure Equilibrium Modules (PEM). The vertical drains consist of a 10 cm drain with a 1 m long screen. The functioning of the PEMs is not known, but one hypothesis is that the effective permeability of the beach is increased. A two-week experiment was conducted at a beach near Holmsland on the west coast of Denmark in order to investigate the hydraulic functioning of the PEMs. Two different experiments were envisaged. A beach-scale experiment where tidal dynamics were monitored in transects with normal observation wells and PEMs, and PEM-scale experiments, where the pressure distribution around a drain was continuously monitored. Unfortunately it was only the beach-scale experiment that was successful.

The experiment was divided into two periods. Period 1 where only 10 cm diameter wells (10 cm screen) were installed with pressure transducers (divers; measurement every 2 minutes) and period 2 where both wells and PEMs were installed, the PEMs also with pressure transducers. Three transects were established. One transect with just wells and no PEMs, which then acted as a reference site, one transect with both wells and PEMs, and then one transect with a few wells and mostly PEMs, which was designed primarily for the PEM-scale experiment. This makes a before-and-after comparison possible, where the tidal response in the wells during period 2 can be compared with the tidal response in period 1 and finally can be compared with the reference site.

The analysis of the data is partly based on the model by Nielsen [1990] and partly on the approach used by Carr [1971]. The model by Nielsen [1990] shows that small increases in the effective permeability of the beach will lead to less reduction in the amplitude of the recorded tidal signal in the wells plus less water table over height (and, thus, lowering of

the water table). Carr [1971] used harmonic analysis to interpret the amplitude damping as a function of distance from the sea.

2 Field site

The field site is located near Holmsland on the West coast of Denmark, Figure 1.



Figure 1: Location of field site

Figure 2 shows the location of the installed wells all with divers measuring the hydraulic head and the Pressure Equilibrium Modules (PEMs) also with divers. The North transect acts a reference site, where no PEMs were installed. The Central transect includes wells spaced about 10 m apart, and with PEMs centrally located in-between (i.e., 5 m spacing to wells). The South transect has only four wells, three nearest to the sea, and one at the other end. Otherwise, this transect mainly consist of PEMs.

All wells were installed starting on 8:00, March 20, 2006. This corresponds to Julian day 79.3. The PEMs were installed on March 26, approximately on Julian day 85.8. The experiment ended on April 2, approximately Julian day 92.7.

The experiment is therefore divided into two experimental periods; Period 1 Julian days 79.3-85.5 (6.5 days), where only wells were installed, and Period 2, Julian days 85.5-

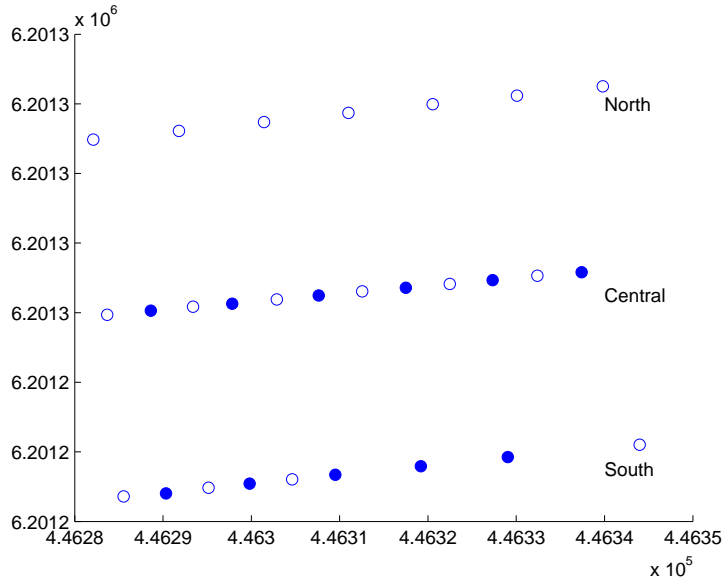


Figure 2: Location of wells with divers (open circle) and pressure equilibrium modules (filled circles)

92.7 (approximately 7.2 days). For reasons discussed below both of these periods will be made shorter.

Figure 3 shows the measured changes in the beach profile (measured on three occasion at every well and PEM). From March 20 to March 26 (i.e., the period without PEMs) there is a change in the beach profile by the addition of sediments to the zone affected by tidal dynamics and waves, which generally causes a decrease in the average slope (inverse of $\cot\beta$, where β is the beach slope, calculated as the distance between end points divided by difference in elevation of the beach at the two end points). The exception is the North transect, where a slight decrease in the elevation of the beach profile at the well nearest to the coast line causes an increase in slope. On the other hand, from March 26 to April 2, there is a decrease in the elevation of the beach profile nearest to the coast line, even below that measured on March 20, causing an increase in slope, Table 1. This change likely happened after March 28-29, during which there was an increase in wave and current activity. Notice the possibility of tidal water being trapped in depressions primarily in the Central and South transects in the latter period.

Figure 4 shows the recorded water level at Hvide Sande. By a coincidence the mean water level can be divided into two periods that more or less exactly matches the two

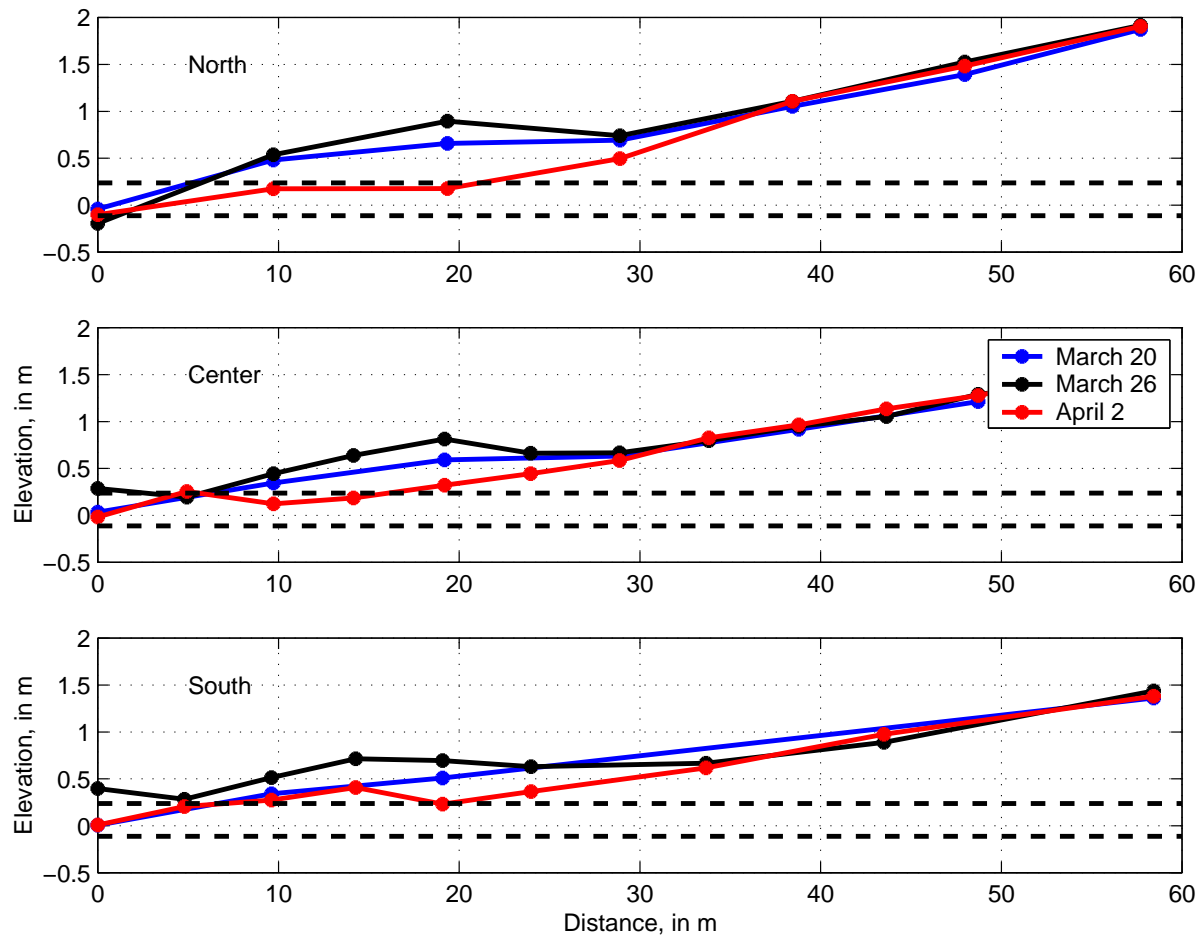


Figure 3: Measured beach profiles on March 20 (blue), March 26 (dark), and April 2 (red) for transects North (top), Central (middle), and South (bottom). The two dashed lines are the MSLs, with the lower and upper lines representing the MSL during periods 1 and 2, respectively.

Transect	Average beach slope		
	March 20	March 26	April 2
North	30.2	27.4	28.8
Central	41.4	48.4	36.2
South	43.2	56.2	42.6

Table 1: Average beach slopes ($\cot\beta$) on March 20, March 26, and April 2.

experimental periods. In period 1, the mean sea water level (MSL) is -0.11 m, while in period 2, the MSL is 0.24 m. This will have an effect on the water table dynamics in the beach. The MSLs are shown on Figure 3. The beach profile measured on April 2 is probably representative for period 2 because the small storm started on March 28. Thus, the MSL moved at least 20 m further inland. The mean amplitude of the water levels at Hvide Sande up to day 83 is 0.36 m. After day 86 and to the end the mean amplitude is 0.49 m.

The hydrogeology of the site is not very well known. The beach mainly consists of sand with embedded gravel layers sometimes up to 0.5-1.0 m in thickness. Grain size analysis shows a d_{10} of about 0.2-0.4 mm. Hazens empirical relation for calculating a hydraulic conductivity (K) is;

$$K = Ad_{10}^2 \quad (1)$$

where $A=1$ if d_{10} is inserted in mm giving K in units of cm/s. Using (1) one can compute K in the range 30-140 m/day.

The other parameter of interest is the drainable or effective porosity, n . For this type of (coarse) sand the drainable porosity is probably close to the total porosity, i.e., 0.2-0.4. However, the effective specific yield (often assumed equal to the drainable porosity) may be much lower due to the presence of the water table near the surface, and, thus, also the capillary fringe, which may become truncated during high tide [Gilham, 1984]. The effective drainable porosity may therefore be less.

Rainfall amounted to about 39 mm over the whole period with the highest rainfall rate of about 14 mm in one day (March 27). At this time of the year recharge is approximately equal to rainfall.

The reported hydraulic heads are based on measurements relative a measuring point found by GPS survey levelling of the wells and PEMS. The precision is about a few cm's

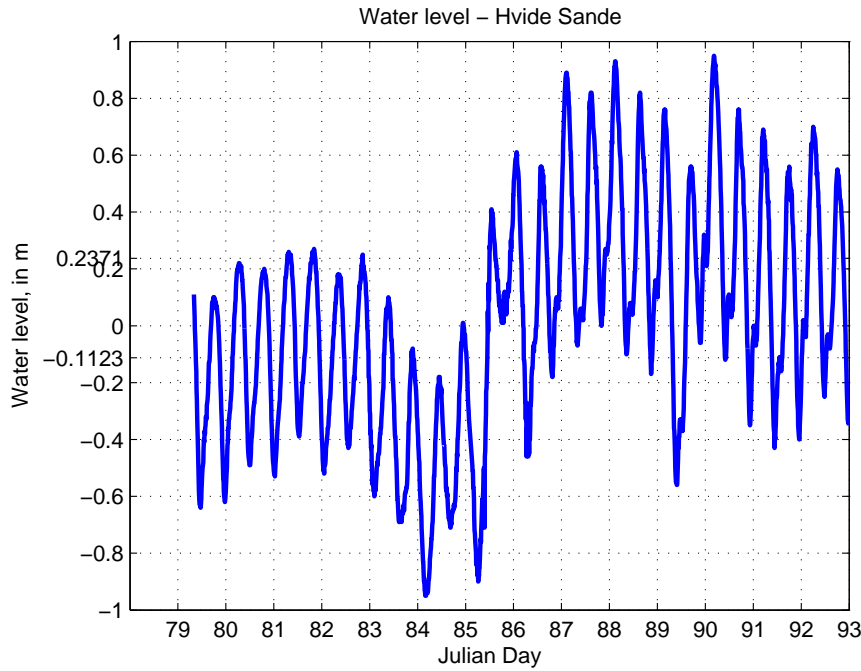


Figure 4: Water level at Hvide Sande

(J. Gregersen, personal communication).

3 Conceptual Model

Nielsen [1990] presented an analytical solution for hydraulic head fluctuations in beaches due to tides. Figure 5 shows a schematic of the considered flow system. The origin of the x axis starts at the intersection of the mean sea level (MSL) and the beach face, and x is positive landward.

The assumptions are;

- A low-permeable layer exist at the bottom of the aquifer. The thickness of the aquifer is D , equal to the distance from the mean sea water level to the bottom.
- The aquifer is homogeneous with an effective hydraulic conductivity, K , and drainable porosity, n .
- The beach has a slope with an angle of β .

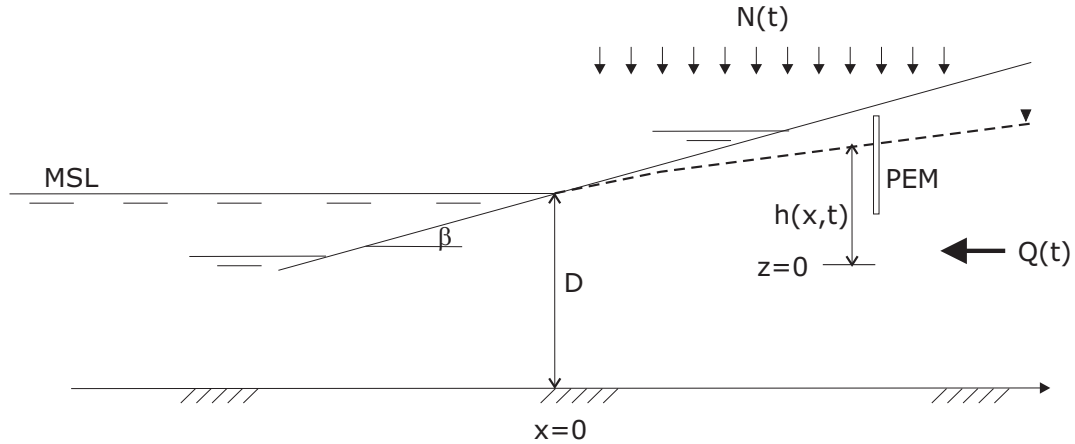


Figure 5: Conceptual model of beach

- Flow is horizontal(Dupuit).
- Single sinusoidal tide with period T .
- Groundwater flow into the coastal aquifer $Q(t)$ is zero.
- Recharge $N(t)$ is zero.
- A seepage face does not develop.
- Capillary effects on water table movement can be neglected.

As mentioned above, the coastal aquifer at Holmsland is likely not homogeneous. However, the analysis will be based on a before-and-after situation, where the PEMs in period 2 may lead to a higher effective permeability because they can lead to an increase in the connectivity between the gravel layers that are known to exist at different elevations.

There is only one harmonics, i.e., the model can not treat low-frequency tides and high-frequency waves at the same time. In the forthcoming analysis the effects of the waves have been filtered out.

Flow is not strictly horizontal at the field site. Raubenheimer et al. [1999] observed that horizontal flow tended to dominate vertical flow, although significant vertical flow did occur during high tide. Likewise Cartwright et al. [2004] found non-hydrostatic pressure distributions in their sand box experiments.

Recharge was not equal to zero during the experimental period. By assuming a drainable porosity of 0.20, then the maximum increase in water table (by neglecting any outflow) from a daily recharge of 14 mm is $0.014/0.2$ or 0.07 m. During most of the days the rate of recharge is less than 5 mm, i.e., an increase in water table of about 0.025 m. However, the effect of the capillary fringe extending all the way to the beach surface, at least during high tide, would mean that the effective specific yield is much less than the drainable porosity [Gilham, 1984]. A few mm of rainfall could therefore easily lead to a higher increase in water table. However, there has been no analysis of when rainfall occurred relative to the tide. For example, if rainfall occurs during high tide then it has much less effect.

One of the most critical assumptions is the that related to the formation of a seepage face. A seepage face occurs because of a decoupling between the falling tide and the water table. The seepage face will form in the active tidal region. The analytical solution given below is therefore only strictly valid upstream to the high water mark.

Capillary effects may play a role, but it is generally accepted that this is most crucial for high-frequency signals (i.e., waves).

Despite these simplifying assumptions the analytical model by Nielsen [1990] may still give some valuable insight into which physical phenomena to look for when comparing the tidal response in the beach before and after the PEMs were installed.

The one-dimensional analytical solution is given as;

$$h(x, t) = D + A \cos(\omega t - kx) e^{-kx} + \varepsilon A \left[\frac{1}{2} + \frac{\sqrt{2}}{2} \cos(2\omega t + \frac{\pi}{4} - \sqrt{2}kx) e^{-\sqrt{2}kx} \right] + O(\varepsilon^2) \quad (2)$$

where $h(x,t)$ is the hydraulic head (m) at position x (m) and time t (days), D is the mean aquifer depth (m), A is the tidal amplitude, $\omega = 2\pi/T$ is the tidal frequency, where T is the tidal period (days), k is the wave number (see below), and $\varepsilon = kA \cot \beta$, where β is the beach slope. The analytical solution was developed from a perturbation analysis using ε as the perturbation parameter. Equation (2) is correct to first order in ε . Thus, ε must be much lower than 1 for (2) to be valid ($\varepsilon \ll 1$, in practise it often suffice that $\varepsilon < 0.5$). Also, it is required that the amplitude is small compared to the mean aquifer depth, i.e., $A \ll D$. Nielsen [1990] also developed a solution that is correct to second order, however, here it will suffice to use (2) to demonstrate the effects of tides on the hydraulic head fluctuations in a sloping beach.

The wave number, k , is defined as;

Parameter	Value
Hydraulic conductivity, K	50, 200 m/day
Porosity, n	0.2
Amplitude, A	0.4 m
Aquifer thickness, D	20 m
Tidal frequency, ω	$2\pi/0.5 \text{ day}^{-1}$
Beach slope, $\cot\beta$	0, 60/1.5

Table 2: Parameters used to simulate tidal dynamics with Nielsen model. Two values for K and the beach slope are used

$$k = \sqrt{\frac{n\omega}{2KD}} \quad (3)$$

where K is the hydraulic conductivity (m/day) and n is the drainable porosity (-). These are the two hydraulic parameters that govern the effects of tidal dynamics on hydraulic head fluctuations. The ration K/n is also called the aquifer diffusivity. The higher the diffusivity the lower is the time scale for transmitting the tidal signal.

The first term in (2) is the mean aquifer depth corresponding to the mean sea water level. For the case of a vertical beach ($\cot\beta=0$) one has $\varepsilon=0$ and the third term cancels out. Thus, the solution represents a pure sinusoidal fluctuation around D, but with a damped signal (Ae^{-kx}) and a phase lag ($\cos(\omega t-kx)$). Figure 6 shows two simulations (black solid and dashed lines) with the parameters in Table 2 (the parameters are close to those representing the field site). Notice that it is $h(x,t)-D$ that is plotted versus time. Both simulations give tidal fluctuations around zero. The phase lag and damping increases with an increase in the wave number corresponding to a decrease in K or increase in n. The case with the high K (200 m/day) thus gives tidal fluctuations that are much higher than the case with the low K (50 m/day). For the high K case, the damping is about $0.23/A=0.23/0.4 = 0.58$ (0.23 m is the peak value). Likewise, for the low K case, the damping is about 0.18. These reductions are also called the tidal efficiency [Carr, 1971].

The third term in (2) accounts for (i) an extra over height and (ii) an extra, but small damping plus a skewing (asymmetry) of the tidal signal $\varepsilon A 2^{1/2}/2(\cos 2\omega t)$. The over height means that the water table is lifted on the mean a factor of $0.5\varepsilon A$ above the mean sea level, which is explained by the fact that it is easier for water to seep into a sloping beach at high tide than to drain away at low tide [Nielsen, 1990]. This is also seen

in the two simulations in Figure 6 where a sloping beach is introduced ($\cot\beta=60/1.5$, red solid and dashed lines). Again the high K case means less damping of the tidal signal, however the mean water level is lifted 0.058 m above the mean sea level. The results are shown at a distance of 50 m from the intersection between the MSL and the beach, i.e., in this case upstream to the high water mark. In the low K case, the water level is lifted 0.11 m. Also, the asymmetry is lower in the high K case.

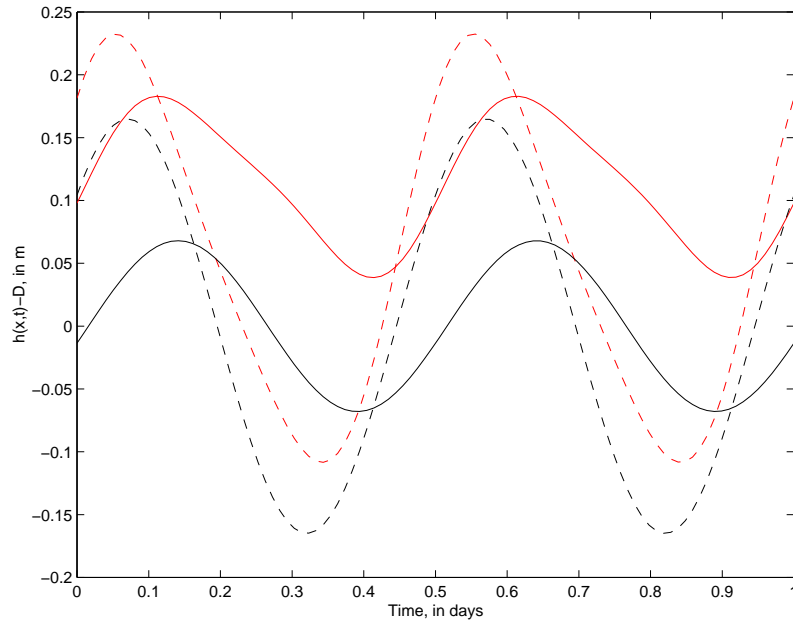


Figure 6: Tidal dynamics at $x=50$ m for 4 different situations. Black indicates a vertical beach ($\cot\beta=0$) and red a sloping beach ($\cot\beta=60/1.5$). Dashed lines are with $K=200$ m/day. Solid lines with $K=50$ m/day.

This leads to the following observations;

- A higher hydraulic conductivity leads to less damping of the tidal signal (and also less phase lag, however this is more difficult to observe)
- A higher hydraulic conductivity leads to a decrease in the so-called water level overhead.
- A higher hydraulic conductivity leads to less asymmetric tidal signals.

4 Presentation of tidal data

Figures 7 and 8 are examples of the recorded tidal signal in wells N1 and N7, respectively. Clearly the signal is composed of low-frequency tide signals and high-frequency waves. At well N7 the high-frequent signals have almost disappeared.

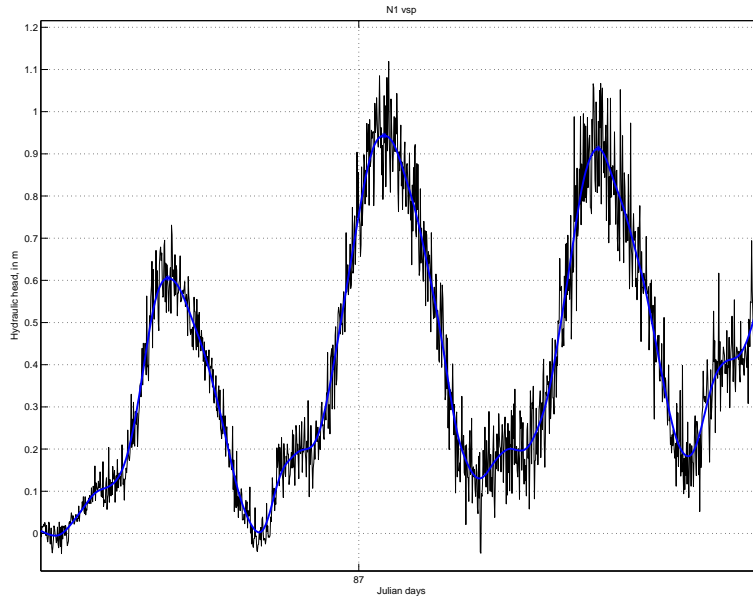


Figure 7: Illustration of the filtering of high-frequency waves in N1. Black line is the recorded signal (every 2 mins). Blue line is the filtered signal.

To make the interpretation easier all recorded signals were filtered using a so-called low-pass band filtering technique, see Appendix A. The results of the filtering are also shown in Figures 7 and 8. The analysis was therefore done exclusively on the filtered signal.

Figure 9 shows the filtered signal in C6. It is clear that during the transition from period 1 to period 2 it is very difficult to pick out low and high tides. This is mainly due to the nature of the sea water level, Figure 4, and the non-linear filtering of the signal due to the beach. The same observation is valid for all wells, except perhaps the wells closest to the sea. The periods of observations have therefore been changed in order to omit this transition period. Thus period 1 ends at day 83 and period 2 starts at day 86. The amount of rainfall in the new periods 1 and 2 are about 3 and 13 mm, respectively. Thus,

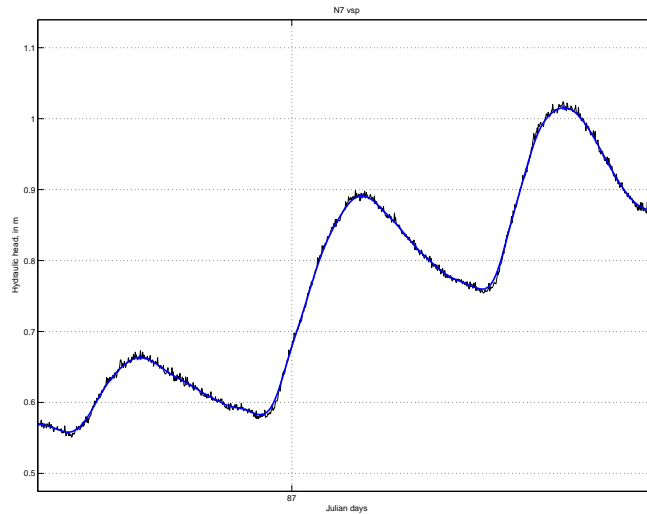


Figure 8: Illustration of the filtering of high-frequency waves in N7. Black line is the recorded signal (every 2 mins). Blue line is the filtered signal.

excluding days 83-86 takes care of the problem with high rates of rainfall with up to 20 mm over 3 days.

The mean hydraulic head in C6 increases from 0.44 m in period 1 to 0.70 m in period 2, which reflects the general increase in mean sea level (0.35 m).

5 Method of analysis

The analysis of the data is performed in the following way;

1. Analysis based on wells only
2. Analysis based on wells and PEMs

5.1 Analysis based on wells

The method of analysis is based on;

- Calculating the amplitude reductions in period 1 and 2 to see if the beach has changed hydraulically by the installation of the PEMs. The PEMs could cause

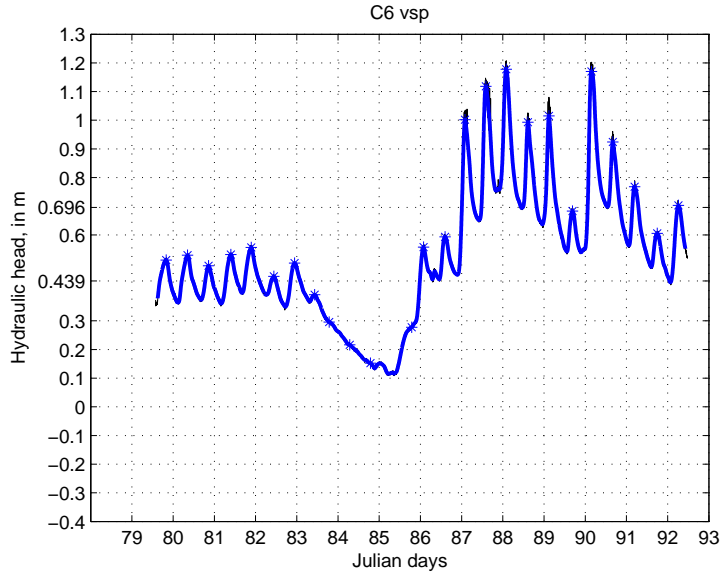


Figure 9: Recorded signal in Well C6. The mean hydraulic head in periods 1 and 2 are, 0.44 and 0.70 m, respectively.

an increase in permeability leading to greater fluctuations during period 2. This approach is similar to that performed by Carr [1971], except that a harmonic analysis is not performed here.

- Calculating the mean water level. The PEMS could cause an increase in permeability leading to less overheight.

The PEMS have not been included in the analysis, i.e., only the wells are included to see how each reacts before and after the installation of the PEMS.

Figure 10 shows the adopted method. For each well the total amplitude has been recorded for each tide. In all there is about 25 low-high tides during the whole period. Because of the exclusion of days 83-86, it amounts to 6 total amplitudes during period 1 and 13 total amplitudes during period 2. Each amplitude is correlated to the same total amplitude in the water levels measured at Hvide Sande, Figure 4. For example, one can have;

$$a_i^r = \frac{a_i^{C6}}{a_i^{HS}} \quad (4)$$

where a_i^r , a_i^{C6} , and a_i^{HS} are the relative amplitude reduction, the total amplitude at C6, and the total amplitude at Hvide Sande for the i 'th tide. The amplitude reduction, a_i^r , is also known as the tidal efficiency [Carr, 1971]. Carr [1971] used harmonic analysis to find the tidal efficiency of three primary tidal components. Cartwright et al. [2003, 2004] similarly used harmonic analysis to find both the amplitudes and phase lags of the single tidal component and the higher order harmonics generated e.g. by the sloping beach and the formation of a seepage face.

The mean amplitude reduction and its standard deviation are calculated for both periods 1 and 2. Recall that only 6 and 13 amplitudes are available, so the standard deviation is uncertain especially for period 1. Furthermore, the mean hydraulic head is calculated for period 1 and 2 in each well.

This procedure assumes that the well response time is short [Black and Kipp, 1977; Horn, 2006], i.e., that the observation well responds more or less instantaneously to changes in pressure outside the well.

All the calculations were done semi-automatically using MATLAB, see also Appendix B.

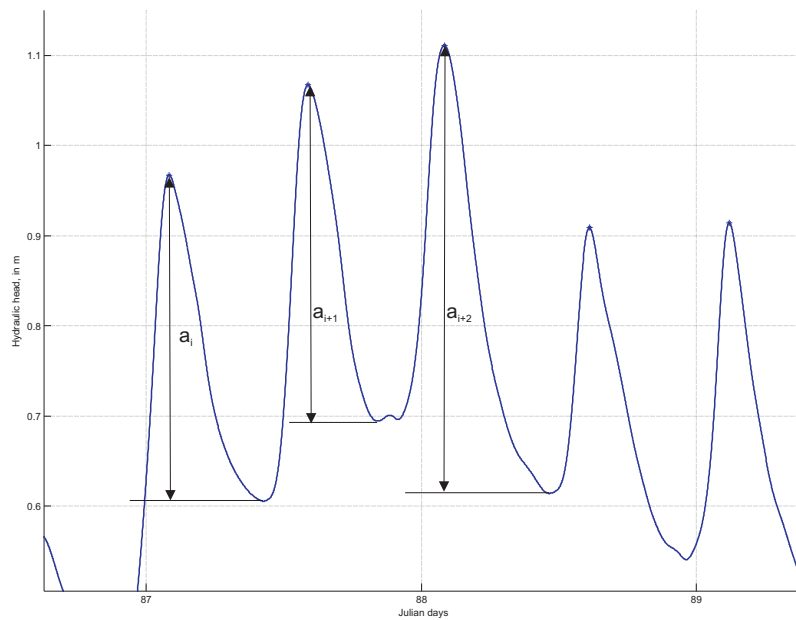


Figure 10: Peak analysis method. Every total amplitude is recorded.

5.2 Analysis based on wells and PEMs

The hydraulic heads were measured with pressure transducers placed near the bottom of the screens of the wells and PEMs, see for example Figure 16. The screen is 1 m long in a PEM and 0.1 m long in a well. The projection of the location of the measurement point of the transducers therefore approximately follows the beach slope.

There are essentially two possibilities for interpreting the tidal response observed in the PEMs;

1. The PEMs act as observation wells with a large diameter and a (relative) long screen.
2. The PEMs act as a drain with water flowing up or down.

Unfortunately it is only possible to investigate the first situation, where the PEMs act as an observation well. Another experiment was designed to closely monitor the head distribution around two PEMs in order to observe significant in/out flows to or from the PEMs. However, this experiment failed. If such a situation is true then inertial effects can become important as has been observed in hydraulic tests of wells. One can not necessarily out rule the possibility of the PEMs draining water from waves in the swash zone, where an analogy to instantaneous hydraulic tests may be made.

The premise for considering the PEMs (and the wells) as observation wells is that the pressure distribution in the well bore is hydrostatic. This means that the hydraulic head inside the well bore represents an average head over the length of the screen. Significant vertical upward or downward flow may exist in the aquifer itself [Cartwright et al., 2003, 2004] although horizontal flow have been shown to dominate at the field scale [Raubenheimer et al., 1999]. The point of measurement is then assumed to be in the middle of the screen, which means that the PEMs measure the hydraulic head about 0.5 m above the wells.

The tidal data from the wells and PEMs have been analyzed to detect possible vertical flows.

6 Results

6.1 Analysis without PEMs

The following analysis is carried out without considering the PEMs. It focuses on a before-and-after situation and a comparison with the reference North transect.

Figures 11, 12, and 13 show the mean amplitude reduction as a function of distance from the first well (N1, C1, or S1). The bars show the plus/minus one standard deviation.

Transect North behaves almost similar from period 1 to 2, although there is a slight tendency to less damping. This may be partly explained by the fact that the MSL moved about 5 m more inland from period 1 to 2 (Figure 4).

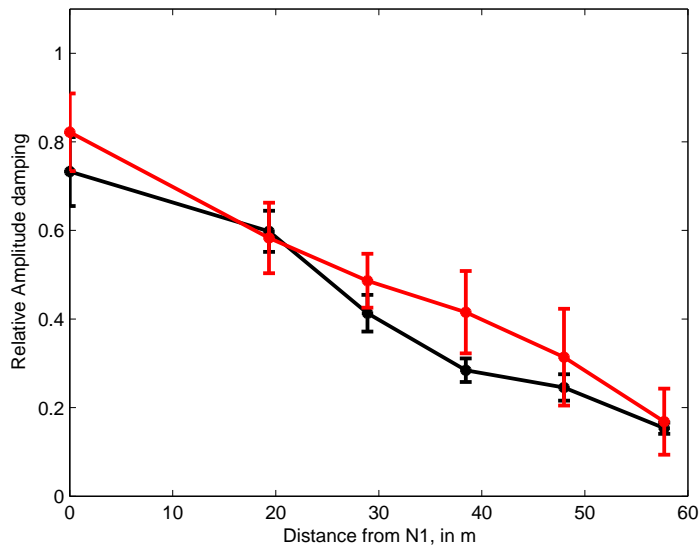


Figure 11: Amplitude damping in transect North. The mean amplitude damping is shown at each well with diver \pm one standard deviation. Black and red lines are period 1 and 2, respectively.

Transects Central and South show a clear tendency towards less damping during period 2, which, again, may be explained by the fact that the MSL moved about 20 m inland, see Figure 3. Figure 22 shows this in another way, where the mean hydraulic heads in the wells have been plotted against the measured beach slope on March 26 and April 2.

Notice that the standard deviation in amplitude reduction is much greater for transects Central and South during period 2. That is, it appears that the beach responds more

erratically during this period.

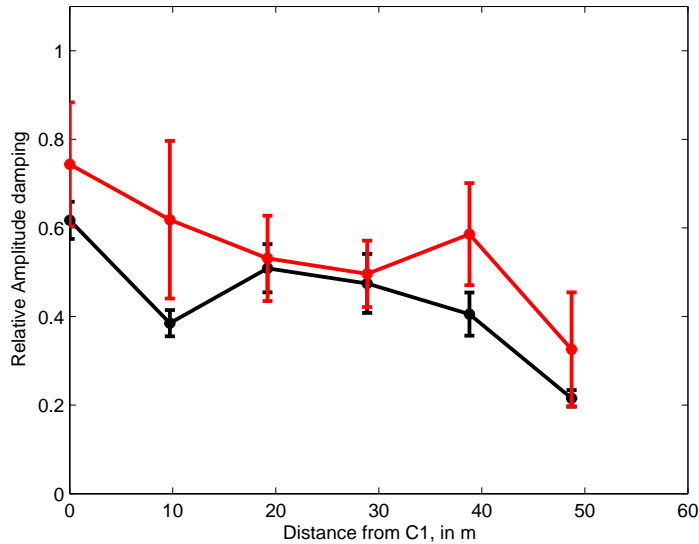


Figure 12: Amplitude damping in transect Central. The mean amplitude damping is shown at each well with diver \pm one standard deviation. Black and red lines are period 1 and 2, respectively.

Figure 14 shows the mean hydraulic head in all wells in the three transects. In all cases the the water table is higher in period 2. This is better seen in Figure 15 where the mean hydraulic head during period 2 was subtracted from the mean hydraulic head during period 1. The three transects show almost identical trends with mean hydraulic heads of 5-35 cm higher in period 2 than in period 1. Recall that Figure 4 showed that the MSL increased by about 35 cm from period 1 to 2. This effectively meant that the MSL moved at least 5-20 m inland. The differences in mean hydraulic heads are less around 10-20 m from the wells nearest to the sea. The reason for this is not known. The micro-topography (Figure 3) would actually trap water in this zone during period 2 and lead to extra infiltration. This would lead to consistently higher hydraulic heads during period 2, and, thus, can not explain the observations. The differences may very well be related to the position of the seepage face during periods 1 and 2. In period 2 the seepage face has likely moved inland. Notice also that the mean hydraulic head is greater during period 2 in the most inland wells up to about 30 cm. This may seem contradictory to the the general behaviour of tidal damping as a function of distance from the coast

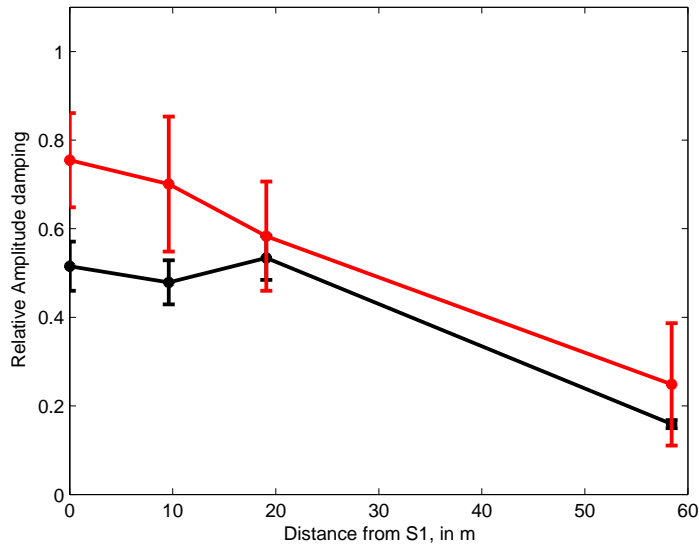


Figure 13: Amplitude damping in transect South. The mean amplitude damping is shown at each well with diver \pm one standard deviation. Black and red lines are period 1 and 2, respectively.

line. This may be explained by the added water table over height or increased inflow of groundwater from upstream areas due to rainfall. The amplitude of the water level at Hvide Sande increases from 0.36 to 0.49 m from period 1 to 2. The water table over height can be computed from $0.5\epsilon A = 0.5A^2 k \cot \beta$, where k is the wave number (3). This relation is strictly only valid for computing the extra over height upstream to the high water mark. This condition is only fulfilled for period 1. Using $A=0.36$ m from period 1 and the parameters from Table 2 together with the estimated hydraulic conductivities (30-140 m/day) gives an extra over height during period 1 of about 11-24 cm. During period 2, with $A=0.49$ m, the over height becomes 20-44 cm depending on the choice of K . Thus, it is likely that natural physical phenomena can explain the extra observed increase in water level in the most inland wells in period 2.

6.2 Analysis including PEMs

Figures 16-21 show a sequence of measured hydraulic heads in the wells and PEMs during low and high tides. Only transect C is analyzed.

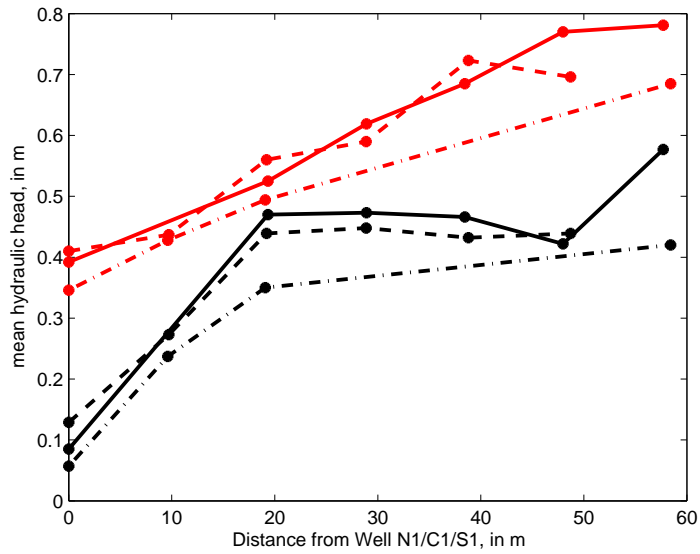


Figure 14: Mean hydraulic head in all wells in the three transect, North (solid), Central (dashed), South (Dash-Dot), with black and red indicating period 1 and 2, respectively

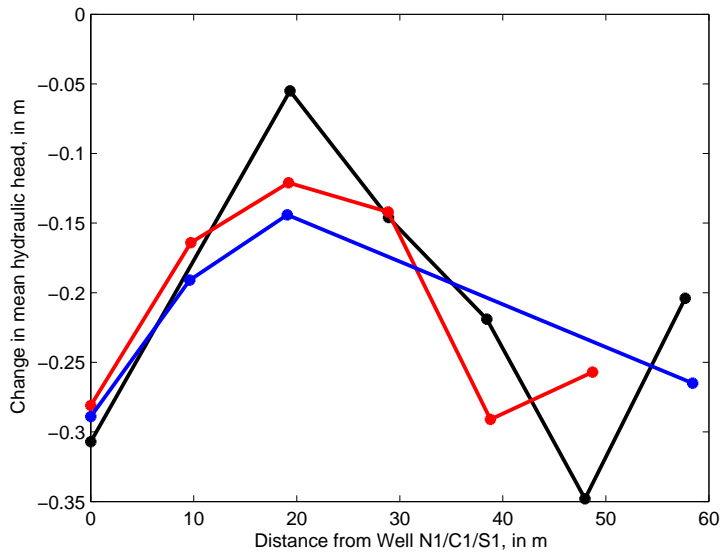


Figure 15: Change in mean hydraulic head in all wells in the three transect, North (black), Central (red), South (blue)

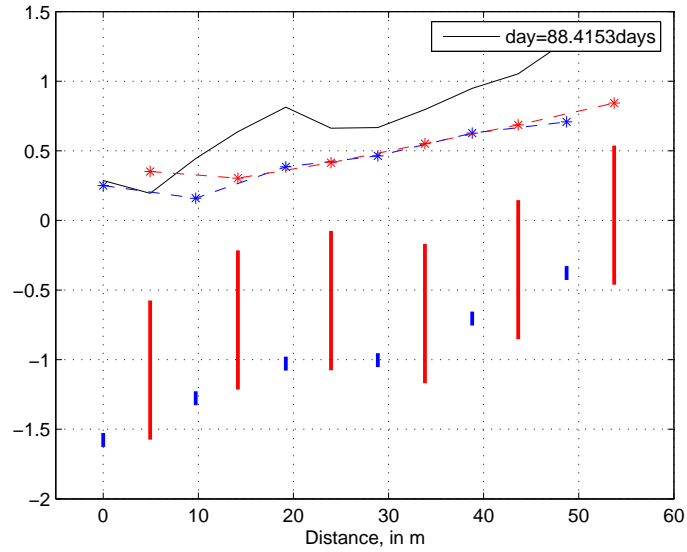


Figure 16: The hydraulic head in period 2 at low tide (88.41 days) for wells and PEMS in transect C. The location of the screens are indicated (red=PEMs, blue=wells)

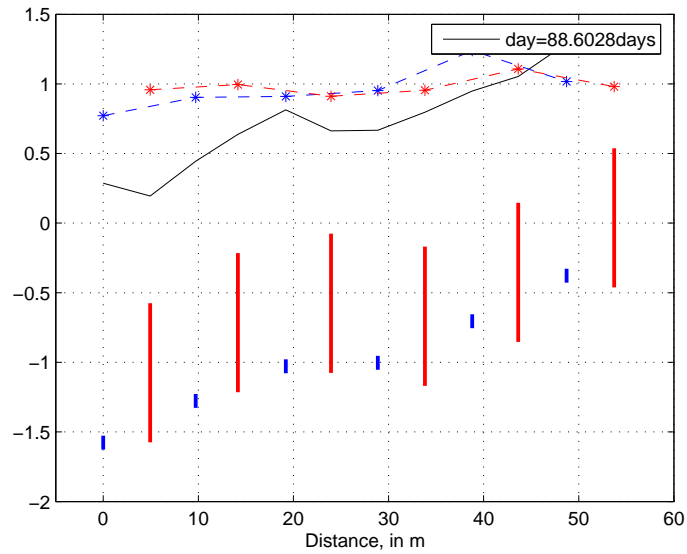


Figure 17: The hydraulic head in period 2 at high tide (88.60 days) for wells and PEMS in transect C. The location of the screens are indicated (red=PEMs, blue=wells)

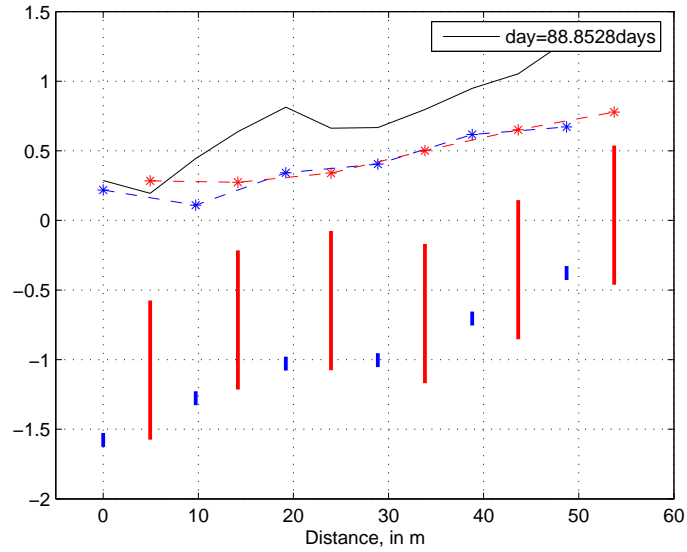


Figure 18: The hydraulic head in period 2 at low tide (88.85 days) for wells and PEMS in transect C. The location of the screens are indicated (red=PEMs, blue=wells)

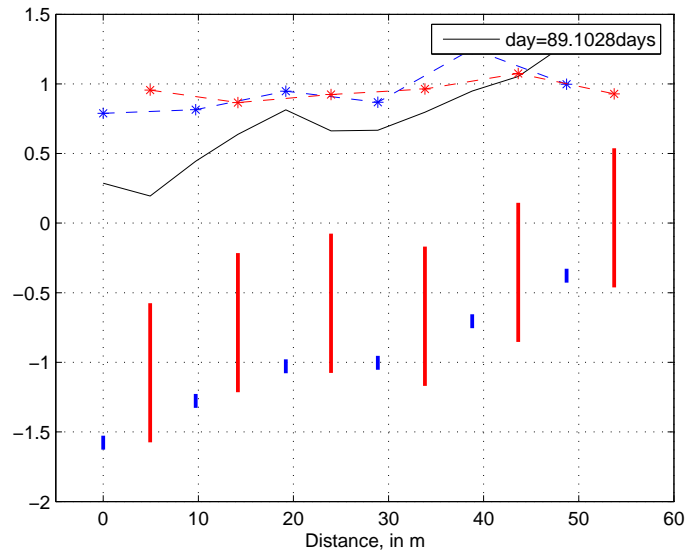


Figure 19: The hydraulic head in period 2 at high tide (89.10 days) for wells and PEMS in transect C. The location of the screens are indicated (red=PEMs, blue=wells)

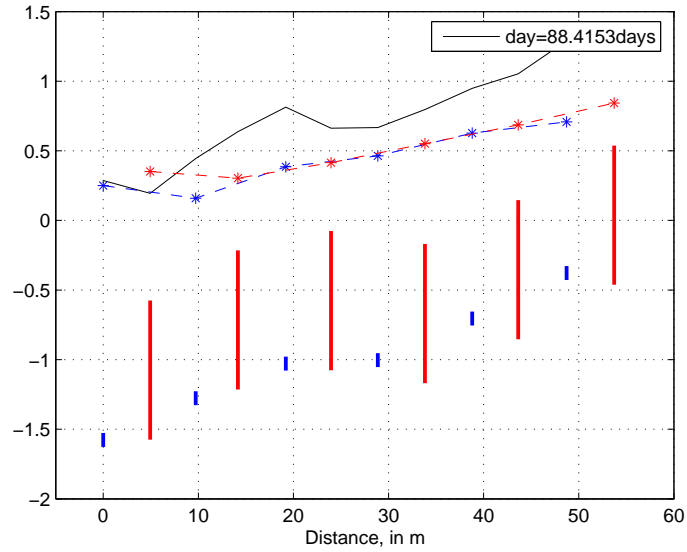


Figure 20: The hydraulic head in period 2 at low tide (89.35 days) for wells and PEMS in transect C. The location of the screens are indicated (red=PEMs, blue=wells)

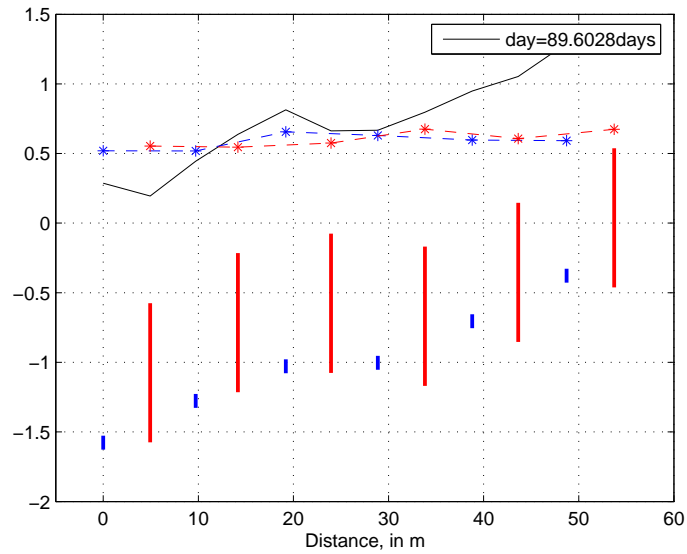


Figure 21: The hydraulic head in period 2 at high tide (89.60 days) for wells and PEMS in transect C. The location of the screens are indicated (red=PEMs, blue=wells)

The hydraulic heads are higher in the PEMs than in the wells in the active forcing zone, 0-20 m, and very similar to the hydraulic heads measured in the wells at distances greater than 20 m (Figures 16-21). Generally, the same pattern is found throughout period 2. Figure 22 show the time mean hydraulic head in the PEMs and wells. Again, the hydraulic heads in the PEMs in the active forcing zone (PEMs Ca and Cb) are higher than in the wells in the same zone (C1, C2, C3). This is consistent with other findings from laboratory experiments [Cartwright et al., 2003, 2004] and field measurements [Raubenheimer et al., 1999], where downward flow was observed during high tide and also as an average over a tidal cycle.

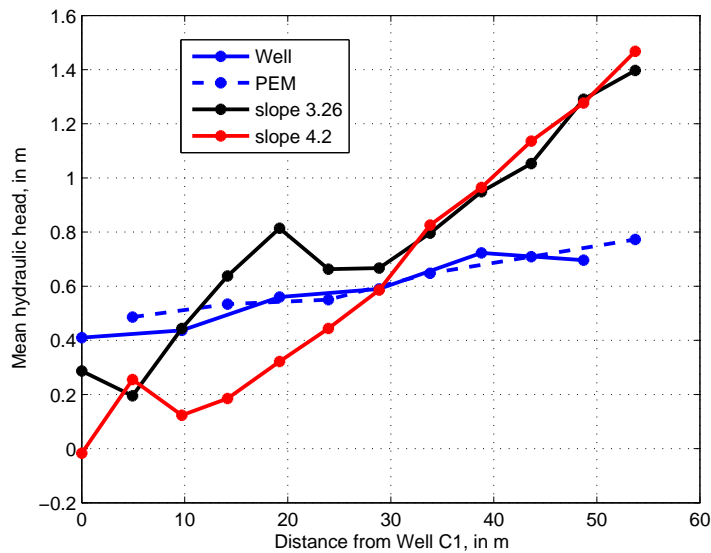


Figure 22: The mean hydraulic head in period 2 for wells and PEMs.

7 Conclusions

An analysis on tidal response in a beach was performed on data from a two-week field-scale experiment at Holmsland.

The analysis is primarily based on a before-and-after situation, where so-called Pressure Equilibrium Modules (PEMs) were installed in week 2. The hydraulic functioning of the beach during week 2 can be compared with week 1 and also compared with a reference site, where no PEMs were installed. The PEMs may result in a more permeable beach

because the long screens can intersect several small gravel layers making the whole beach more conductive. Infiltrating water could thereby drain better away.

The analysis is exclusively performed on tidal data where the high frequency waves have been filtered out.

The hydraulic behaviour of the beach in damping the tidal signal was investigated and compared between week 1 and week 2. The analysis is based on similar principles as applied by Carr [1971], model predictions by Nielsen [1990] for beaches of different permeability, and observations in laboratory and field experiments by Cartwright et al. [2003, 2004]; Raubenheimer et al. [1999].

This leads to the following conclusions;

- The damping is less in period 2 (week 2), which is explained by the fact that the mean sea level moved 5-20 m more inland due to a combination of increase in water level at Hvide Sande and a change in beach profile.
- The temporal mean hydraulic heads increased in reasonable correspondence with the observed water levels at Hvide Sande and the fact that a sloping beach leads to an extra water table over height at inland wells.
- A comparison of the mean hydraulic heads in the wells and PEMs suggest that there is a downward flow in the tidal active zone. This is in agreement with laboratory and other field-scale findings.
- In all cases the transect with both wells and PEMs (Central) act very similar to the transect with just wells in both period 1 and 2. Any differences can be explained by the differences in beach profile.

In summary, it is concluded that, for this beach-scale analysis, the PEMs seem to have little effect on the tidal dynamics. The observed differences between periods 1 and 2 and between the Central and North transects can be explained by the physical situation (beach profile) and physical flow processes.

8 Appendix A: Least square filter, FIR

The design of the filter was originally proposed by Bloomfield [1976]. The FORTRAN programs developed by Bloomfield [1976] were rewritten in the MATLAB script language

by Boon [2004]. These MATLAB scripts were modified as a part of this project. The method is also known as the Finite Impulse Response (FIR) filter.

The idea of a filter is to smooth a time series by removing all periodic motion oscillating above a specified cutoff frequency while retaining oscillations at or below the exact same frequency unmodified [Boon, 2004]. First of all, the linear filter is based on a weighted moving average

$$h'_t = \sum_{k=a}^b w_k h_{t-k} \quad (5)$$

where w_k is a series of weights and h_t and h'_t are the observed and filtered data at time t .

Bloomfield [1976] gives a nice example of how one should choose the weights very carefully. For example, a linear filter

$$h'_t = \frac{1}{3}(h_{t-1} + h_t + h_{t+1}) \quad (6)$$

with $w_k=1/3$ (constant) and $h_t=A\cos(\omega t-kx)$, i.e., a pure sinusoidal signal, will produce an output (h'_t) that is unmodified for frequencies near zero, whereas frequencies $\omega=2\pi/3$ will be removed completely.

However, an optimal filter can be designed [Bloomfield, 1976]. Ideally one would like a filter with the following characteristics;

$$M(\omega) = 1(0 \leq \omega \leq \omega_c) \quad (7)$$

$$= 0(\omega_c \leq \omega \leq \pi) \quad (8)$$

where ω_c is a cutoff frequency. Ideally, if one could have a filter like $M(\omega)$ then it would be possible to filter out all data with frequencies above the cutoff frequency (e.g. high frequency waves). M is also called a response curve.

Without going into details it is possible to show that the weights can be computed as

$$w_0 = \frac{\omega_c}{\pi} \quad (9)$$

$$w_k = \frac{\sin\omega_c k}{\pi k} \quad (10)$$

where $k=1, m$, and m is the width of the filter. The width of the filter specifies the steepness of the response curve. The larger the width the steeper the response curve gets.

In practice it is not possible to specify an exactly abrupt response curve and one is left with what is called the transition band. To get a small transition band also requires that one is prepared to sacrifice $2m$ values, i.e., the first m values and the last m values. Also, it is often found that the response curve can over- and undershoot (oscillate around 1 and 0). This can be reduced by multiplying the filter weights with a convergence factor, i.e.,

$$w_k = \frac{\sin\omega_c k}{\pi k} \left(\frac{\sin 2\pi k / (2m + 1)}{2\pi k / (2m + 1)} \right) \quad (11)$$

9 Appendix B: Test of method

Figure 23 shows the simulated tidal response in two wells located a distance of 20 and 50 meters from the position of the mean sea water level for the conditions of a vertical beach (i.e., $\cot\beta=0$). When the beach is vertical there is no lifting of the water table, and the only difference in the tidal signal is the significant damping at $x=50$ m.

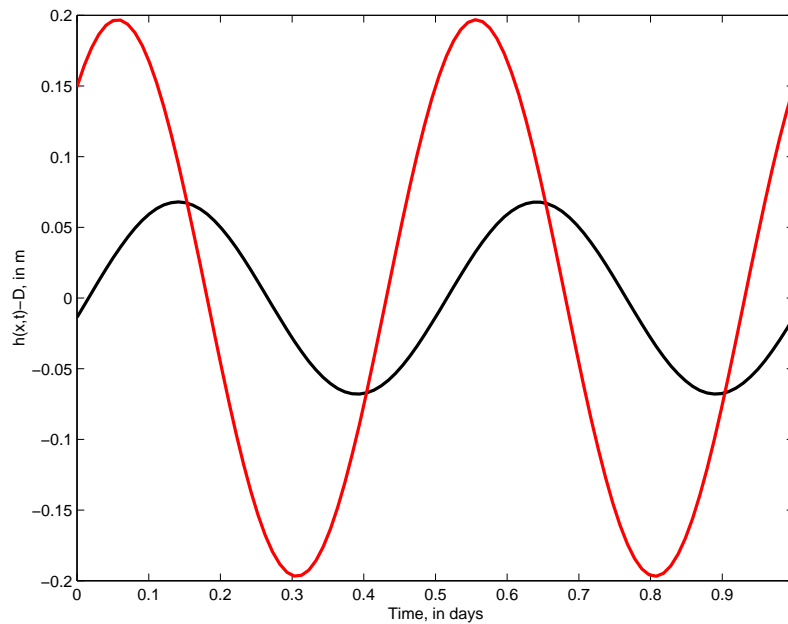


Figure 23: Simulated tidal responses in two wells at $x=20$ m (red) and $x=50$ m (black) for a vertical beach. Parameters can be found in Table 2

By use of (2) the relation between the total amplitudes can be given as;

$$\frac{a_{50}}{a_{20}} = e^{-k\Delta x} \quad (12)$$

where a_{50} and a_{20} are the total amplitudes at $x=50$ m and 20 m, and Δx is the distance between the two wells, i.e., 30 m. The total amplitudes are 0.3927 and 0.1359 m at $x=20$ and 50 m, respectively, and the wave number can be computed as $k=0.0355$. By use of (3) it is possible to calculate n/K , the two hydraulic parameters. For example, assuming the porosity $n=0.20$ is known (i.e. used in the model), one can calculate that $K=49.98$ m/day, very close to the input value that was used to generate the tidal responses shown in Figure 23.

Figure 24 shows the same type of simulation, but now with a sloping beach, Table 2.

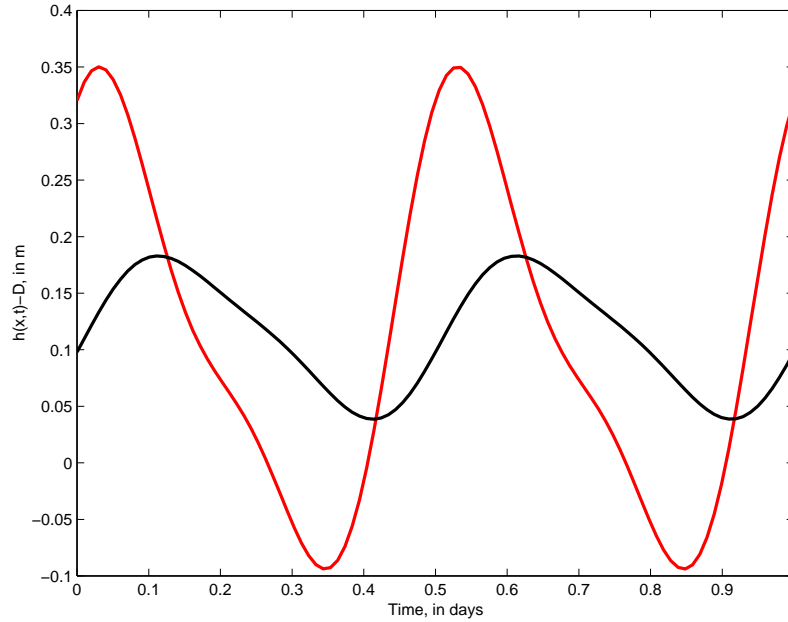


Figure 24: Simulated tidal responses in two wells at $x=20$ m (red) and $x=50$ m (black) for a sloping beach. Parameters can be found in Table 2

As mentioned in Section 3 the effect of a sloping beach is to lift the mean water level recorded in the well a quantity $\epsilon A/2$ above the mean sea level, where $\epsilon=kA\cot\beta$. For example, the mean water level in Figure 24 is 0.1133, or $\epsilon=0.5664$. Thus, the wave number can be calculate to be $k=0.0354$, and by use of (2) the hydraulic conductivity can be computed to be 50.13 m/day under the same assumption that the porosity is known, $n=0.2$. This value is very close to the value used to generate the curves in Figure 24.

If the same method is used as in the case of the vertical beach (total amplitude) then K is computed to 44.77 m/day, about 10 % lower than the input value. This is because

there is a small damping effect in the third term in (2) not accounted for by the simple amplitude reduction equation (12). However, if $K=200$ m/day was used to generate the tidal signal, then K can be calculated to be 194.31 m/day, relatively closer to the true value.

References

- Black, J. H. and K. L. Kipp (1977). Observation of well response time and its effect upon aquifer test results. *J. Hydrol.*, 34, 297–306.
- Bloomfield, P. (1976). *Fourier analysis of time series: An introduction*. John Wiley and sons.
- Boon, J. D. (2004). *Secrets of the tide: Tide and tidal current analysis and predictions, storm surges and sea level trends*. Horwood Publishing, Chichester, England.
- Carr, P. A. (1971). Use of harmonic analysis to study tidal fluctuations in aquifers near the sea. *Water Resour. Res.*, 7, 632–643.
- Cartwright, N., P. Nielsen, and S. Dunn (2003). Water table waves in an unconfined aquifer: Experiments and modeling. *Water Resour. Res.*, 39.
- Cartwright, N., P. Nielsen, and L. Li (2004). Experimental observations of watertable waves in an unconfined aquifer with a sloping boundary. *Ad. Water Resour.*, 27, 991–1004.
- Gilham, R. W. (1984). The capillary fringe and its effect on water-table responses. *J. Hydrol.*, 67, 307–324.
- Horn, D. (2006). Measurements and modelling of beach groundwater flow in the swash-zone: A review. *Continental Shelf Research*, 26, 622–652.
- Nielsen, P. (1990). Tidal dynamics of the water table in beaches. *Water Resour. Res.*, 26, 2127–2134.
- Raubenheimer, B., R. T. Guza, and S. Elgar (1999). Tidal water fluctuations in a sandy ocean beach. *Water Resour. Res.*, 35, 2313–2320.

Appendix 3
Numerical modelling (written by Peter Engesgaard, KU)

Simulation of tidal effects on groundwater flow and salt transport in a coastal aquifer with artificial drains (Pressure Equilibrium Modules)

Peter Engesgaard
Department of Geography and Geology
University of Copenhagen

FINAL REPORT to Danish Coastal Authority
May 2008

Content

1. Introduction and objectives	3
2. Model setup	3
2.1 2D Flow and transport models	3
2.2 Including Pressure Equilibrium Modules as drains	3
2.3 Beach geometry, boundary conditions and choice of parameters	4
3. Results	7
3.1 General simulation results on flow and salt distributions	7
3.2 Flow balances	19
3.3 Effect of disconnecting the gravel layer from the sea	23
3.4 Low permeable layers	24
3.5 Effect of having several gravel layers connected by PEMs	26
3.6 Effect of tides	27
3.7 Comparing different scenarios	28
3.8 Effect of PEMs on Darcy fluxes and hydraulic gradients across beach face	29
3.9 Simulations with higher and lower inflow	33
3.10 Effect of depth of PEMs	37
4. Conclusions	39
5. References	41

1. Introduction and objectives

The results of a numerical study of groundwater flow and the movement of salt in a coastal aquifer are reported. The research objective has been to numerically investigate the effects of Pressure Equilibrium Modules (PEMs) on groundwater flow in a coastal aquifer, especially their draining effect. A number of simulation scenarios have been investigated representing different flow systems. Furthermore, a small sensitivity study was carried out looking into the effects of the permeability contrast between the beach and a higher- or lower permeable layer in the beach and how the connectivity of this layer to the sea on how PEMs affect draining.

2. Model setup

Different flow systems have been investigated where freshwater inflow to the beach is varied from almost no inflow to a very high inflow. The base case is developed to approximate the conditions at Holmsland at the West coast of Denmark. For all systems the effects of having a gravel layer present were simulated with and without PEMs. Additional simulation studies were carried out having one or two layers of contrasting permeability (gravel to clay) present or not. The effect of disconnecting the gravel layer with the sea was also investigated.

The conceptual simulation model is a two-dimensional cross-section of the beach system with or without PEMs. The width of the cross-sections is assumed to be 1 m.

2.1 2D Flow and mass transport models

The flow and salt transport models assume the following;

- 2D variably-saturated groundwater flow and density-dependent transport of salt
- The hydraulic properties of the unsaturated zone are described by the van Genuchten equations relating soil moisture with hydraulic tension and conductivity
- The flow equations are formulated in terms of fresh water head
- The PEMs are simulated as flow pipes (Hagen-Poiseuille flow).

The set of equations for 2D variably-saturated flow and density-dependent transport of salt are well-known and will not be given here. A description of how to incorporate the pressure equilibrium modules are given below. The simulation code FeFlow was used (Diersch, 2006).

2.2 Including Pressure Equilibrium Modules as drains

The pressure equilibrium modules are inserted as so-called discrete feature elements in the model. Flow in the PEMs is assumed to follow axi-symmetric Hagen-Poiseuille flow in a pipe of radius R (pure translation of flow and no inertial effects). This means that flow can be described as an equivalent to Darcy flow according to

$$q = Kf_{\mu} \left(\frac{\partial h}{\partial z} + \frac{\rho - \rho_o}{\rho_o} \right) \quad (1)$$

where f_μ is the ratio of the viscosity of freshwater (μ_o) and saltwater (μ). The density of freshwater and saltwater is given as ρ_o and ρ , respectively. The ratio $(\rho-\rho_o)/\rho_o$ is called the density ratio. The equivalent hydraulic conductivity K for a pipe is;

$$K = \frac{r_{hydr}^2 \rho_o g}{2\mu_o} = \frac{R^2 \rho_o g}{8\mu_o} \quad (2)$$

where r_{hydr} is the hydraulic radius of a pipe ($R/2$). Thus, by specifying the radius it is possible to simulate flow in discrete elements (pipes) embedded in the porous matrix elements. For example, with $\rho_o=1000 \text{ kg/m}^3$, $\mu_o=1.3e^{-3} \text{ Pas}$, and $g=9.81 \text{ m/s}^2$ one can calculate an equivalent hydraulic conductivity of about 1500 m/s ($1.3*10^8 \text{ m/day}$) for a pipe with radius of 0.04 m . This is a factor of 5 million higher than the hydraulic conductivity of a sandy porous medium (like what is used for a beach in the current study). Thus, the pipes are very conductive to flow.

Since the model is two-dimensional this also means that the width of the model is 1 m . It is implicitly assumed that the pipes fill out all of the width, which is of course not true. In fact, for the current system a pipe only occupies 0.08 m per 1 m width.

2.3 Beach geometry, boundary conditions and choice of parameters

Figure 1 shows the idealized model setup of a beach system. The section is 100 m long with a sloping beach face from -2 m to $+2 \text{ m}$. The amplitude of the tide is assumed to be $A=0.5 \text{ m}$, Figure 2. The high and low water mark (HWM and LWM) are indicated on Figure 1. Mean sea level (MSL) is 0 m and cuts the beach at the location $x=20 \text{ m}$.

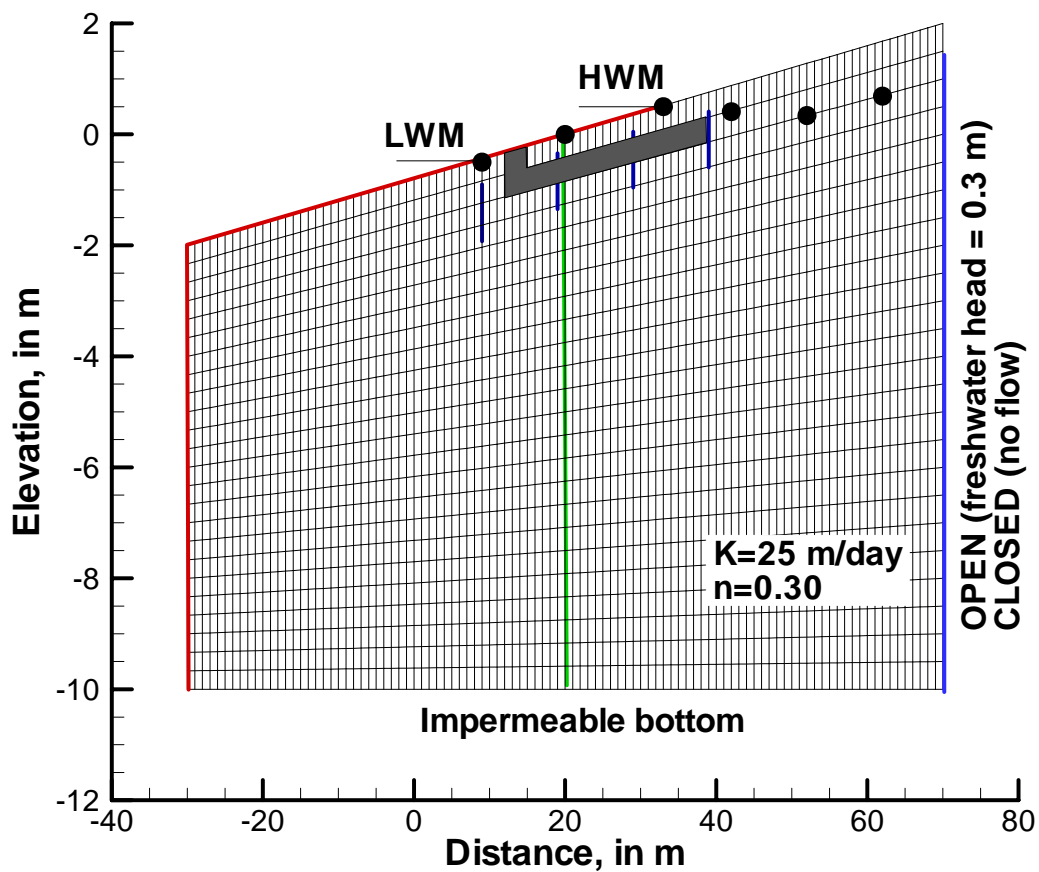


Figure 1 Model geometry and grid, boundary conditions, and flow balance sections. The solid red line indicates the section where the tidal cycle is applied. The blue solid line indicates the freshwater boundary condition (fixed head of 0.3 m). The solid red line also indicates the section where inflow and outflows through the beach section have been recorded for flow balances. The dark solid circles indicate points where the tidal attenuation and damping have been recorded. The black area indicates the presence of the gravel layer alternatively a clay layer. The small heavy blue lines near the gravel layer indicate the approximate location of the screens in the PEMs.

The boundary conditions are as follows;

- The red line indicates the section where a tidal boundary condition (Figure 1) is applied. However, for each nodal point the tide is adjusted to provide the equivalent freshwater head according to elevation. The details of this will not be given here.
- A seepage face is also specified between LWM and HWM, which means that it is assumed that the water table follows the beach for example when going from high to low tide. When the seepage face is active, only outflow is allowed. This is incorporated in the model using so-called boundary constraints. It means that the water table can detach from the beach when going from high to low tide.
- The rest of the upper boundary is assumed to be a water table with zero influx.

- The bottom is assumed impermeable giving a variable thickness of the coastal aquifer (8-12 m).
- The right boundary (blue line) is a fixed head boundary condition (head of 0.3 m). The choice of a head of 0.3 m is based on a calculation of how much water should discharge to the coast from the strip of land separating the ocean and Ringkøbing Fjord. With a precipitation of around 800-1200 mm/year, assuming that 50% infiltrates in the sand dunes, and taken the half-width of the length of the strip of sand (650 m) one can calculate an approximate discharge of 0.9 m²/day. When the tide is at MSL there is a head gradient of 0.3-0.0 m from the freshwater boundary to the point where the MSL cuts the beach. From Darcys law one can compute a freshwater inflow of about 1.7 m²/day. However, as Nielsen (1990) pointed out there will be a water table overheight. Without showing the details here (see Engesgaard, 2006) the overheight amounts to about 0.25 m, although Niensens analytical solution is not strictly valid for the selected system. Thus, the inflow will be reduced. The mean inflow over a tidal cycle for a homogeneous beach has later been simulated to be approximately 0.65 m²/day. Including a gravel layer and PEMs will increase this average inflow because of a higher permeability of the beach.

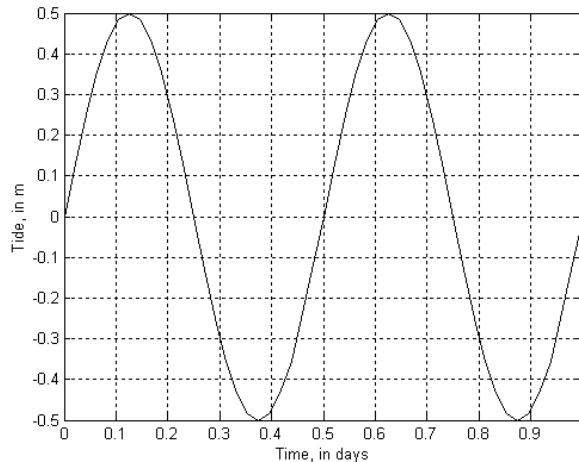


Figure 2 Tidal fluctuation with MSL of 0 m and amplitude of $A=0.5$ m. This tidal boundary condition is modified in the model to correspond to the equivalent freshwater head at the given nodal elevation.

An approximate 0.5 m thick gravel or clay layer can be present in the beach. This layer may connect to the sea or not. The PEMs are modelled as pipes and their positions are also indicated in the figure. It is only the 1 m slotted screen of the PEMs that have been included.

The model parameters are given in Table 1. It is assumed that the sand in the beach has a hydraulic conductivity of 25 m/day and that the gravel layer has a hydraulic conductivity that is a factor of 10 higher. This layer will be also be simulated as a silt/clay layer with a hydraulic conductivity a factor of 10-100 less than that of the sand. The discretization is 1 m in the horizontal direction (100 elements). In the vertical direction 25 elements have been used given a variable mesh length.

The PEMs were located at $x=9$ m, 19 m, 29 m, and 39 m and 0.5 m below the beach face. In the experiments reported by Engesgaard (2006) the screens of the PEMs were located approximately 0.8 m below the beach face, however, due to the choice of discretization in the vertical direction

(0.5 m) it was not possible to exactly match this position. The effects of locating the PEMs one meter deeper is investigated.

Parameter	Value	Unit
Saturated hydraulic conductivity for sand, $K_x=K_z$	25)	m/day
Saturated hydraulic conductivity for gravel, $K_x=K_z$	250 (0.25, 0.025)	m/day
Porosity, n	0.3	-
van Genuchten max. saturation	1	-
van Genuchten min. saturation	0.0025	-
van Genuchten fitting coefficient A	4.1	1/m
van Genuchten fitting exponent n	1.964	-
Longitudinal dispersivity	1.0	m
Transverse dispersivity	0.02	m
Molecular diffusion coefficient	$8.64 \cdot 10^{-5}$	m^2/day
Freshwater and saltwater density	1000 and 1029	kg/m^3
Density ratio	0.029	-
Viscosity	$1.3 \cdot 10^{-3}$	Pas

Tabel 1 List of parameter values used in model scenarios. The values in parenthesis are values used in different sensitivity studies.

3. Results

All simulations were run to quasi-steady state by repeating the tidal cycle for about 50 days. The results in this section are from one tidal cycle after that.

3.1 General simulation results on flow and salt distributions

Figure 3 shows a close-up view of the simulated water table at low tide (LWM), mean tide (MSL), and high tide (HWM). Recall that the fixed head is 0.3 m at the freshwater boundary. At low tide there is a significant head gradient towards the sea, while at high tide the gradient is opposite, with flow from the sea into the fresher part of the aquifer. The simulated water content above the water table at low tide ranges from 100% saturation at the LWM to about 50% at the HWM.

Figure 4 shows the simulated distribution of salt water at low and high tide for a homogeneous beach, i.e., no gravel/clay layer or PEMs. It is the relative mass fraction that is displayed, where a mass fraction of 1 is salt water and a mass fraction of 0 is fresh water. A secondary plume of saltwater develops at the high water mark. This is in agreement with other findings (e.g. Robinson et al., 2007ab). If the back-ground freshwater flow was higher a freshwater outflow tube could develop between this secondary plume and the saltwater wedge.

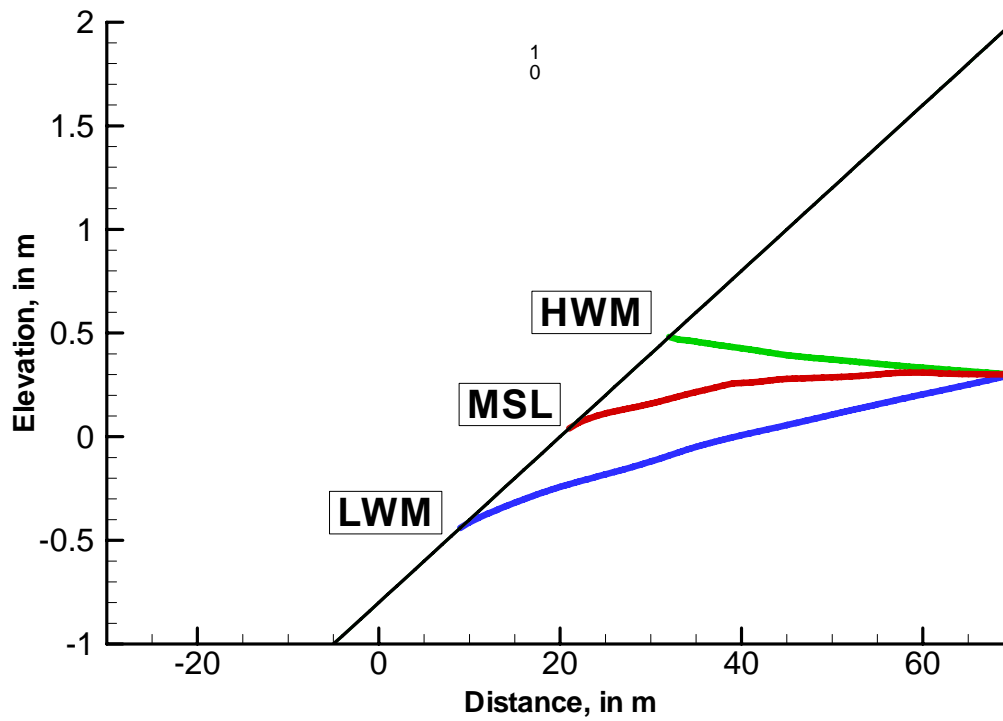


Figure 3 Simulated water table at low, mean, and high tide for the homogeneous case.

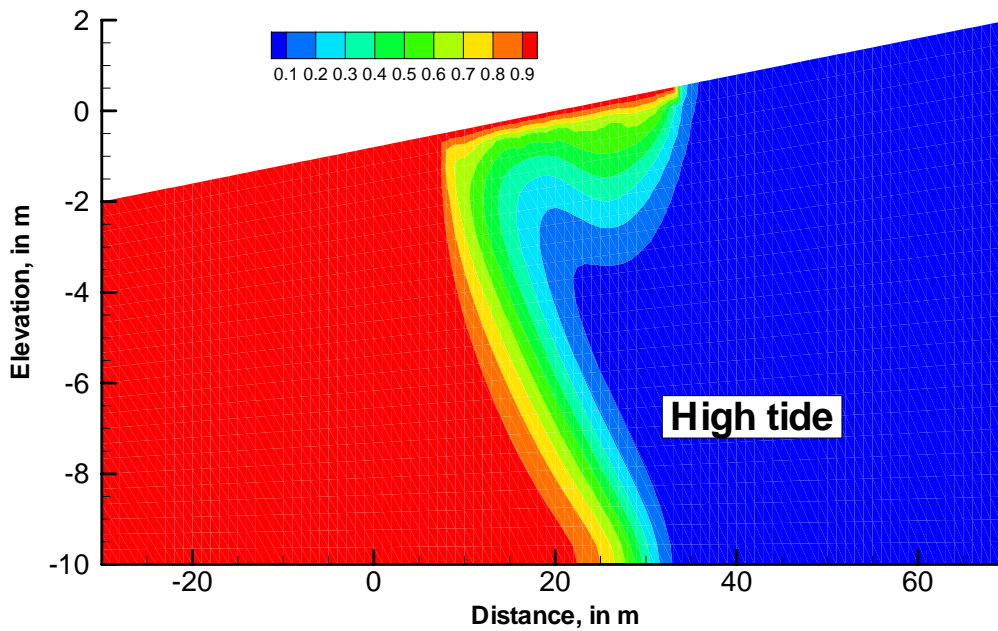
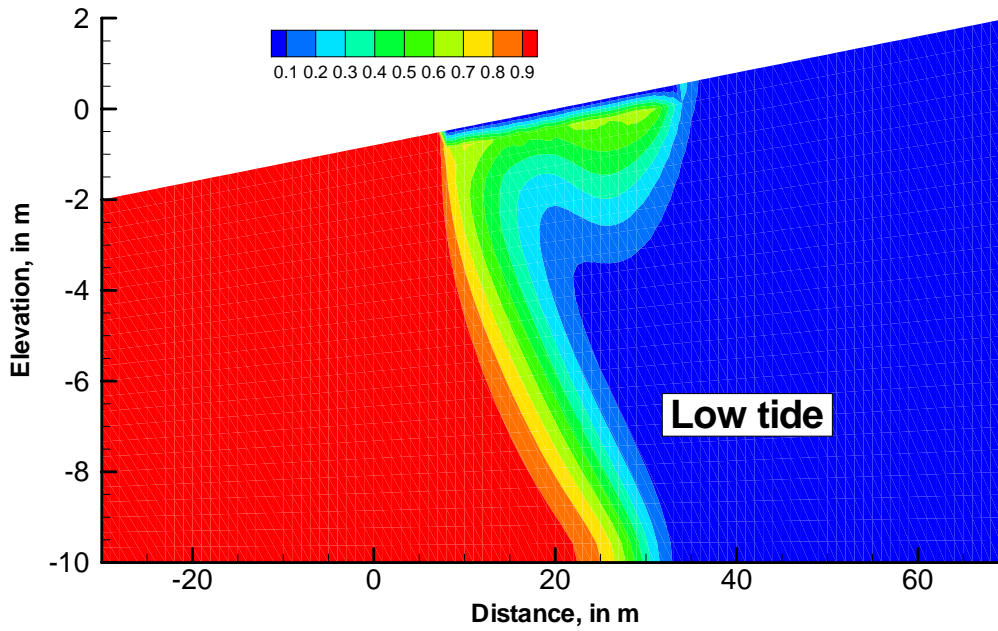


Figure 4 Simulated mass fraction distribution for homogeneous beach (without gravel/clay layer and PEMs) at low tide (upper) and high tide (lower). A mass fraction of 1 is salt water, a mass fraction of 0 is fresh water.

Figures 5 and 6 show the same results but now plotted with velocities also. At low tide the zone of discharge is close to the LWM with maximum velocities of 1.0 m/d. At high tide there is a rather complicated flow field with both inflow and outflow. Inflow takes place from the LWM and

seaward and around the HWM. In-between there is outflow. Maximum velocities are 0.3 m/d near the HWM.

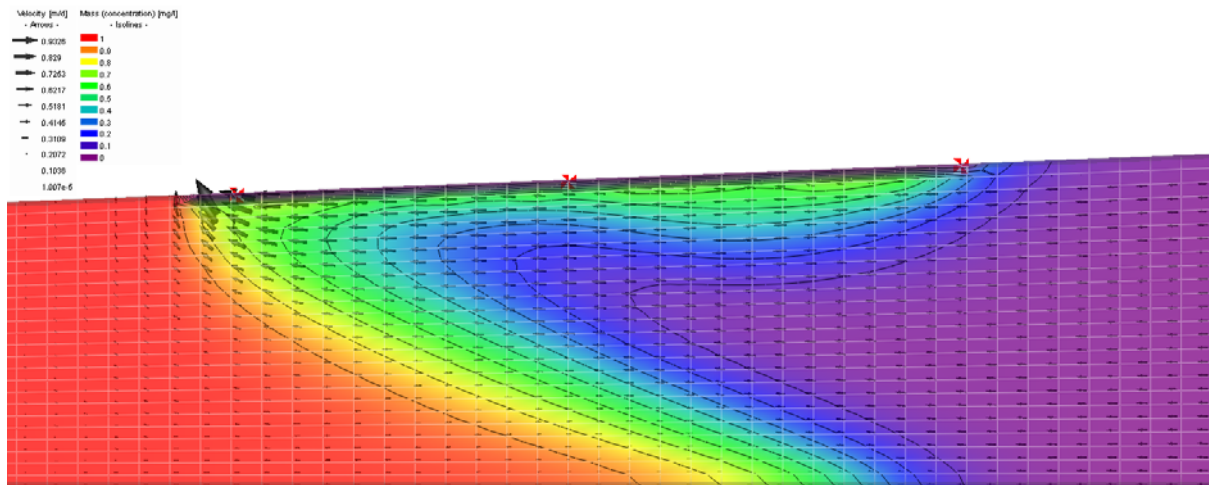


Figure 5 Close up view of the simulated distribution of mass fraction and velocities at low tide in an open system with no gravel layer or PEMs. The three markers show LWM, MSL, and HWM. The arrows indicate direction and strength.

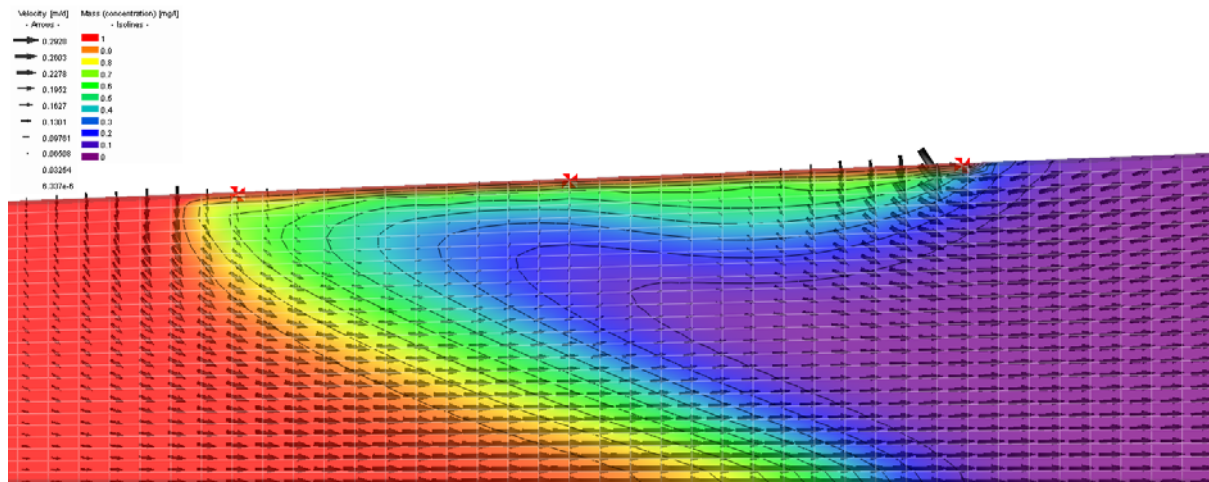


Figure 6 Close up view of the simulated distribution of mass fraction and velocities at high tide in an open system with no gravel layer or PEMs. The three markers show LWM, MSL, and HWM. The arrows indicate direction and strength.

Figures 7 and 8 show the results with a gravel layer. At low tide, the highest velocities are now found in this layer, but the gravel layer has the effect of providing a slightly more diffuse outflow with maximum velocities now only up to 0.7 m/day. Notice that at high tide the flow field is quite different in that now only inflow occurs primarily through the gravel layer.

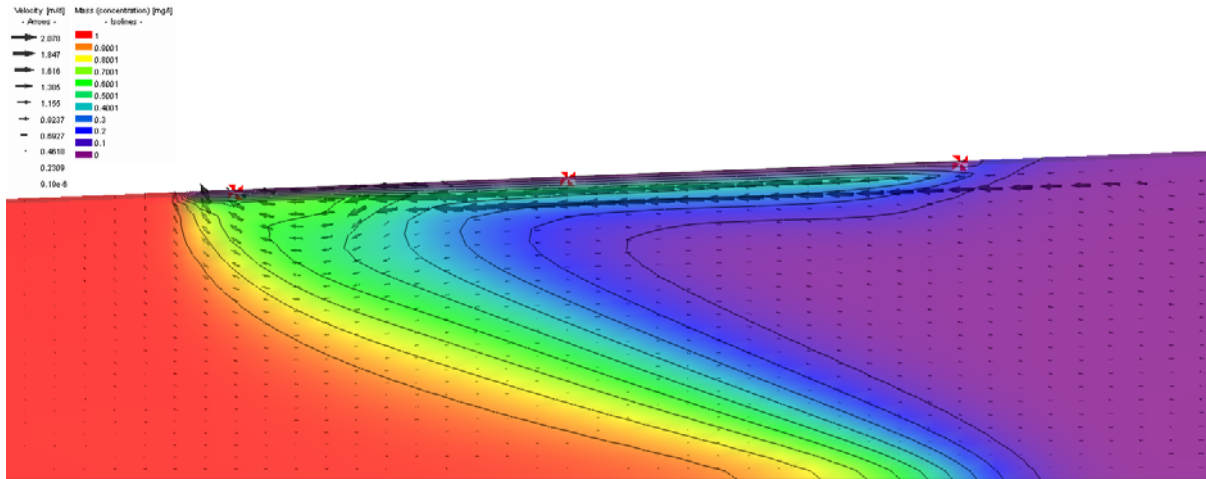


Figure 7 Close up view of the simulated distribution of mass fraction and velocities at low tide in an open system with a gravel layer but no PEMs. The three markers show LWM, MSL, and HWM. The arrows indicate direction and strength.

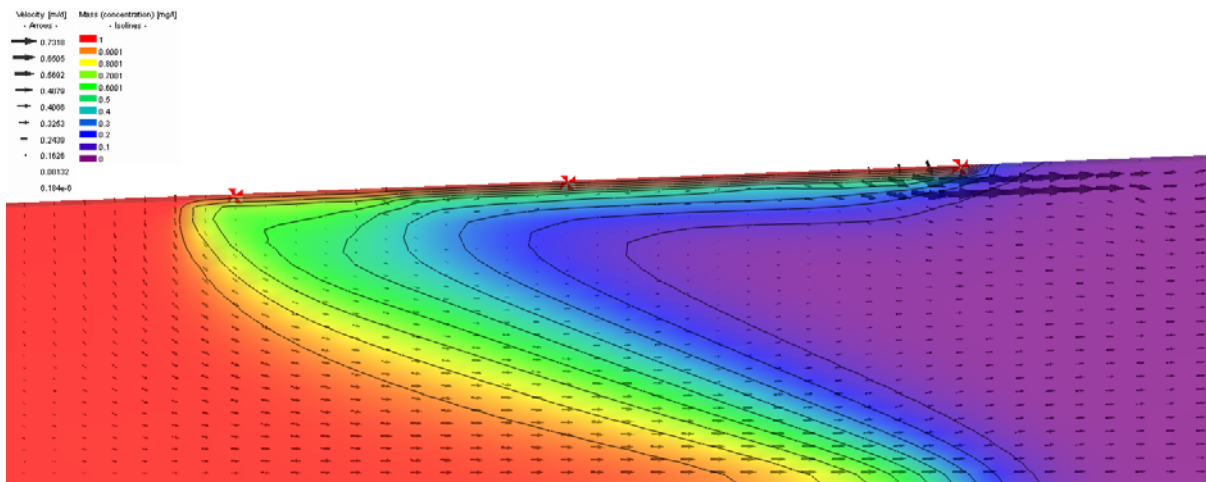


Figure 8 Close up view of the simulated distribution of mass fraction and velocities at high tide in an open system with a gravel layer but no PEMs. The three markers show LWM, MSL, and HWM. The arrows indicate direction and strength.

Figures 9-10 show similar results but now for a system with no gravel layer but 4 PEMs. The location of the PEMs can be seen in Figure 1. Two sets of figures are shown in each figure; top figure shows the saltwater distribution together with two types of velocities; bullets and arrows. The bullets do not show the magnitude of the velocities, only direction. The arrows show magnitude and direction. The bullets are included to show the general flow system, otherwise, because of the high velocities in the PEMs, only these would be visible. The bottom figure shows the freshwater head distribution together with the logarithm to the velocities, i.e., $\log(\text{velo})$, plotted then only as a line with an arrow.

At low tide the PEM near the low water mark is most active with very high velocities 180 m/d or approximately 0.2 cm/s. In the bottom figure it looks like the almost horizontal flow velocities are deflected towards the bottom of the PEMs and out of the PEMs near the top. All PEMs show vertical velocities, which seems intuitively correct.

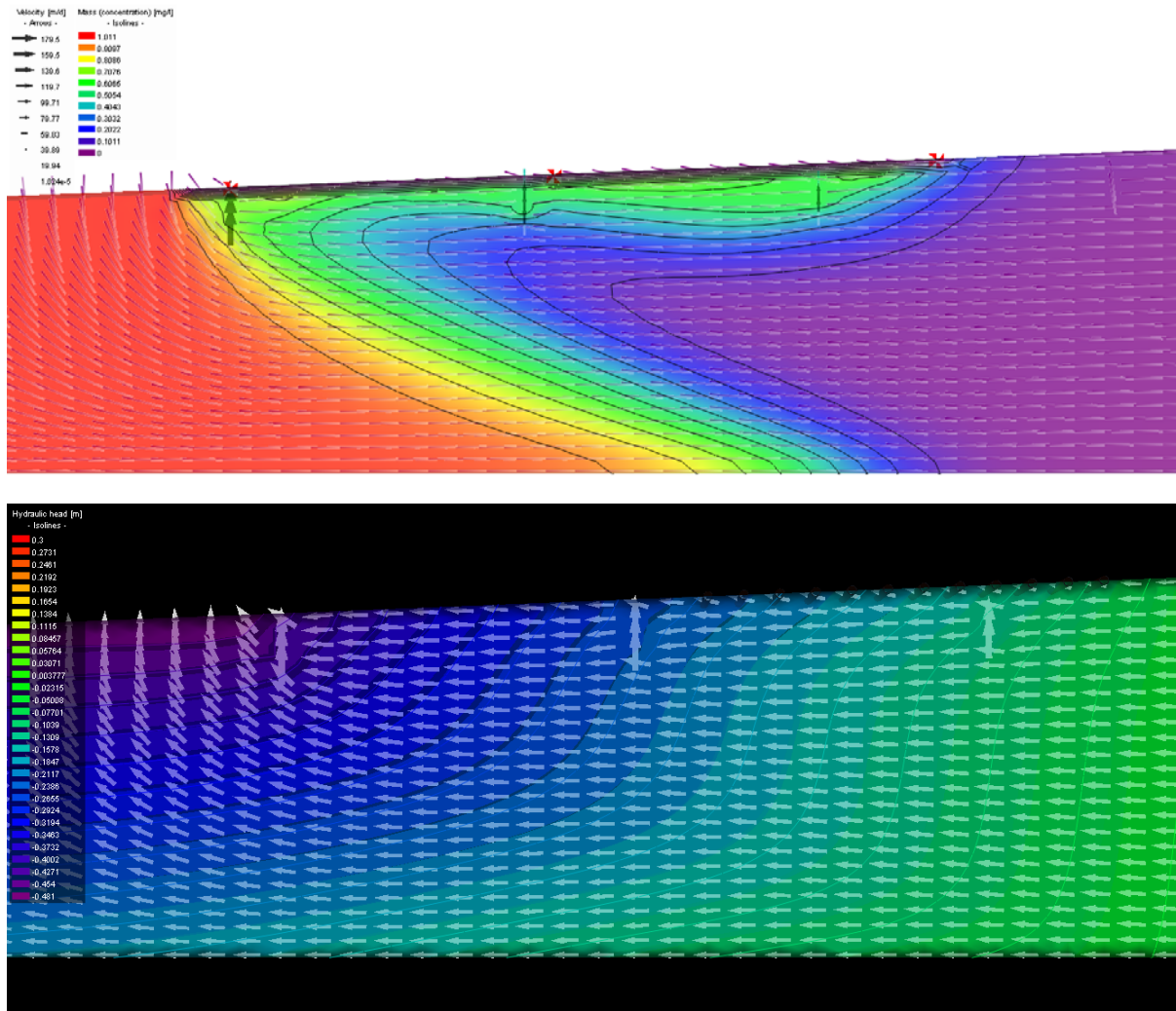


Figure 9 Close up view of the simulated distribution of mass fraction and velocities (top) and freshwater head and \log (velocities) (bottom) at low tide in an open system with no gravel layer but 4 PEMs. The three markers show LWM, MSL, and HWM.

At high tide, Figure 10, it is the PEM near the high water mark that is most active (top figure). It is clear that the PEMs affect the saltwater distribution, see also later. The effect of the PEMs on the velocity distribution is much more apparent at high tide (bottom figure). Again all PEMs show upward flow, despite that flow just outside the PEMs can be downward. The left-most PEM shows a circulation, where flow moves down and into the PEM and then back up through the PEMs. The head distribution around the bottom and top of the PEMs confirm that flow is into the PEM at the bottom and out through the PEM at the top. It is not clear why this circulation comes about. Perhaps a combination of buoyancy effects and flow driven by forced convection. At the middle PEM the flow distribution is clearer. Flow diverges upward, enters the bottom of the PEM and exits at the

top. At the right most PEM there is again flow down along the PEM, but now part is (apparently) diverted up through the PEM again and parts is flowing towards the landside. Still we see the characteristic head distribution indicating flow into the PEM and out of the PEM. At the beach face flow is outward right at the three PEMs in the tidal zone.

Later it is discussed that numerical oscillations is believed to cause inaccuracies when the tide rolls past a PEM. Thus, this may also have affected the simulated flow fields in the figures above.

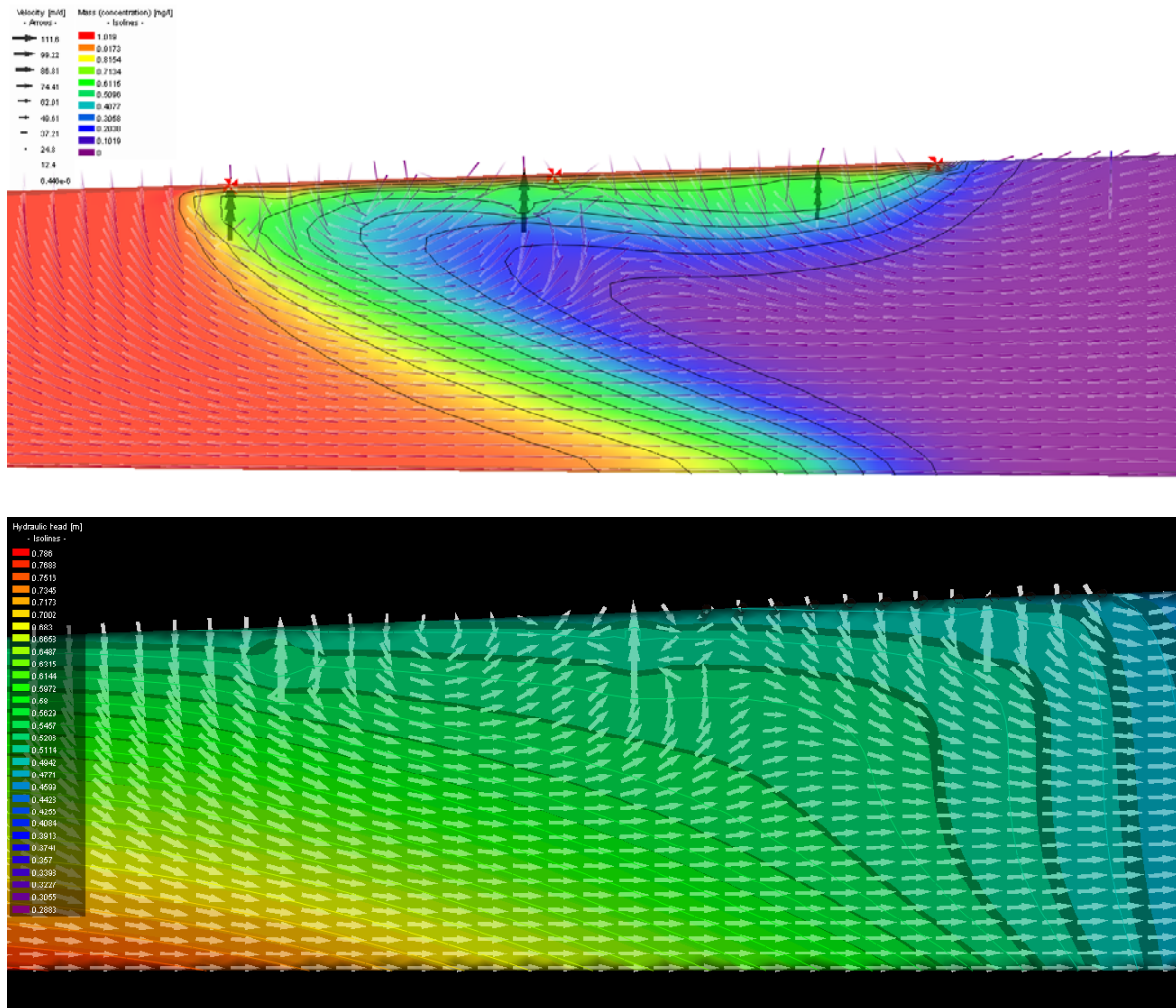


Figure 10 Close up view of the simulated distribution of mass fraction and velocities (top) and freshwater head and \log (velocities) (bottom) at high tide in an open system with no gravel layer but 4 PEMs. The three markers show LWM, MSL, and HWM.

Figure 11 shows the damping of the tidal signal as a function of distance from the sea. The location of the observation points are shown in Figure 1. The red line is from the point at the low water mark and is identical to the tidal signal (corrected for freshwater head). The dark line is at the mean sea water level and shows the development of the seepage face, where the water table detaches from the beach. This takes place when the tide reaches the beach level $h=z=0$. Because of the high hydraulic

conductivity and the freshwater inflow the tidal signal is quickly dampened and attenuated (peak occurs later more inland).

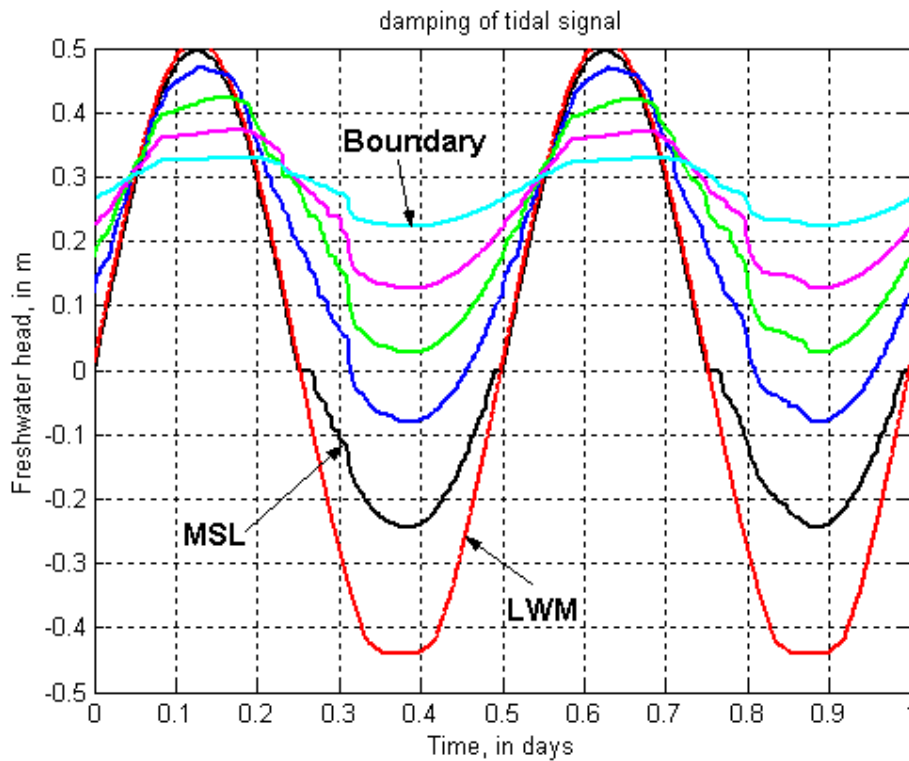


Figure 11 Simulated freshwater head in 6 observations points (see Figure 1). The red and black lines are identical to the applied tidal signal at the LWM and MSL, respectively.

Figures 12 and 13 summarize the simulation results for the salt distribution at low and high tides. In all cases a secondary salt plume may be found at the high water mark. The presence of the gravel layer results in a slightly smaller plume due to the preferential channelling of freshwater through this layer. The presence of PEMs also has an effect on the saltwater distribution. At the bottom of the PEMs the concentration is slightly higher than outside at high tide, while at the top of the PEMs the concentration is slightly lower. The latter is likely due to the preferential upward discharge of water seen in Figure 10.

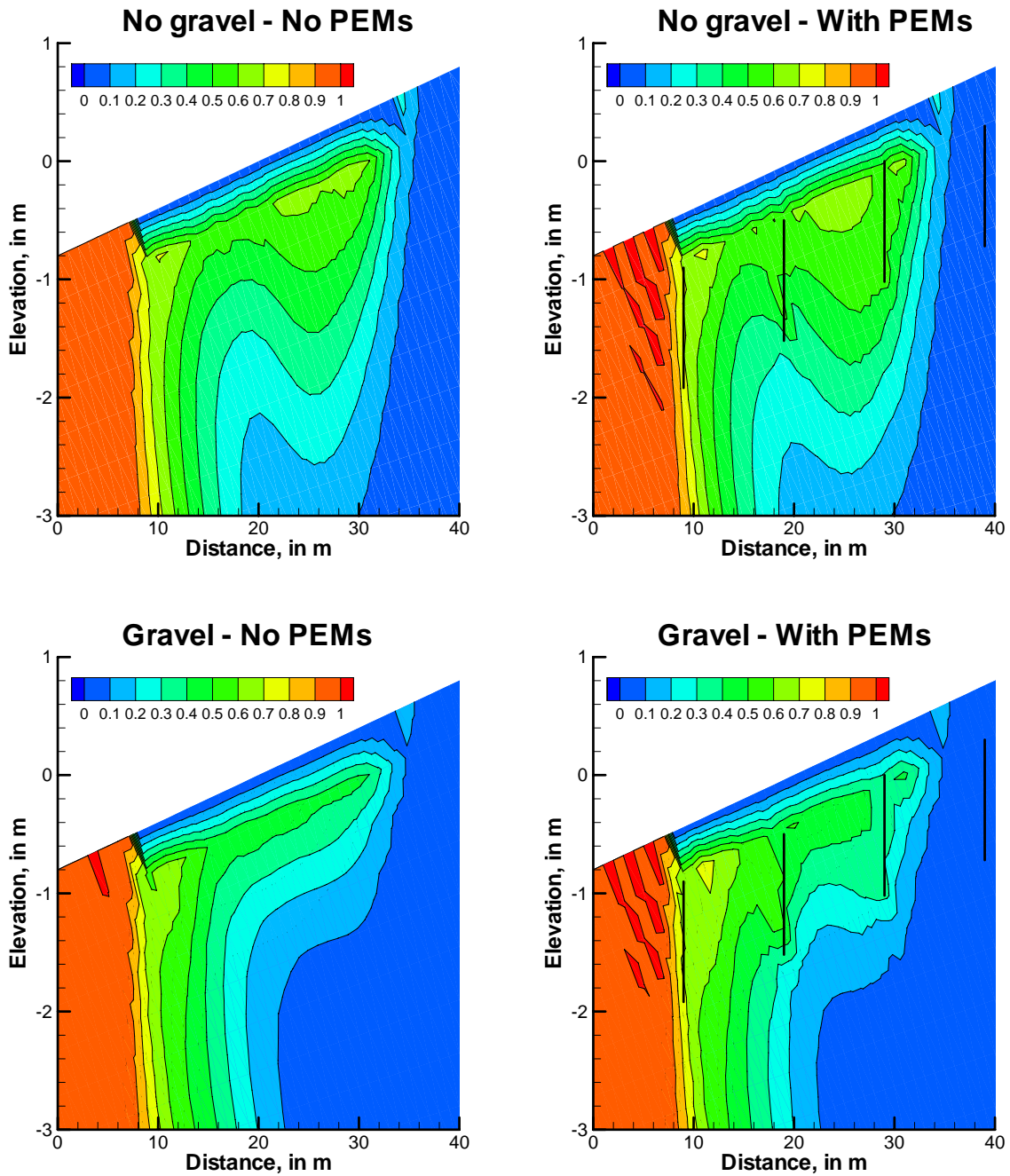


Figure 12 Simulated salt distribution at low tide for four different cases. The locations of the PEMs are shown with solid dark lines.

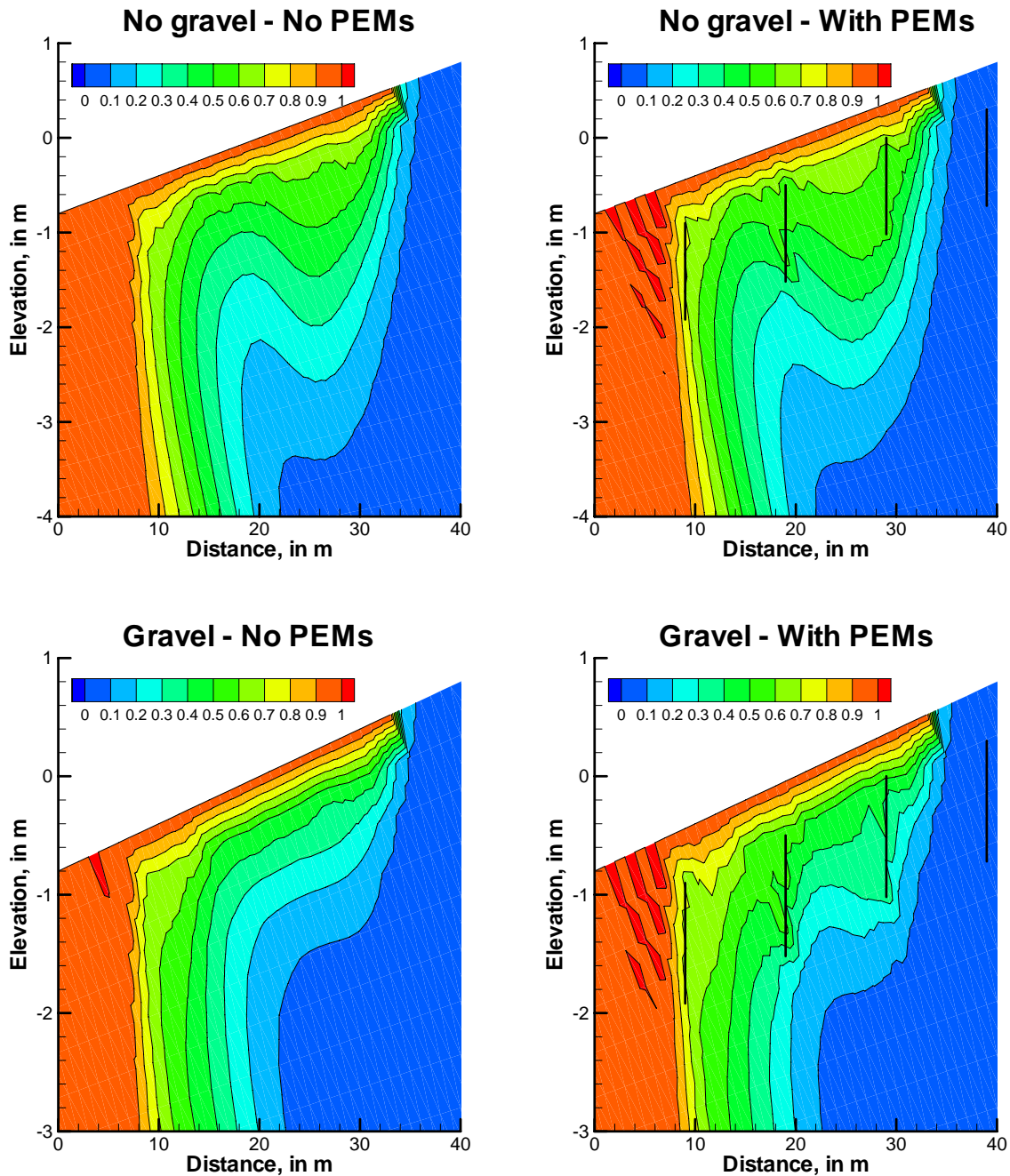


Figure 13 Simulated salt distribution at high tide for four different cases. The locations of the PEMs are shown with solid dark lines.

The simulated spatial distribution of the absolute magnitude of the velocity is shown in Figure 14 for the case of no gravel layer with PEMs. The four PEMs are not active in a uniform way. At low tide, it is the PEM near the LWM that is active with upward directed velocities near 200 m/day (0.2 cm/s), while at high tide, it is the corresponding PEM near the HWM that is most active. Between the most active PEMs, the velocities are in the range 0.2 m/day (high tide) to 0.5 m/day (low tide).

Figure 15 shows a close-up view of the velocity distribution at low tide with and without PEMs. Without PEMs the highest flow rates (0.8 m/day), is found near the LWM. With PEMs it is the PEM near the LWM that is most active channelling flow upwards, but notice that flow exits the PEM and is reduced to the same order of magnitude in velocity as without the PEMs.

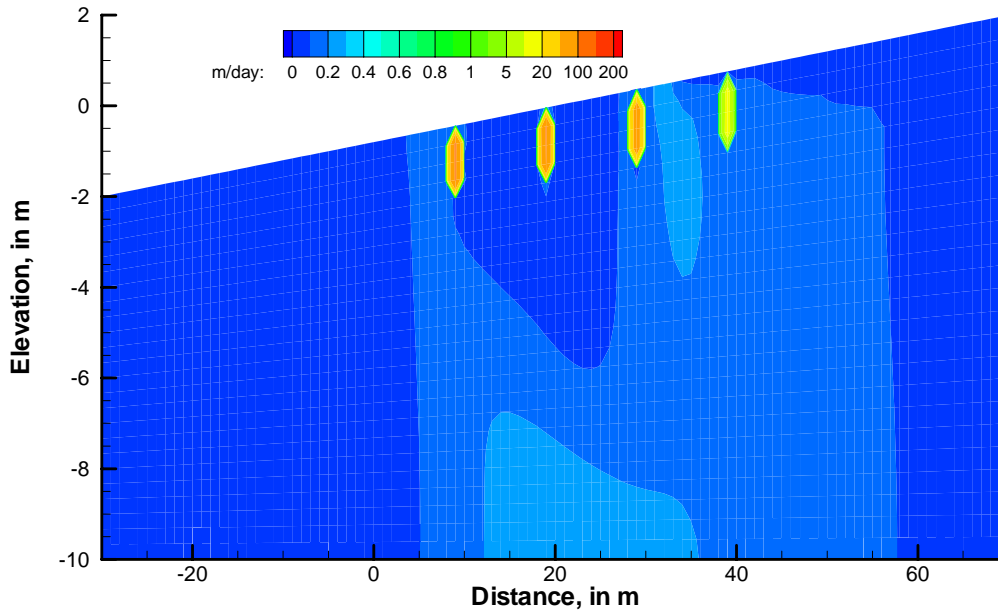
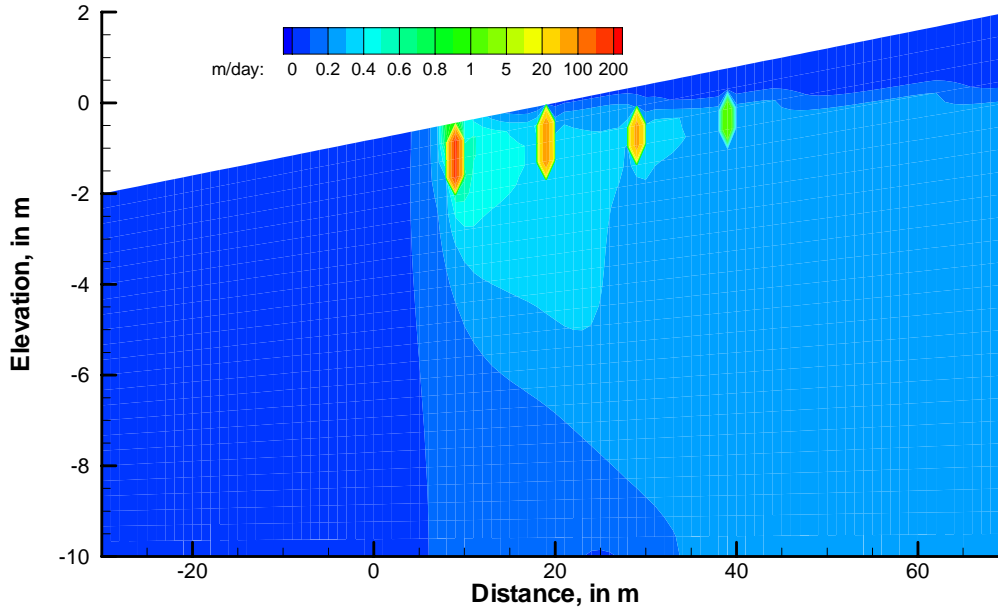


Figure 14 Simulated magnitude of velocities at low tide (upper) and high tide (lower). Notice, it is the absolute value of the velocity that is plotted, i.e., it does not show direction. Units are in m/day.

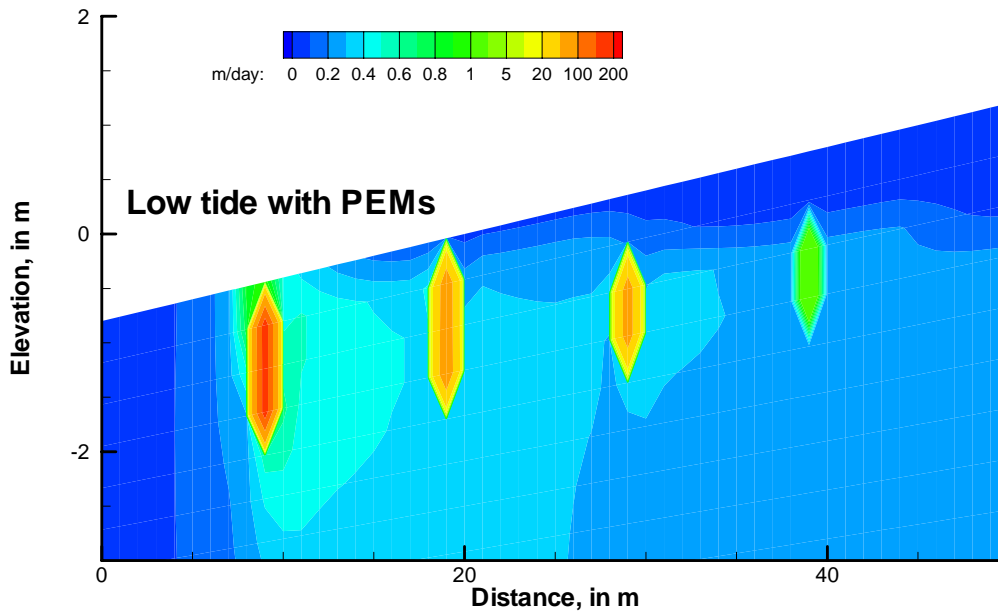
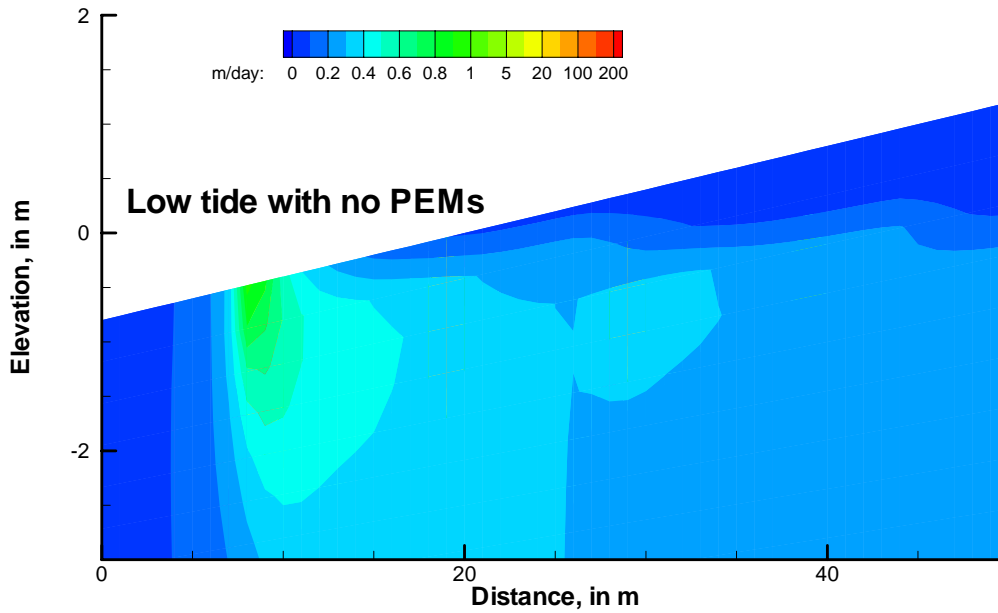


Figure 15 Close-up view of velocity distribution at low tide with and without PEMs. Units are in m/day. Figure 16 shows the tidal changes in the velocities at the mid-point of the four PEMs for the case without a gravel layer. Recall that the PEMs are located near the LWM, MSL, and HWM (one just below and one just above). There are peak flows of up to 0.2-0.3 cm/s in the two PEMs closest to

the sea, whereas the two other PEMs located above the MSL is much more inactive likely because the water table during low tides drops below the PEMs. It is also apparent that the two most active PEMs have peak flows at different times during the tidal cycle. At low tide it is the PEM near the LWM that is most active, and, vice versa, at high tide it is the PEM near the HWM (but below) that is most active.

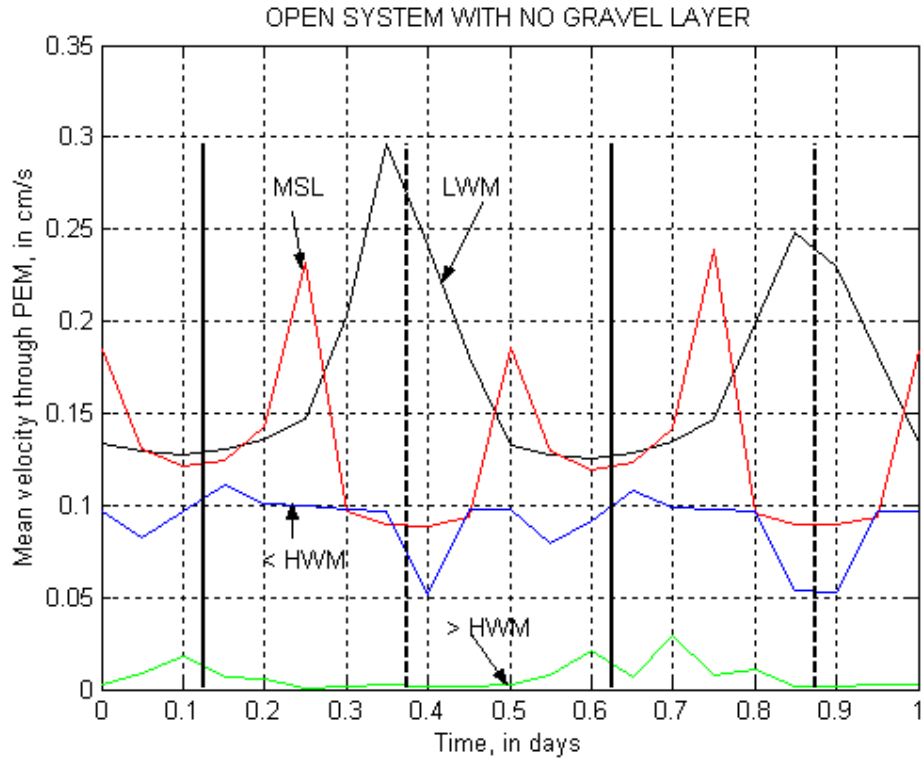


Figure 16 Simulated velocities at the mid-point of the four PEMs over a tidal cycle. Black line (x=9 m, LWM), red line (x=19 m, MSL), blue line (x=29 m, <HWM), and green line (x=39 m, >HWM). High and low tides are indicated with vertical solid and dashed lines, respectively.

3.2 Flow balances

Figure 17 and 18 show the simulated results for an open system without and with PEMs. The freshwater flux is on the order of $2.5 \text{ m}^2/\text{day}$ entering the beach at low tide and $-1.0 \text{ m}^2/\text{day}$ leaving the beach at high tide for the homogeneous case without PEMs. These fluxes increase slightly when including a gravel layer and PEMs because of the increased bulk permeability of the aquifer.

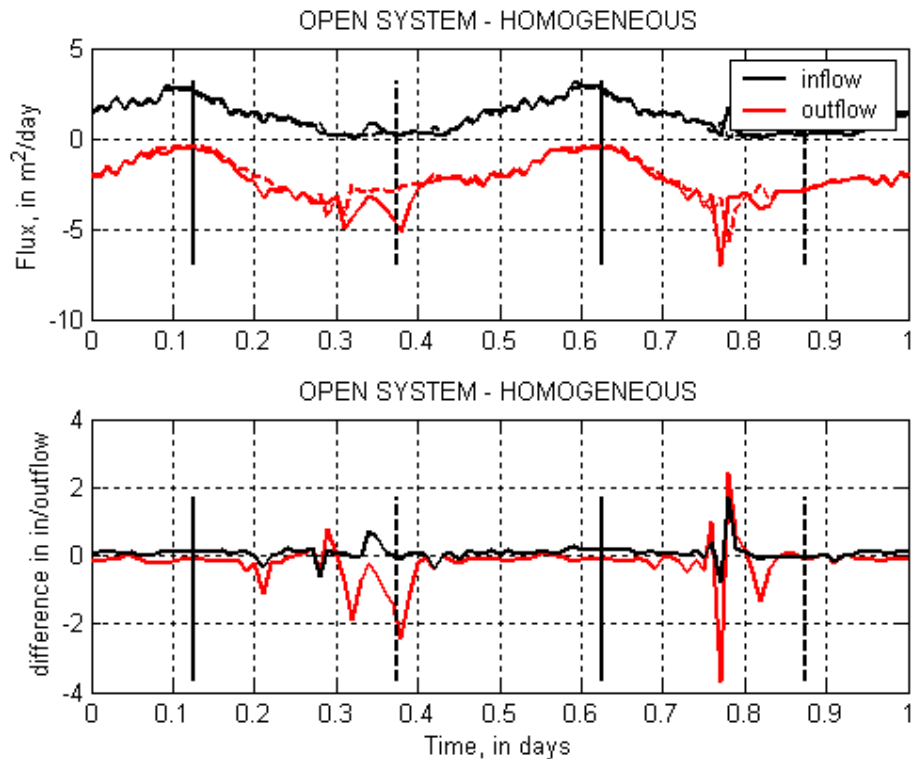


Figure 17 Simulated inflow and outflow in beach section (see Figure 1) for an open system with no gravel layer. Top figure, simulations with PEMs are shown with solid lines, simulations without PEMs with dashed lines. Bottom figure, shows differences in inflow and outflow with and without PEMs. High and low tides are indicated with vertical solid and dashed lines, respectively.

The smallest (least negative) outflow occurs during high tide and the highest during low tide. The bottom figure in Figures 17 and 18 show the differences between simulation without and with PEMs for inflow as well as for outflow. In the case of a homogeneous beach (Figure 17) one can note that the in- and outflows are not identical over a tidal cycle, e.g. outflow is clearly different at the two times in between low and high tide. The reason for this is not known precisely, but can be related to numerical difficulties because the boundary condition in the tidal zone is continuously changing from a fixed head boundary to that of an only outflow seepage boundary. This can be the cause of the small (non-symmetric) bumps in the curves for the simulation without PEMs. The simulations with PEMs show greater fluctuations in the in- and outflows. As shown in Figure 3 the water table moves up and down along the PEMs during a tidal cycle. This causes a very complicated flow field around the PEMs (see also Figures 9-10 and 14), which leads to greater oscillations.

Nevertheless, Table 2 shows the integrated in- and outflow for homogeneous case. The in- and outflows represent the area under each curve in Figure 17 (top figure). The differences in flows have been calculated, where a positive difference means that flow is greater with PEMs. A negative flow means less flow with PEMs. For the homogeneous beach the PEMs cause both greater inflow and outflow. The inflow increases from 1.16 m²/day to 1.25 m²/day, ie. 0.09 m²/day, or about 7%. Outflow increases by 0.21 m²/day or about 10%. So more water flows out than flows in. The difference (0.21-0.09=0.12 m²/day) is approximately 5-10% of inflow/outflow.

	Inflow (m ² /day) – difference in %			Outflow (m ² /day) – difference in %		
	No PEM	With PEM	Difference	No PEM	With PEM	Difference
Homogeneous (Figure 17)	1.16	1.25	7	-2.09	-2.30	10
Gravel Layer (Figure 18)	1.64	1.74	6	-2.79	-2.69	-3
Gravel Layer w. no connection (Figure 20)	1.37	1.49	9	-2.62	-2.36	-10
“Silt” Layer 0.1*K (Figure 21)	1.17	1.27	8	-1.88	-1.98	6
“Clay” Layer 0.01*K (Figure 22)	0.97	1.34	37	-1.69	-1.75	4
2 Gravel layers (Figure 24)	1.95	1.89	-3	-3.07	-3.19	4

Table 2 Summary of simulations showing inflow and outflow.

In the case with a gravel layer the increase in inflow is about the same, however the outflow is now smaller with PEMs than without. Thus, there is a negative influence of the PEMs. These differences are small when compared to the total in- or outflows.

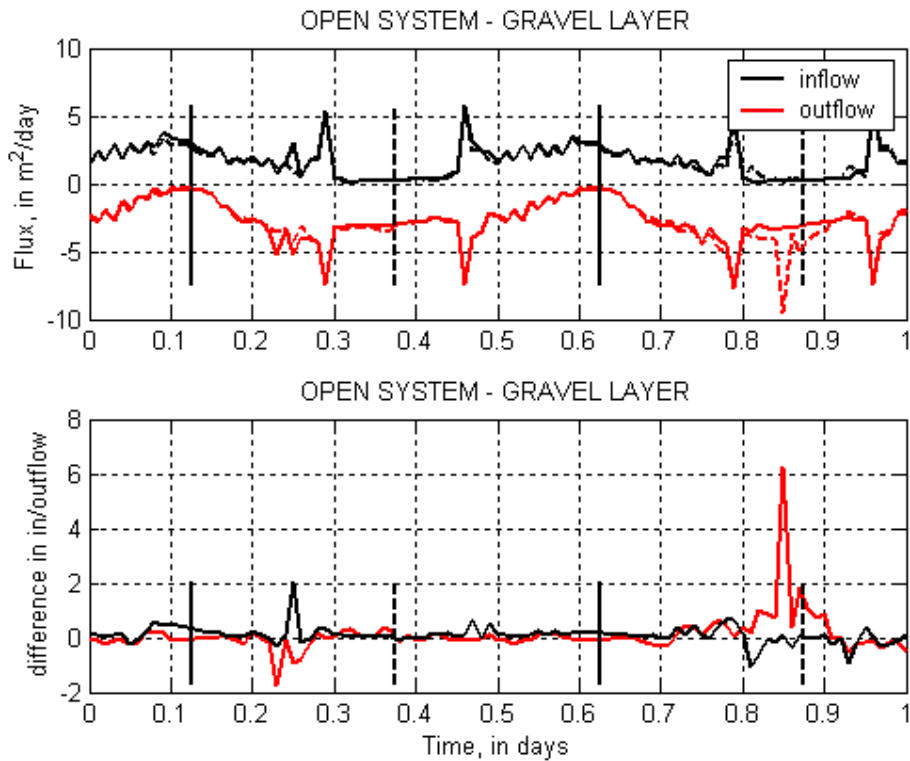


Figure 18 Simulated inflow and outflow in beach section (see Figure 1) for an open system with a gravel layer. Top figure, simulations with PEMs are shown with solid lines, simulations without PEMs with dashed lines. Bottom figure, shows differences in inflow and outflow with and without PEMs. High and low tides are indicated with vertical solid and dashed lines, respectively.

Figure 19 shows the ratio of the sum of the total flows through the 4 PEMs vs. the absolute value of the net inflow and outflow to the sea (magnitude of inflow minus outflow). This is for the case without a gravel layer. The flow through one PEM is simply calculated as $Q=V \cdot A$, where V is the mean velocity of the 3 nodes representing a PEM and A is the cross-sectional area of the pipe. The PEMs transport a lot of water, approximately 50% of the net inflow/outflow. Inflow is very low at low tide so here one can say that the PEMs almost transport all of the water eventually discharging to the sea. However, it is important to remember that it is not the same as saying that the PEMs discharge directly to the sea. Instead one can say that water is quickly routed vertically one meter before again being transported much more slowly through the porous media. For example, Figure 15 shows very high absolute velocities in the PEM near the low tide but also increased velocities in the porous medium right above the PEM. At high tide it is much more difficult to interpret the results since, as Figure 10 shows, there is both inflow and outflow.

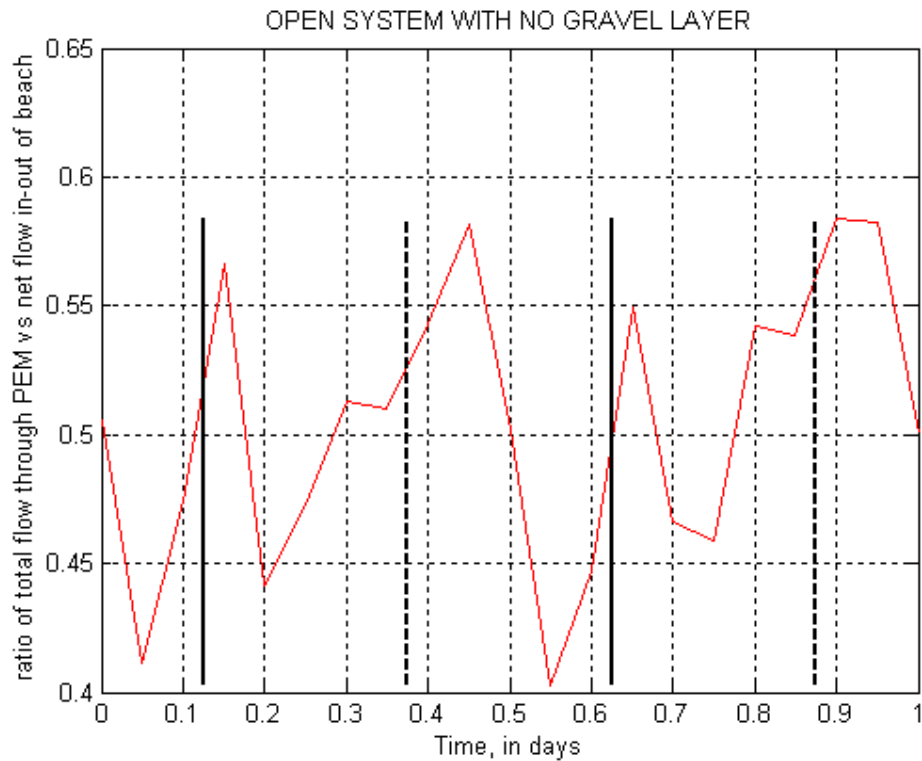


Figure 19 Ratio of total sum of flow through four PEMs vs total outflow through beach. High and low tides are indicated with vertical solid and dashed lines, respectively.

3.3 Effect of disconnecting the gravel layer from the sea

In this set of simulations the gravel layer is disconnected from the sea by removing the three gravel cells in the top row (see Figure 1), thus, these three cells now consist of sand. Figure 20 shows that this has a negative effect on the draining (outflow) capacity of the PEMs. At low tide the simulations with PEMs discharge less when compared to the case without PEMs. It is not entirely clear why this happens. One explanation can be that at low tide only two PEMs are active, the two most upstream PEMs are now located in the unsaturated zone. The majority of the outflow is captured by the two active PEMs, so instead of discharging directly to the sea over a short distance groundwater flows up in one PEM and then transported laterally in the gravel layer for 5-10 m before again being released to the sand and finally to exit near where the low tide meets the beach.

Table 2 shows that the in- and outflows are reduced, but also that the existence of PEMs enhances inflow but restricts outflow.

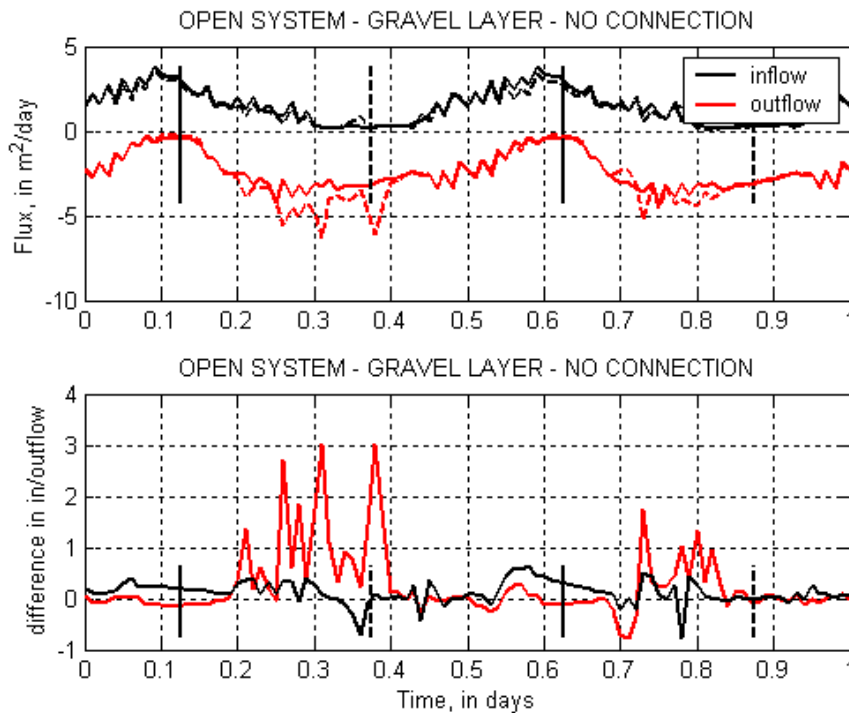


Figure 20 Simulated inflow and outflow in beach section (see Figure 1) for an open system with a gravel layer but with no connection to the sea. Top figure, simulations with PEMs are shown with solid lines, simulations without PEMs with dashed lines. Bottom figure, shows differences in inflow and outflow with and without PEMs. High and low tides are indicated with vertical solid and dashed lines, respectively.

3.4 Low-permeable layers

Two sets of simulations were conducted, where the hydraulic conductivity of the layer was decreased to 2.5 m/day and 0.25 m/day, which is a factor of 10 and 100 less than the hydraulic conductivity of the sand.

Figures 21 and 22 show the results of these simulations. The gravel layer is now no longer a “gravel” layer but rather a silt/clay layer that lies as a cap beneath the beach in the tidal zone, where the discharge to the sea mainly occurs. The PEMs therefore will penetrate this capping layer allowing water to access the sea more easily. The figures show that this will both lead to increased inflow and outflow. With a “silt” layer approximately just as much water flows in as flows out, Table 2. With a “clay” layer up to more than 37% now flows in with PEMs, while the increased outflow is much less. The PEMs therefore have a negative effect. One explanation can be the density effect where the pipes are more active.

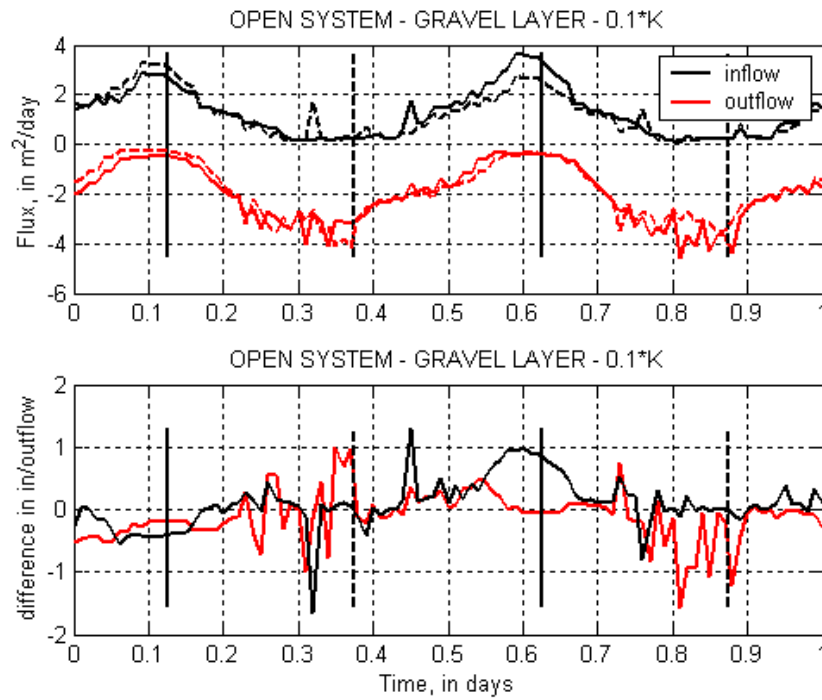


Figure 21 Simulated inflow and outflow in beach section (see Figure 1) for an open system with a “silt” layer with a $K=2.5$ m/day (factor of 10 less than the K in the sand). Top figure, simulations with PEMs are shown with solid lines, simulations without PEMs with dashed lines. Bottom figure, shows differences in inflow and outflow with and without PEMs. High and low tides are indicated with vertical solid and dashed lines, respectively.

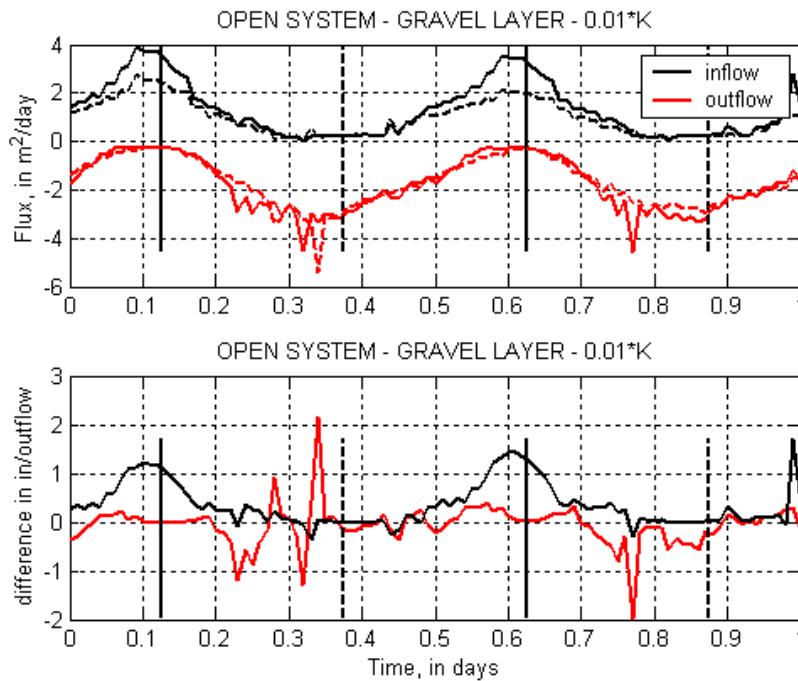


Figure 22 Simulated inflow and outflow in beach section (see Figure 1) for an open system with a “clay” layer with a $K=0.25$ m/day (factor of 100 less than the K in the sand). Top figure, simulations with PEMs are shown with solid lines, simulations without PEMs with dashed lines. Bottom figure, shows differences in

inflow and outflow with and without PEMS. High and low tides are indicated with vertical solid and dashed lines, respectively.

3.5 Effect of having several gravel layers connected by PEMS

Figure 23 shows the case with two gravel layers and extended PEMS. These are now 2 meters long. The upper layer is the same as before and connects to the sea. The PEMS connect the two gravel layers.

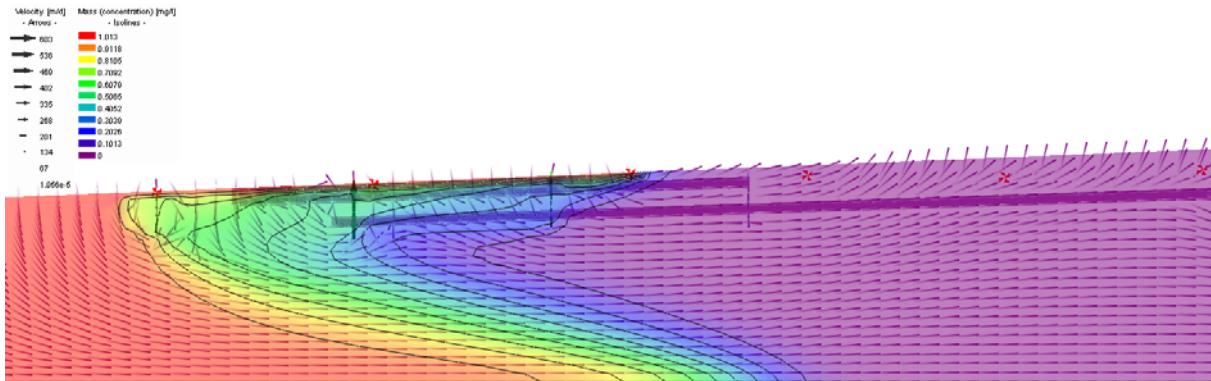


Figure 23 Simulated saltwater distribution and flow (high tide) in the case with two gravel layers and PEMS.

Figure 23 shows that both layers are active in transporting water at high tide. It is also clear that the saltwater distribution is affected.

Figure 24 shows the simulated in- and outflow. As before the PEMS both cause extra inflow and outflow. However, this time the net inflow is less with PEMS, while net outflow is increased. The PEMS therefore have a positive effect, albeit very small when compared with the absolute magnitude of in- and outflow.

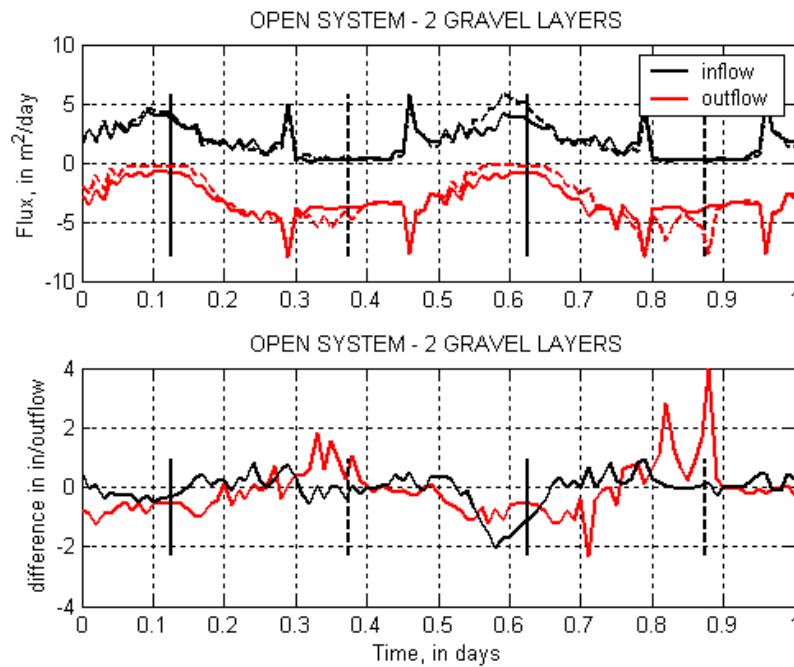


Figure 24 Simulated inflow and outflow in beach section (see Figure 1) for an open system with two gravel layers, an upper gravel layer identical to that in Figure 1 and a layer 1 m below, which is not connected to the sea. The PEMs have been extended to cross both layers. Top figure, simulations with PEMs are shown with solid lines, simulations without PEMs with dashed lines. Bottom figure, shows differences in inflow and outflow with and without PEMs. High and low tides are indicated with vertical solid and dashed lines, respectively.

3.6 Effect of tides

The effects of the tides have been investigated by running the model to steady-state using the open system and a sea level of 0 m corresponding to MSL (however, corrected for freshwater head).

Flux (m ² /day)	Gravel		No gravel	
	No PEMs	With PEMs	No PEMs	With PEMs
Inflow	0.86	1.16	0.44	0.84
Outflow	-2.01	-2.32	-1.26	-1.68

Table 3 Steady inflow and outflow

The presence of a gravel layer increases both inflow and outflow. The PEMs cause a higher inflow and outflow with approximately the same amount. The changes caused by the PEMs are generally high 13-53% but the net result is about zero change in the two systems (i.e., just as much higher inflow as outflow).

3.7 Comparing different scenarios

Figure 25 shows the simulated saltwater fluxes (inflow and outflow, g/day) through the beach. It was not possible to compute water fluxes in this way; however the absolute value of the Darcy fluxes across the beach face is discussed in Section 3.8. The balance only accounts for flow through the nodes which connects to the sea, i.e., from the HWM and seawards. The figure shows three systems; homogeneous beach, a beach with a gravel layer, and a beach with a clay layer.

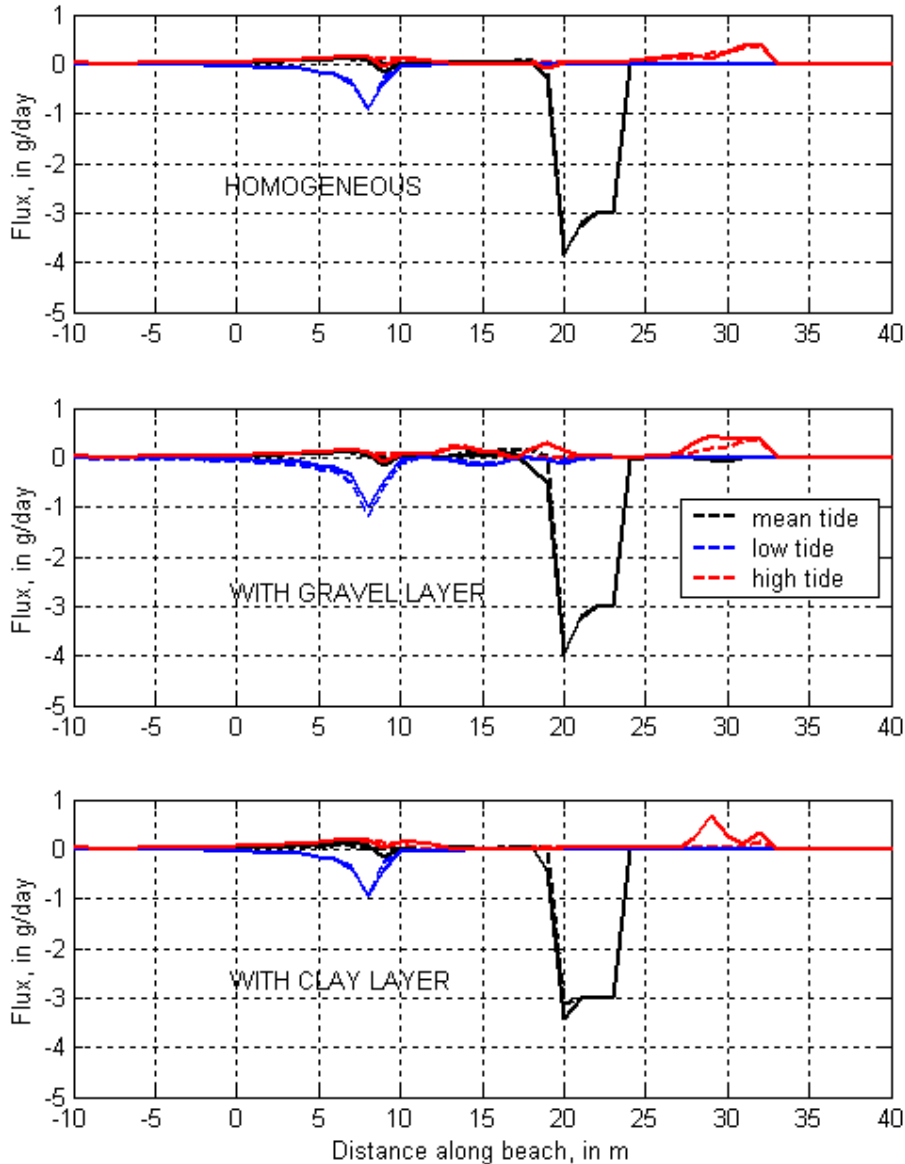


Figure 25 Simulated inflows (positive) and outflow (negative) through the beach at nodes that connect with the sea. The solid and dashed lines represent simulations with and without PEMS, respectively.

Three things may be noted; (1) at low tide the gravel layer actually results in slightly higher outflow, (2) at the mean tide the PEMs generally results in a slight increase in outflow, and (3) at high tide the PEMs significantly increases inflow. However, the differences between the simulations with and without PEMs are small.

Figure 26 shows the same results but now for the case of a steady system, i.e., no tides. Only the cases with a homogeneous beach and a beach with a gravel layer were simulated.

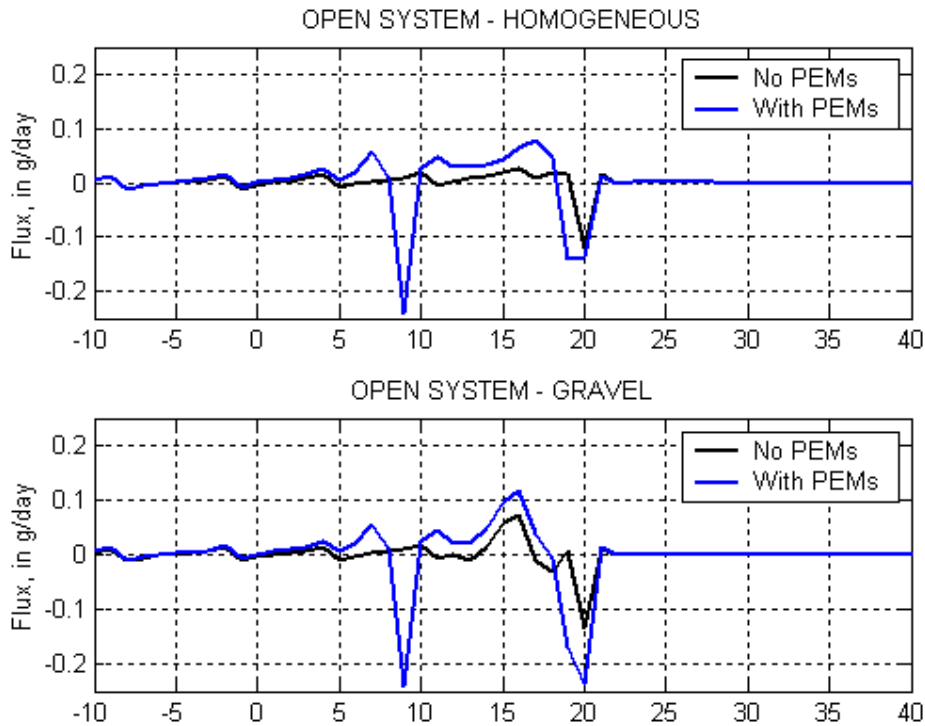


Figure 26 Simulated steady inflows (positive) and outflow (negative) through the beach at nodes that connect with the sea. The black and blue lines represent simulations without and with PEMS, respectively.

Again, inflow is positive, and outflow is negative. Remember that MSL cuts the beach at $x=20$ m. From the case with no PEMs it can be seen that outflow takes place near MSL and is constrained to a zone with a width of about 1-2 m. The effects of the PEMs at $x=9$ and 19 m are clearly seen resulting in an extra outflow, but also a wider discharge zone, now 2-3 m. However, the PEMs also induce extra inflow. The gravel layer also has an effect mostly by causing an extra inflow where the layer cuts the beach ($x=13-16$ m). The tides do not have a similar effect of the width of the discharge or recharge zone.

3.8 Effect of PEMs on Darcy fluxes and hydraulic gradients across beach face

The effects of the PEMs on the water fluxes and hydraulic gradients across the beach face have been investigated for the homogeneous case. This means that it is mainly when the tide gets above 0.3 m (near high tide) that inflow will take place (excluding that due to density effects).

Feflow can compute the absolute value of the water (Darcy) flux (q) in any line segment given by the user, e.g., along the beach face. Since it is the absolute value, it tells nothing about direction. The gradient can be computed from Darcys law;

$$q = K * i$$

where K is the hydraulic conductivity (here 25 m/d) and i is the gradient in the direction of flow. Thus in the present case;

$$i = \frac{q}{K} = \frac{q}{25}$$

With salt transport the hydraulic gradient i represents that of forced and free convection. Forced convection is caused by hydraulic gradients (any direction), free convection is caused by density differences (vertical).

Figure 27 shows the simulated salt distribution and flow field without PEMs at high tide. This figure corresponds to Figure 6.

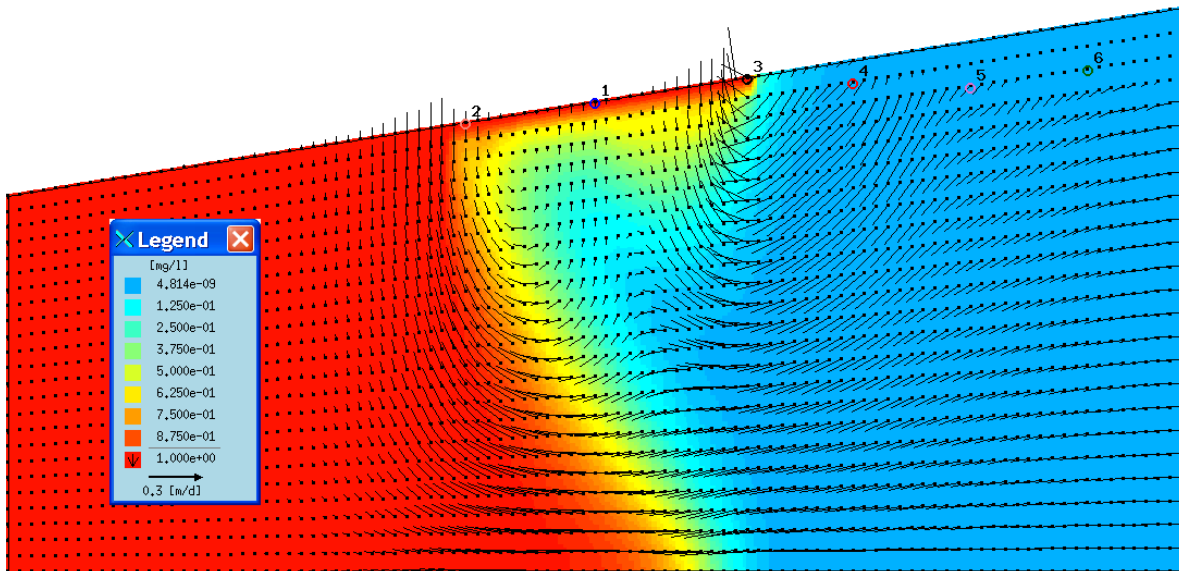


Figure 27 Simulated salt distribution and flow field for the homogeneous case without PEMs (high tide) and a fixed head of 0.3 m at the right boundary

Notice that there are two areas with inflow and an area in between with outflow. The areas with inflow have Darcy fluxes around 0.3 m/d (see velocity scale in legend), thus the inflow gradient is around 0.012. Figure 28 shows the situation at mean tide, when the tide is going from high to low tide (draining). Discharge is out of the beach right at MSL. The maximum outflow Darcy flux is around 1 m/d, thus the maximum outflow gradient is around 0.04. Figure 29 shows the situation at low tide. Flow is outwards mainly at the LWM. The maximum outflow Darcy flux and gradient is slightly smaller than at mean tide.

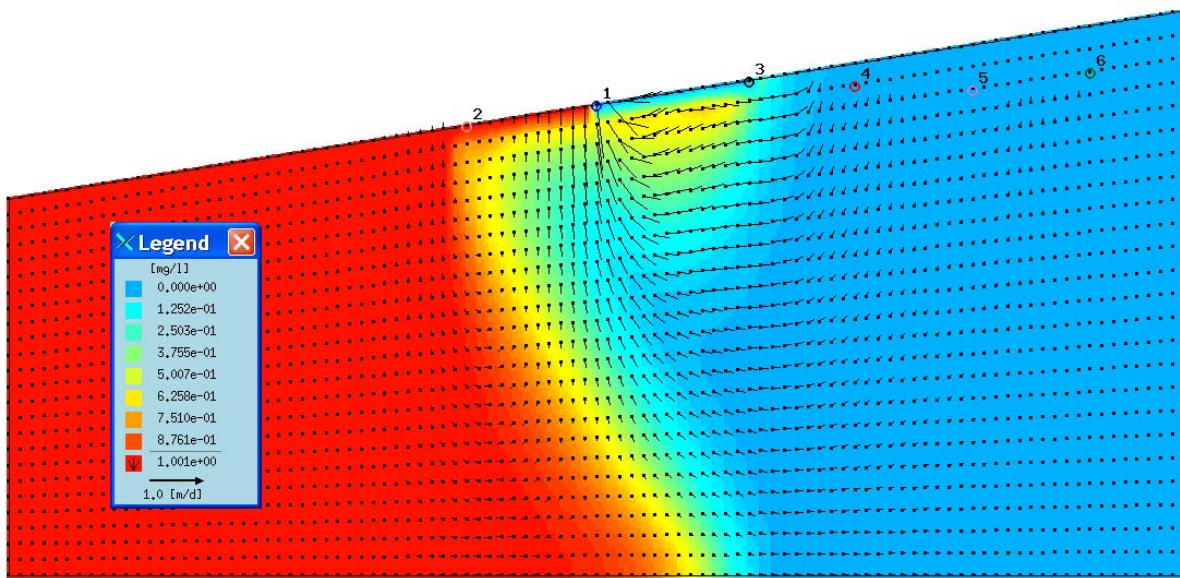


Figure 28 Simulated salt distribution and flow field for the homogeneous case without PEMs (mean tide) and a fixed head of 0.3 m at the right boundary

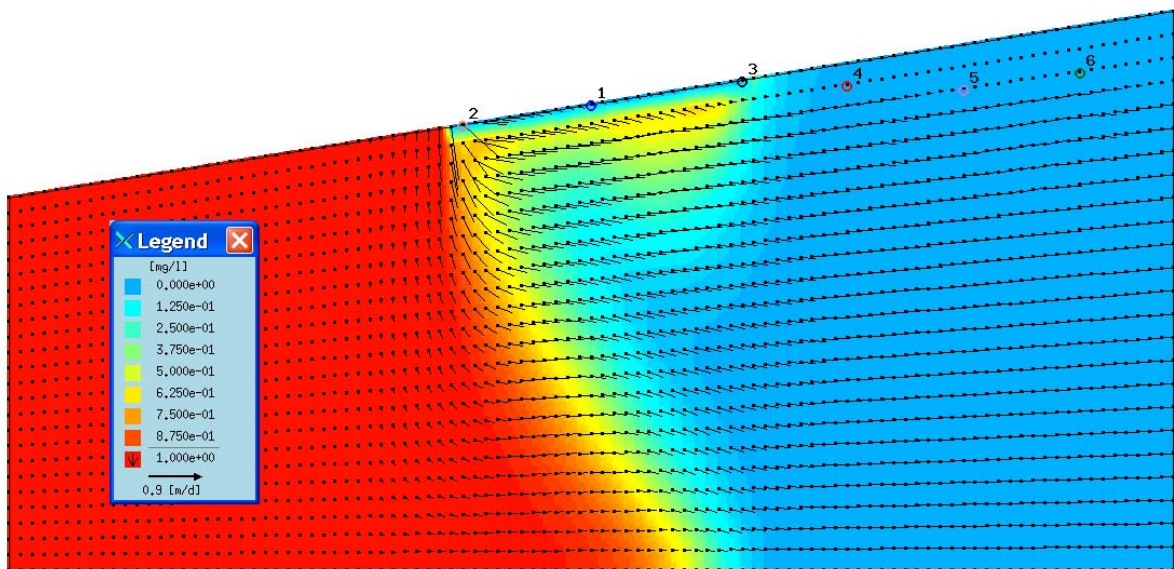


Figure 29 Simulated salt distribution and flow field for the homogeneous case without PEMs (low tide) and a fixed head of 0.3 m at the right boundary

Similar figures for the cases with PEMs are not shown simply because the velocities in the PEMs are so much higher than outside in the porous medium; instead refer to Figures 9 and 10. Recall that at high tide flow was outward across the beach face right at the three PEMs in the tidal zone due to the observed circulation around a PEM.

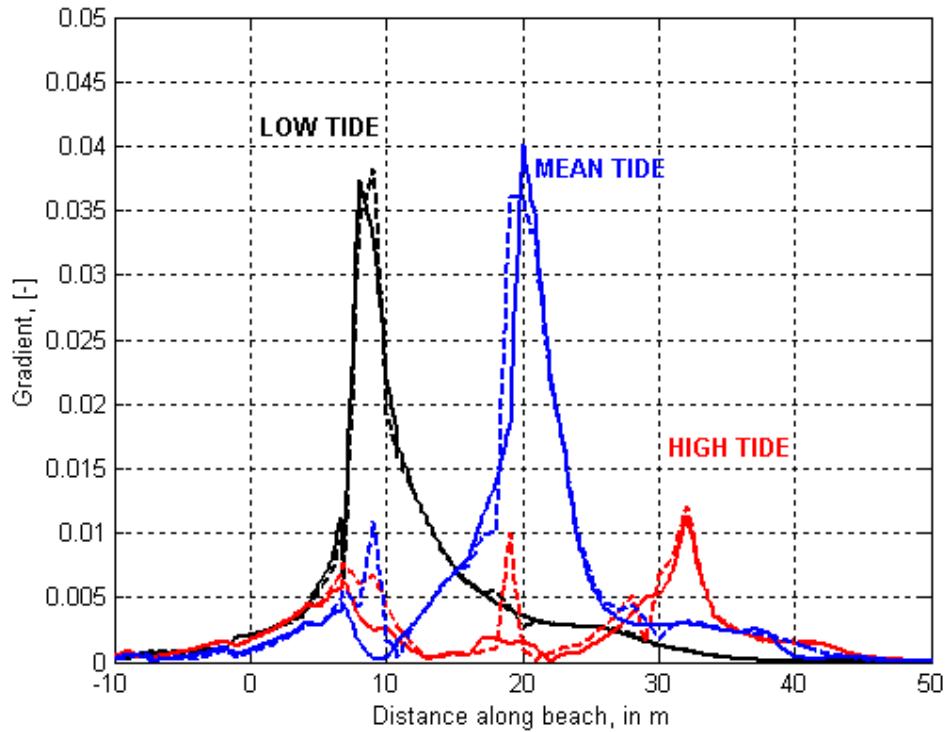


Figure 30 Absolute values of hydraulic gradients across beach face at low, mean and high tide. The gradient says nothing about direction.

Figure 30 shows the absolute values of the hydraulic gradients across the beach face at low, mean, and high tide. The gradients are calculated based on the simulated absolute values of the water fluxes at the beach face. Two sets of simulations are shown; solid and dashed lines are without and with PEMs, respectively. Recall that direction is not indicated, thus this figure can only be understood by also referring to Figures 27-29. In the cases of low and mean tide flow is always out, however at high tide flow is in and out. Referring to the high tide case with no PEMs, the two peaks at 8 m (LWM) and 33 m (HWM) correspond to the inflow shown in the figure above, and the peak in-between at around 20 m (MSL) is outflow. The gradients are highest in the cases of low and mean tide, around 0.35-0.04. The area of outflow tracks the receding water table very closely. However, notice that in the cases with PEMs (dashed lines) the two peaks are off-set by about 1-2 m. This is because the PEMs are located at 9 and 19 m, 1 m off the point where the low and mean water table cuts the beach. The PEMs therefore mainly redirects the point of maximum outflow during a receding tide. It is also seen that the PEM near the low tide line actually generates a higher gradient (and outflow) than in the case without a PEM. Otherwise, the simulated results are very alike. In the high tide case the two simulations are almost identical except that the three main active PEMs in the tidal zone (9, 19, and 29 m) generate outflow and not inflow due to the observed circulation. Thus, the not only are the gradients different, also direction.

3.9 Simulations with higher and lower inflow

Two other sets of simulations were carried out; (a) with a higher freshwater inflow using a fixed head of 1.5 m at the upstream boundary and (b) with a lower freshwater inflow using a fixed head of 0 m (=MSL). The two cases are compared with the base case (fixed head of 0.3 m) in Figure 31 for the situation of a homogeneous beach.

Freshwater inflow oscillates between 6.8-8 m²/day in the higher inflow case and oscillates between -2.4 to +1.2 m²/day in the lower inflow case. The high negative outflow in the last situation occurs because at high tide there is a significant head gradient inland.

Figure 31 demonstrates that the freshwater inflow has a significant impact on the saltwater distribution, here shown at high tide. With higher inflow the saltwater wedge is pushed back, while the lower inflow case results in significant buoyancy effects because a denser fluid overlies a lighter fluid that is almost stagnant.

Table 4 and 5 summarize the results. The most interesting cases are the high inflow case with a clay layer and all low inflow cases. When a clay layer is present in a high inflow case there is a significant relative extra inflow when the PEMs are present, see also Figure 25. Outflow is also higher when including PEMs. In absolute fluxes the outflow is much greater, 0.79 m²/day, in comparison to only 0.22 m²/day for inflow. Overall the PEMs therefore have a positive effect, on the order of 10%.

	Inflow (m ² /day) – difference in %			Outflow (m ² /day) – difference in %		
	No PEM	With PEM	Difference	No PEM	With PEM	Difference
Homogeneous	1.09	1.17	7	-8.45	-8.56	1
Gravel Layer	1.17	1.20	3	-9.50	-9.55	0.6
Clay Layer	0.72	0.94	31	-7.16	-7.95	11

Table 4 Summary of simulation results with a higher freshwater inflow using a fixed head of 1.5 m.

In the low inflow case the presence of PEMs have a positive effect ranging from 9-29%. Again, when a clay layer is present there is a notable effect increasing drainage by 29%, while changes in inflow are small. This is interesting as the base case, Table 2, showed that the clay layer scenario only had a minor impact on the drainage effect of the PEMs. However, outflow is now very small, about half of the inflow.

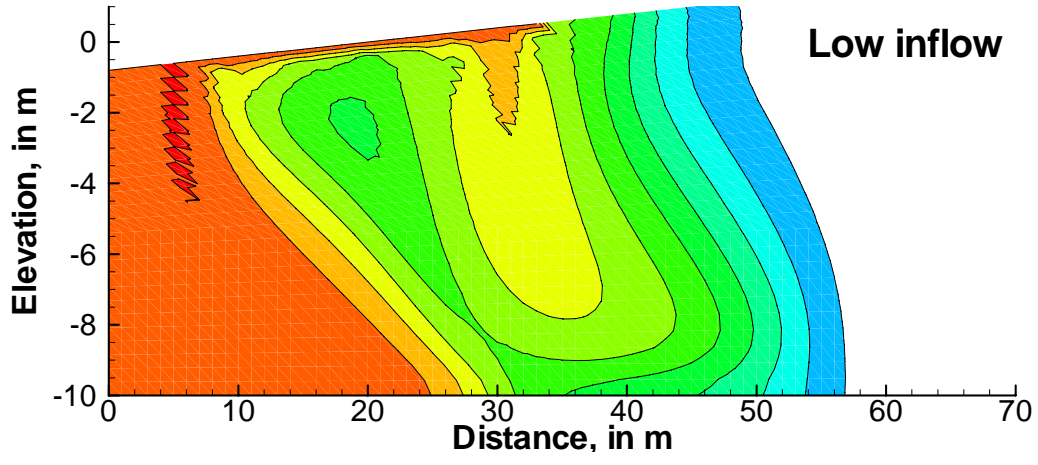
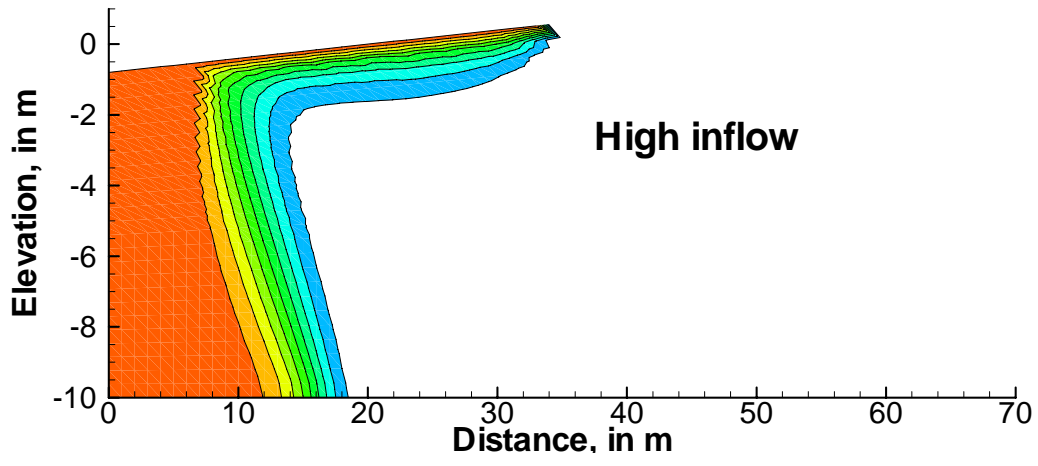
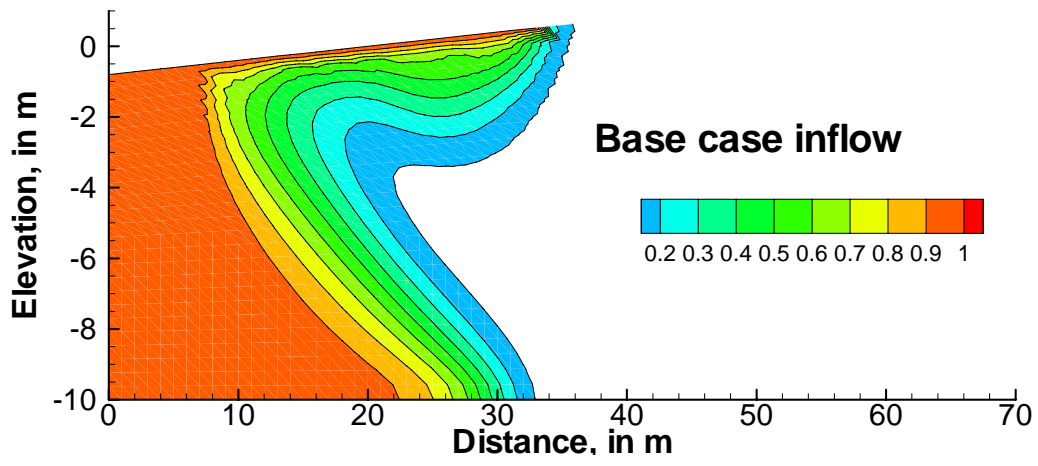


Figure 31 Simulated salt distribution at high tides for three case of freshwater inflow.

	Inflow (m ² /day) – difference in %			Outflow (m ² /day) – difference in %		
	No PEM	With PEM	Difference	No PEM	With PEM	Difference
Homogeneous	2.12	2.09	-1	-1.11	-1.25	13
Gravel Layer	2.84	2.86	1	-1.91	-2.08	9
Clay Layer	1.71	1.78	4	-0.79	-1.02	29

Table 5 Summary of simulation results with a lower freshwater inflow using a fixed head of 0.0 m.

The effect of the PEMs on the hydraulic gradients across the beach face were investigated for the low inflow case ($h=0.0$ m at right boundary). When the tide rises from mean to high tide, inflow will be generated due to a gradient.

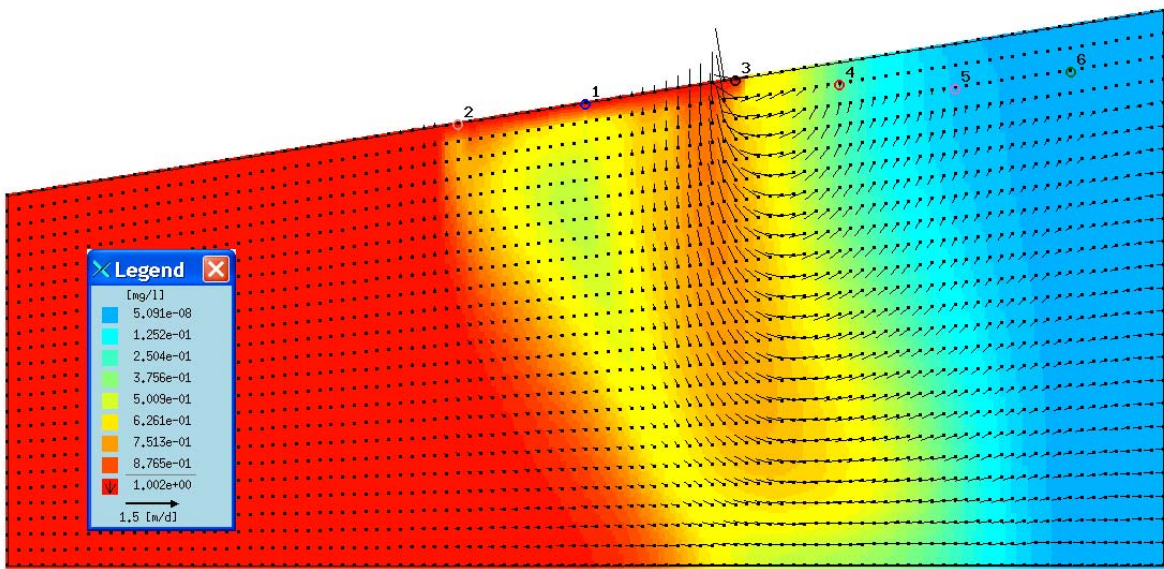


Figure 32 Simulated salt distribution and flow field for the homogeneous case without PEMs (high tide) and a fixed head of 0.0 m at the right boundary

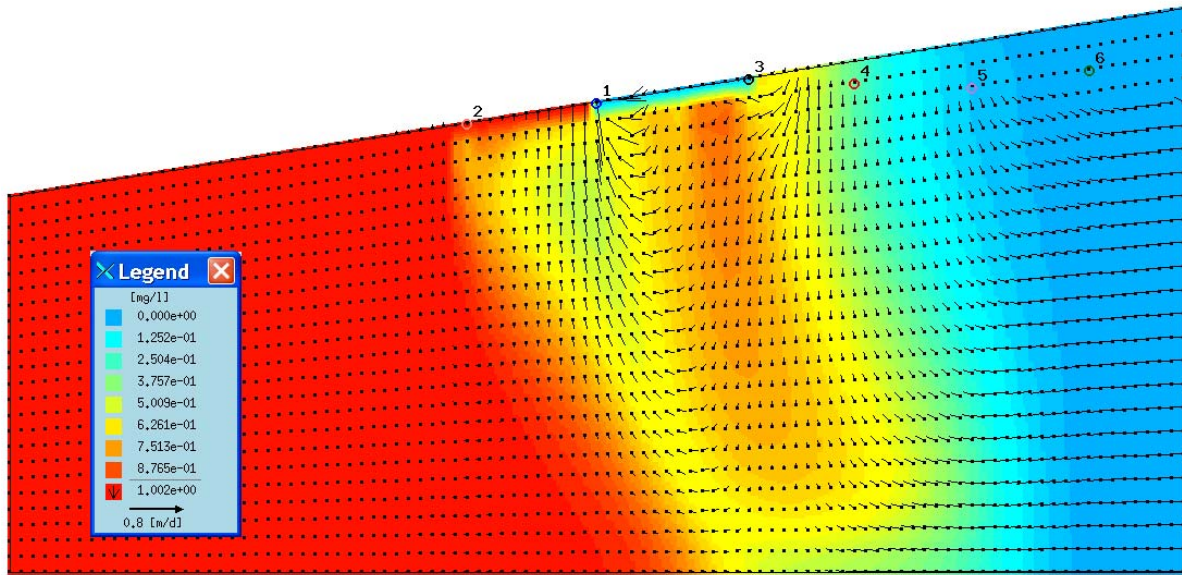


Figure 33 Simulated salt distribution and flow field for the homogeneous case without PEMs (mean tide) and a fixed head of 0.0 m at the right boundary

Figure 32 shows the simulated salt distribution and flow velocities. Inflow takes place near the HWM. The maximum Darcy fluxes are around 1.5 m/d or $i=0.06$. Figure 33 shows the situation at mean tide. Density effects are greatest at this point. The flow field is rather complicated, where (dense) water either flows from the zone between MSL and HWM towards the right boundary or towards the MSL. Maximum Darcy flux is outward at MSL, but only half of that during high tide.

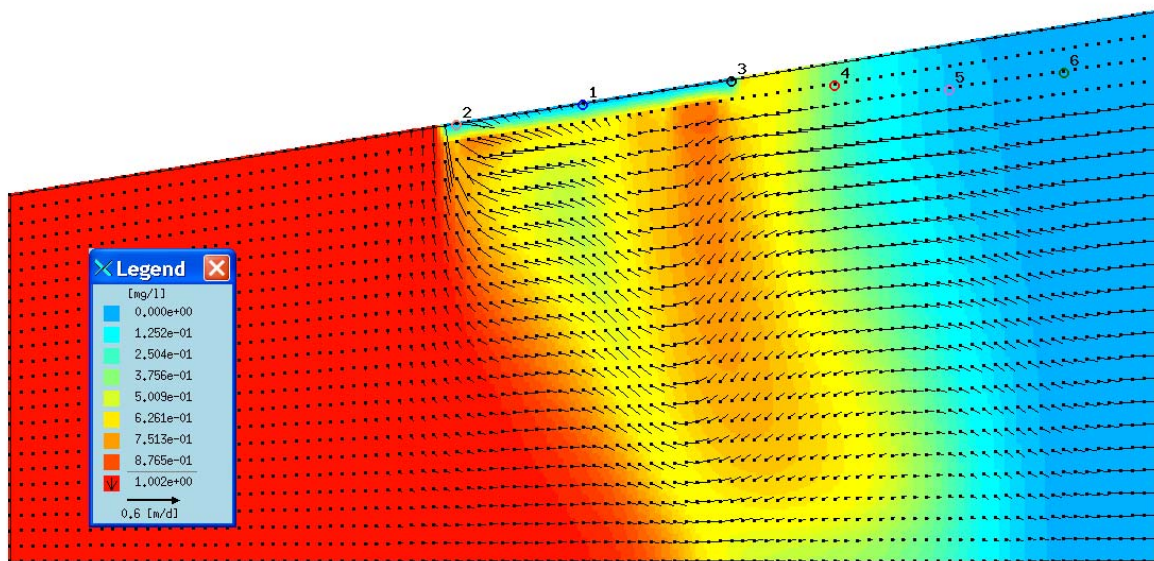


Figure 34 Simulated salt distribution and flow field for the homogeneous case without PEMs (high tide) and a fixed head of 0.0 m at the right boundary

Figure 34 shows the situation at low tide. The salt water distribution affects the flow pattern below the tidal zone, but, generally flow is outward near the LWM, with a smaller gradient than at mean tide.

Figure 35 shows the calculated hydraulic gradient across the beach face. The (inflow) gradient at high tide is now higher than in the case with a high freshwater inflow, almost 0.06. The effects of an outward gradient near the three active PEMs are still seen, although the effect of the PEM at $x=29$ m is less due to the relative stronger inflow. The (outflow) gradients in the low and mean tide cases are a little lower than in the case with higher freshwater inflow. The same phenomena with PEMs generating outflow in the PEMs away from the water table line is still seen.

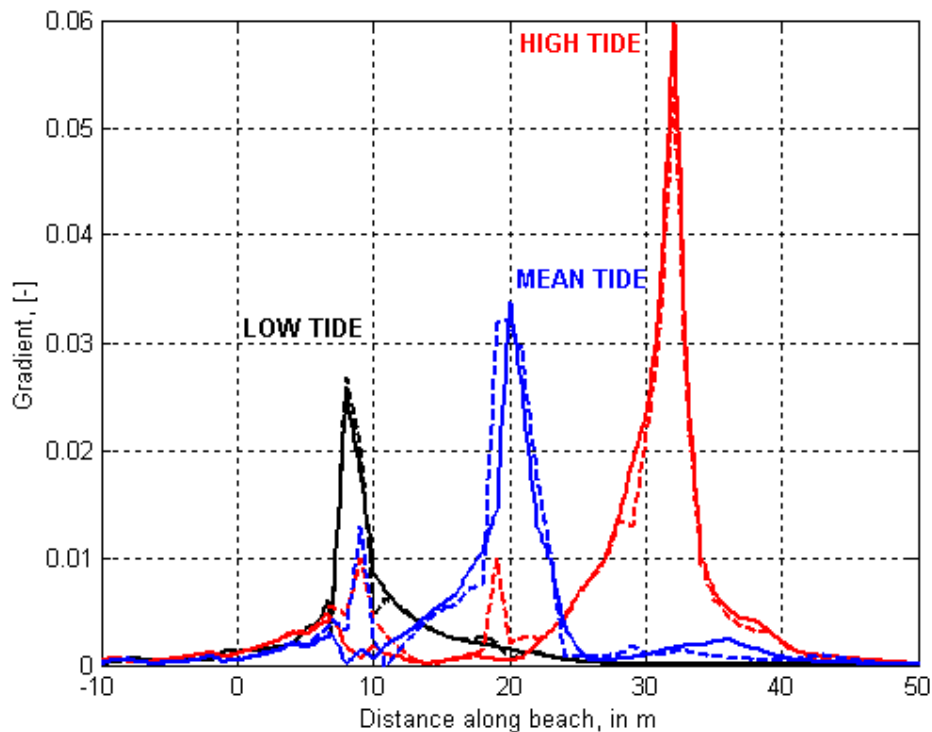


Figure 35 Absolute values of hydraulic gradients across beach face at low, mean and high tide. The gradient says nothing about direction.

3.10 Effect of depth of PEMs

The effects of placing the PEMs 1 m deeper in the coastal aquifer was investigated for the homogeneous case.

Figure 36 shows the simulated hydraulic gradients, which again is compared to the situation without PEMs. The main difference is now at high tide. At low and mean tides the results are almost similar.

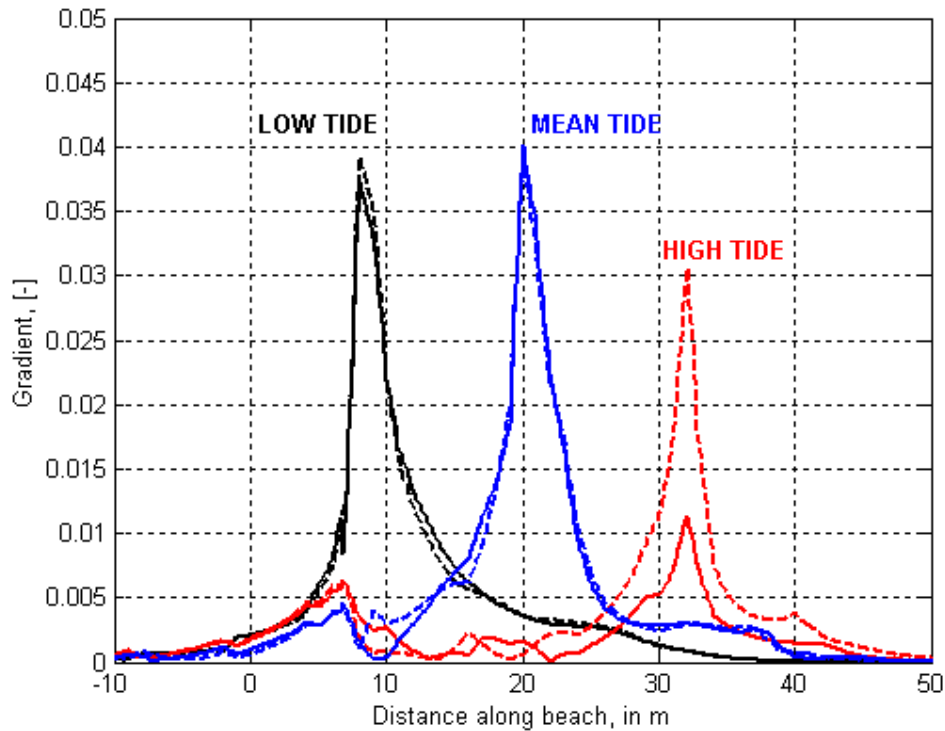


Figure 36 Absolute values of hydraulic gradients across beach face at low, mean and high tide for the case with PEMs located 1 m deeper. The gradient says nothing about direction.

The differences at high tide are caused by the circulation now taking place deeper in the coastal aquifer when the PEMs are located 1 m deeper. A new set of simulations were conducted with a refined mesh around the PEMs. Figure 37 and 38 show the results for the two situations near the PEM at the HWM; Figure 37 where the PEMs are located from 0.5-1.5 m below the beach face, and Figure 38, where they are located 1 m deeper.

The circulation pattern is clear in both cases, but in Figure 37 it results in flow outwards at the beach face. When the PEMs are located one meter deeper the flow is inward at the PEM. Thus, the observed differences in Figure 36 are primarily due to a change in flow direction.

If the two most inland PEMs were excluded then the two sets of simulations in Figure 36 were almost identical.

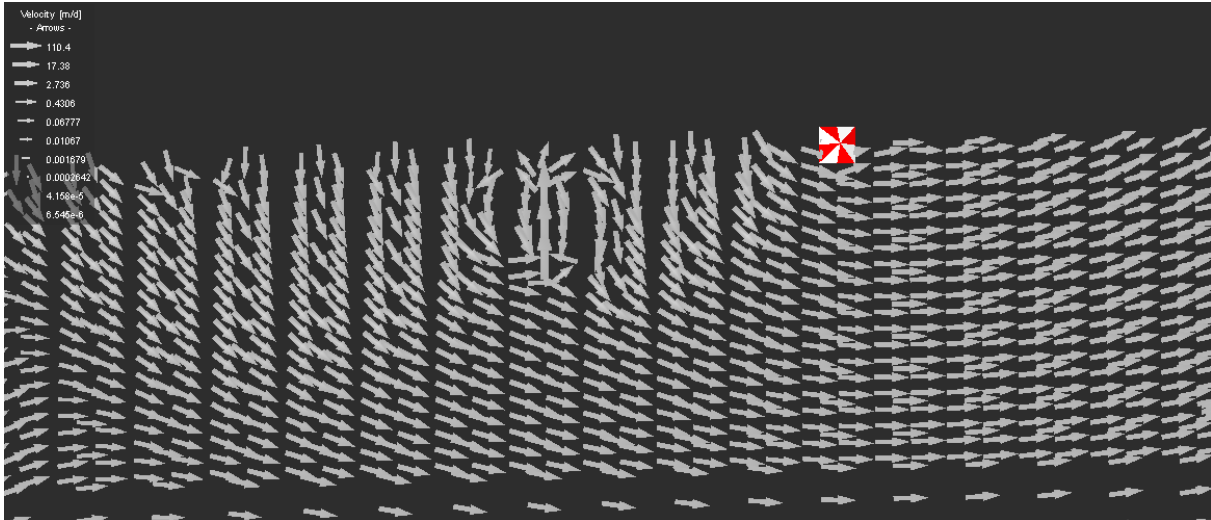


Figure 37 Simulated *log* velocities in the case of PEMs located from 0.5-1.5 m below beach face. The marker shows the location of the HWM. The PEM with circulation is to the left of the HWM.

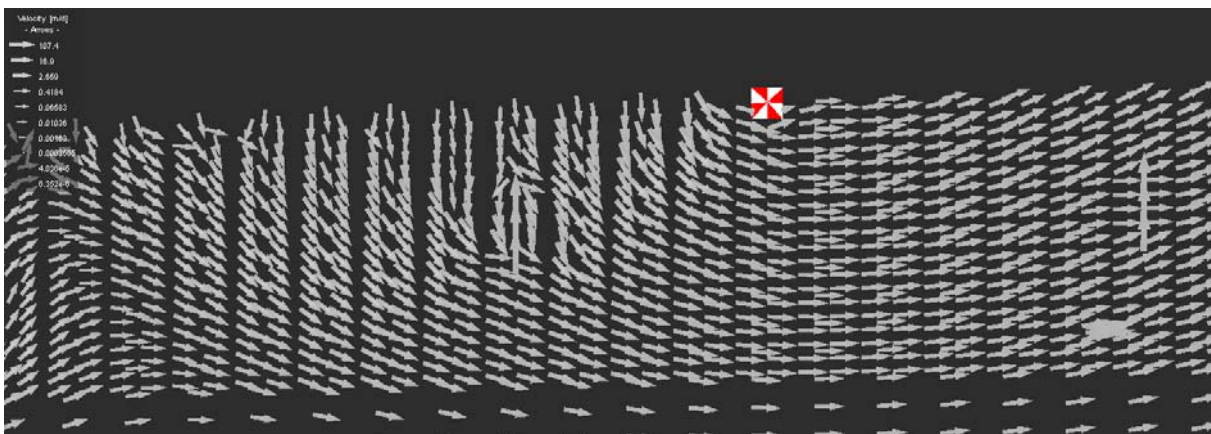


Figure 38 Simulated *log* velocities in the case of PEMs located from 1.5-2.5 m below beach face. The marker shows the location of the HWM. The PEM with circulation is to the left of the HWM.

4. Conclusions

The effects of tides on groundwater flow and salt transport have been simulated in an idealized cross-section using the numerical model Feflow. The conceptual model was created in order to mimic the conditions at Holmsland on the West coast of Denmark (Engesgaard, 2006). Thus, the numerical model is two-dimensional. The model simulates variably-saturated flow with density-dependent flow and salt transport. Furthermore, it allows for a seepage condition at the tidal zone.

Several scenarios were simulated. The base case assumes an open system with a freshwater inflow corresponding to what might be realistic at the field site. Several other freshwater inflows were simulated with higher inflow and lower inflow. The numerical study compares the results without

and with PEMs in order to investigate the effects of including PEMs. The PEMs were simulated as pipes with a much higher hydraulic conductivity and were placed in the beach approximately according to how real PEMs are installed. It is only the slotted screen of a PEM that is included. The effect of having the PEM connect to a gravel layer or penetrate a lower-permeable layer was investigated. Finally, the effects of having a gravel layer connect to the sea or not were evaluated.

The numerical model still only resembles field conditions in an approximate way;

- It is a 2D model, which means that 3D flow phenomena around the PEMs (pipes) are not included. More importantly the pipes will over-represent the effects in the 2D model. The width of the model is implicitly assumed to be 1 m, while in reality the diameter of the pipes in the model is only 0.08 m.
- The discretization in the vertical direction (approximately 0.5 m) controls the thickness of the gravel/silt/clay layers. Whether these layers are thinner or thicker is not known.
- The hydraulic conductivity of the gravel layer in the base case is rather high. One may speculate whether this is a reasonable assumption given that small sand grains might fill up the pore space between the gravel yielding a hydraulic conductivity that is more comparable to that of sand. The hydraulic conductivity of the silt/clay layers are realistic.
- The PEMs all connect with the layers, which of course is not necessarily the case in a real situation.

The following observations are made;

- There is a complicated flow field in the tidal zone, where the water table detaches from the beach and drops to below the PEMs. In almost all cases this results in a tidal response that is not symmetric, i.e., the observed fluxes are not the same at the two low/high tides during one tidal cycle. This could be the result of this non-linear behaviour of the water table dropping and rising along the length of the PEMs. The PEMs are active one by one as the tide rolls past a PEM. It was observed that the PEMs always carried water upward due to a circulation pattern where water enters the PEMs near the bottom and exits at the top. This seems intuitively correct at low tide, however it also occurs at high tide, where flow is also downward. This downward flow seeps into the PEMs and flows vertically upward.
- The PEMs have an effect on the salt distribution near the PEMs in the tidal zone. The PEMs transport a lot of water, for example approximately 50% of that discharging to the sea at low tide in the base case. However, this is not the same as saying that they increase discharge with this amount, because in reality they just move water to another area with sand or gravel. Flow inside the PEMs are of the order 0.2-0.3 cm/s.
- The PEMs allow water and salt to flow slightly more rapidly into and out of the beach. In most cases they have an effect both ways sometimes resulting in a negative effect of the PEMs, sometimes in a positive effect. Despite this, the effects (positive or negative) are generally small when compared with the integrated outward or inward flux during a tidal cycle. In the base case (homogeneous beach) the extra outflow caused by the PEMs is on the order of 5%. Only in the case with a very low freshwater inflow are the changes in in- and outflow higher than this.
- There seems to be a positive effect of the PEMs in the case where a clay layer is present (and connected to the sea and thus acting as a low-permeable barrier to flow). This effect is most pronounced in the high and low freshwater inflow case, while in the base case it is less apparent.

- The PEMs do not appear to increase the width of the discharge zone significantly. Only in the case of steady flow is the width increased from 1-2 m to 2-3 m.
- The effects of changing the hydrogeological conditions (gravel/silt/clay layer, freshwater inflow) have a larger impact on inflow and outflows across the beach than having PEMs or not.
- The depth of the PEMs has an effect on the fluxes/gradients at the beach face. If they are close to the beach face the circulation pattern means that flow is generally outward at the beach face. If they are located 1 m deeper flow the circulation pattern does not influence the gradients at the beach face and flow is inward.

5. References

- Engesgaard, P., Effect of vertical drains on tidal dynamics in beaches, report to KDI, June 2006, 2006.
- Robinson, C., L. Li, and H. Prommer, Tide-induced recirculation across the aquifer-ocean interface, *Water Resour. Res.*, 43, W07428, doi:10.1029/2006WR005679, 2007
- Robinson, C., L. Li, and D.A. Barry, Effect of tidal forcing on a subterranean estuary, *Ad. Water Resour.*, 30, 851-865, 2007
- Diersch, H.-J.G., FEFLOW 5.3, Users's Manual, WASY software, Institute for Water Resources Planning and Systems Research, 2006.
- Nielsen, P. (1990). Tidal dynamics of the water table in beaches. *Water Resour. Res.*, 26, 2127–2134.

Appendix 4: Undulations alongshore.

The observed accretion along the shore may stem either from the PEM-system or be due to natural coastal processes.

It is well known that a coast exposed to obliquely incoming waves can cause undulations in the beach-width. The scale of these undulations are typical: wavelength 1-4 km, amplitude 10-50 m, and down drift migration velocity: 50-500 m/year. Very large undulations along the Danish coast is for instance observed at Uggerby just East of Hirtshals, and at Gl. Skagen at the North tip of Jutland. At both locations, the coast are exposed to very obliquely incoming waves.

At Nymindegab, the angle between the coastline and the dominating incoming waves are in the neighborhood of 45 degrees, see figure 1, so also here it is most likely that large-scale undulations will exist.

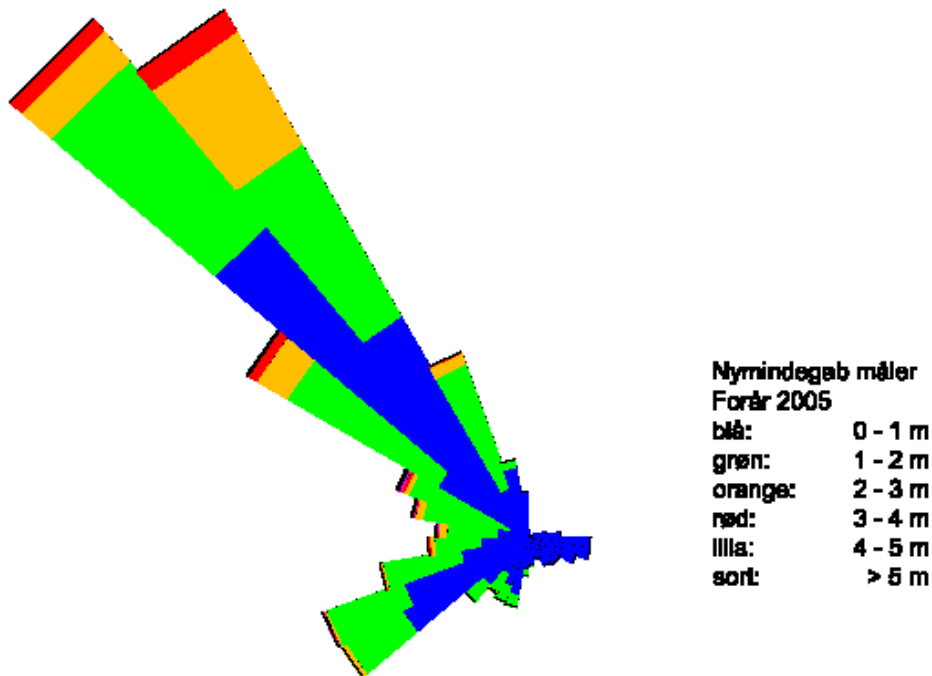


Figure 1A. Wave-rose based on spring measurements in 2005.

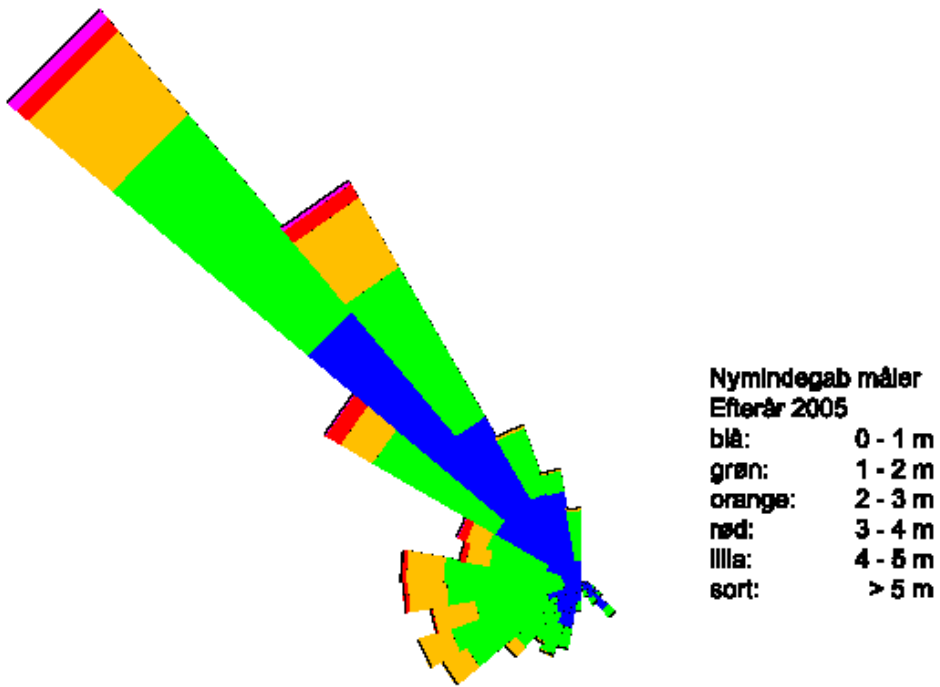


Figure 1B: wave-rose based on fall measurements in 2005.

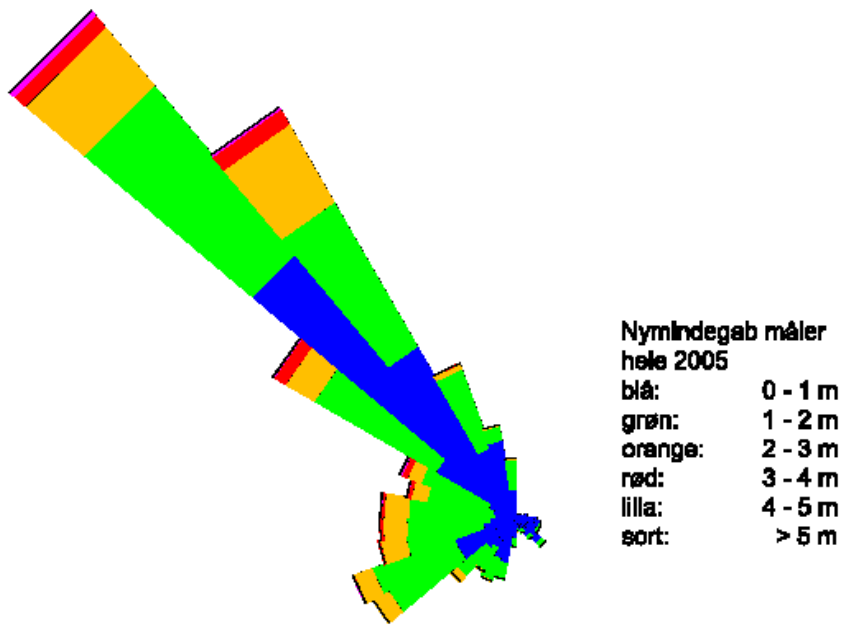


Figure 1C. Wave-rose including all measurements in 2005.

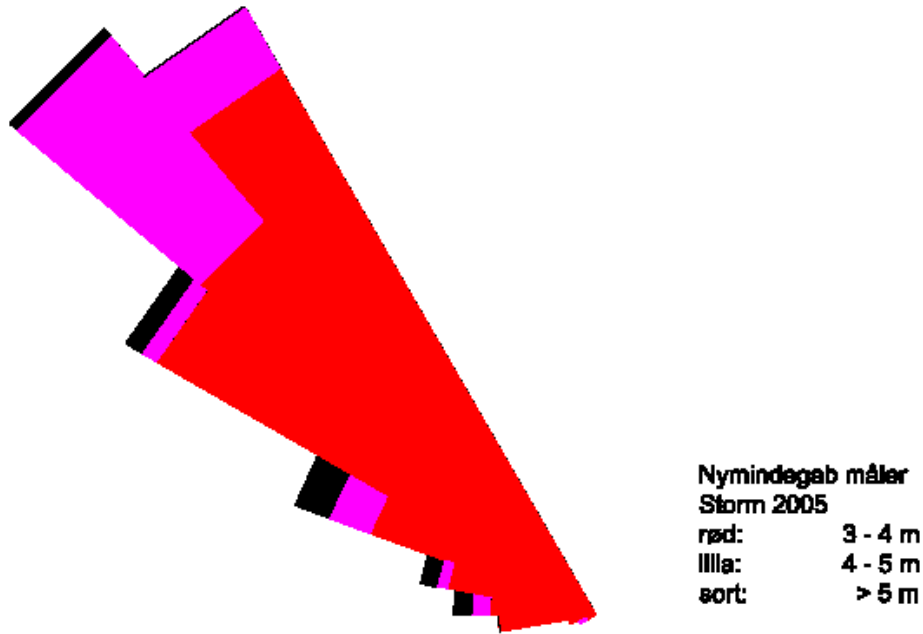


Figure 1D: Wave-rose: Storm waves: all waves larger than 3 m based on all measurements in 2005.

From figure 1 it further becomes evident that the sediment drift is in the Southern direction (with the wave climate shown in figure 1, the CERC-formula suggest an annual rate of around 2 million cbm).

By inspection of satellite-photos large-scale undulations can be identified, but their behavior (change of shape and migration) is quite stochastic and not so easy to identify during the relative short time of period of the present experiment.

Undulations have been observed at the location of the experiment also before the PEM-experiment was started, so the presence of undulations cannot only be due to the implementation of the PEM-system. Figures 2 a and b show the measured long shore variation in beach-width in May 2000 (yellow). August 2002 (blue plus brown) and September 2005 (blue plus dark blue). Also a fit with a polynomial is included in the figures. First of all, undulations can be detected from this figure. Secondly, they seem to migrate in the down drift (Southern) direction, around 1000-1300 meters during the 5 years. The wavelength of the very large undulations is around 6 km, and it is observed that the undulation which in year 2000 had its peak in "rør 1" now has been wider, while the other undulation, which was located on the border between "ref 2" and "rør 2" now has been narrower.

Kystliniebugtninger 2000-2002

Tegn. Nr. 2

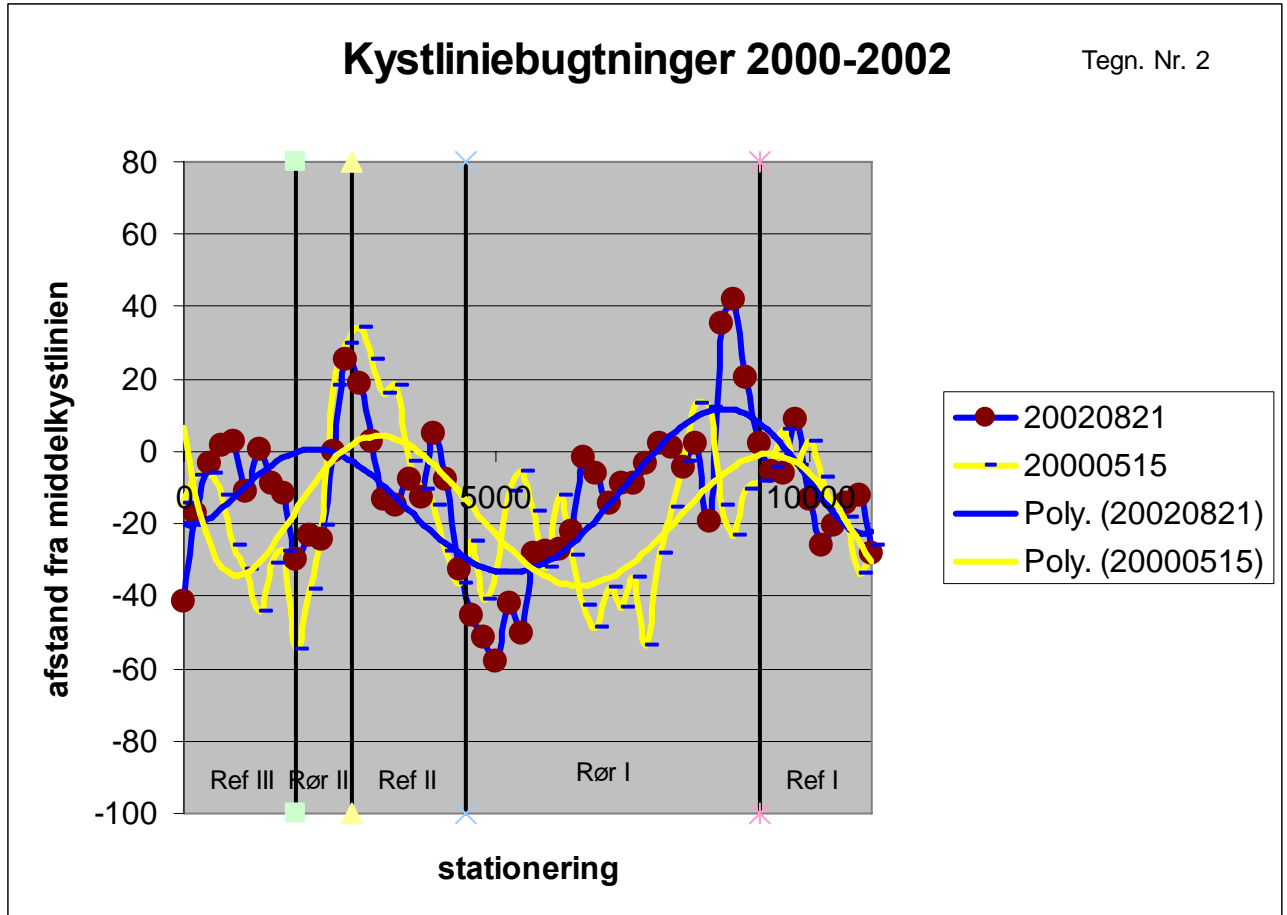


Figure 2a: Variation in beach width in two years from 2000-2002 (Produced by KDI).

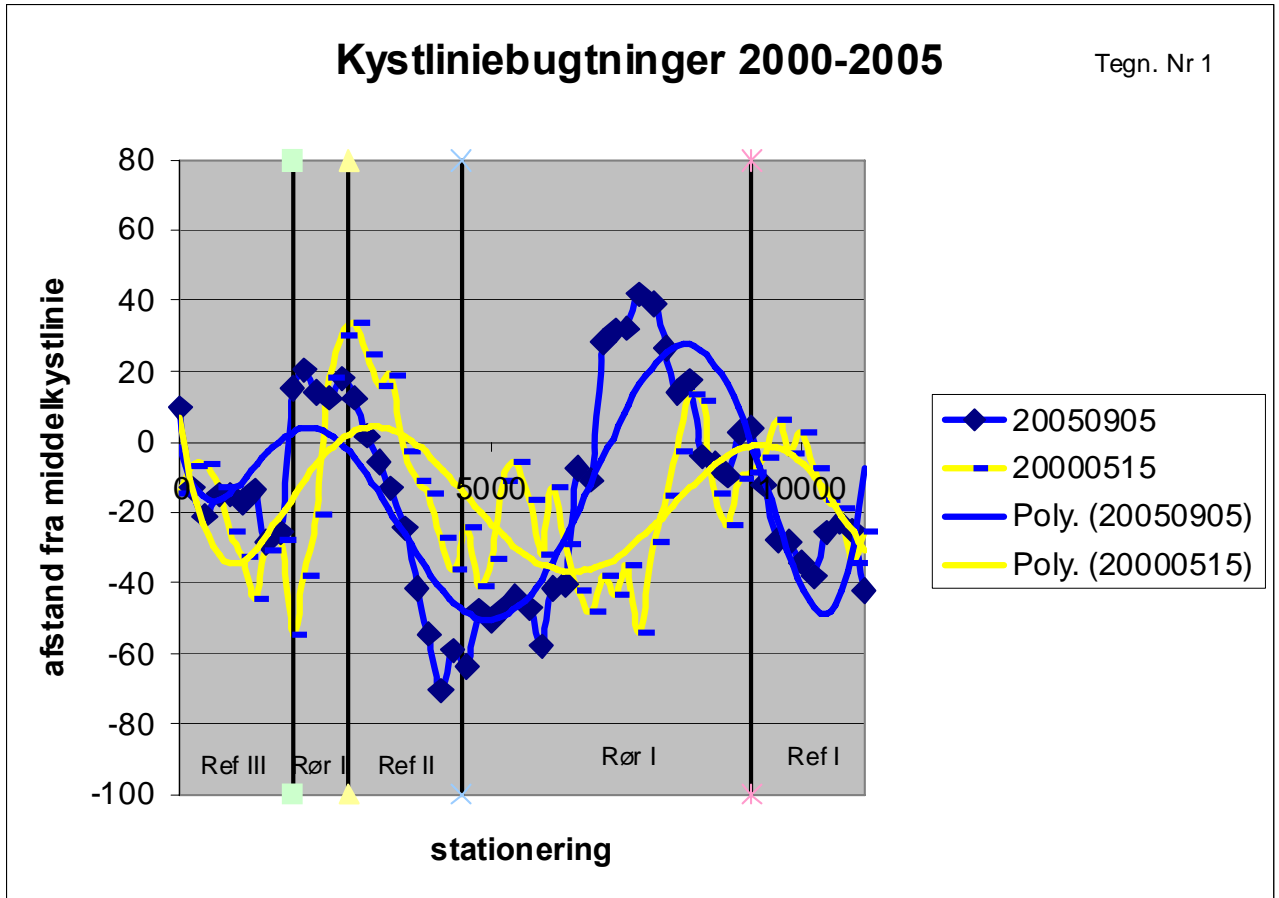


Figure 2b: Variation in beach width during five years from 2000-2005 (Produced by KDI).

The migration of the undulations will cause a rhythmic pattern of erosion and deposition along the coast as sketched in figure 2c.

The local variation in sediment transport q along the undulations with the shape $h=h(x)$ is given by

$$\frac{\partial q}{\partial x} = -T \frac{\partial h}{\partial t}$$

where T is the average thickness of the beach.

If we assume the undulations migrate with a steady shape and a migration velocity a , we have

$$h = h(x - at) \text{ and } \frac{\partial h}{\partial t} = -a \frac{\partial h}{\partial x}$$

so

$$\frac{\partial q}{\partial x} = aT \frac{\partial h}{\partial x}$$

If we take $a=250$ m/year and $T=2$ m, the accretion of the beach will be 100 cbm/year on a location, where the beach widens 10 meter over a 50 meter long distance, which is not unusually on the test site.

The average transport in one “long shore wave” is

$$q = \frac{1}{2} a \Delta W T$$

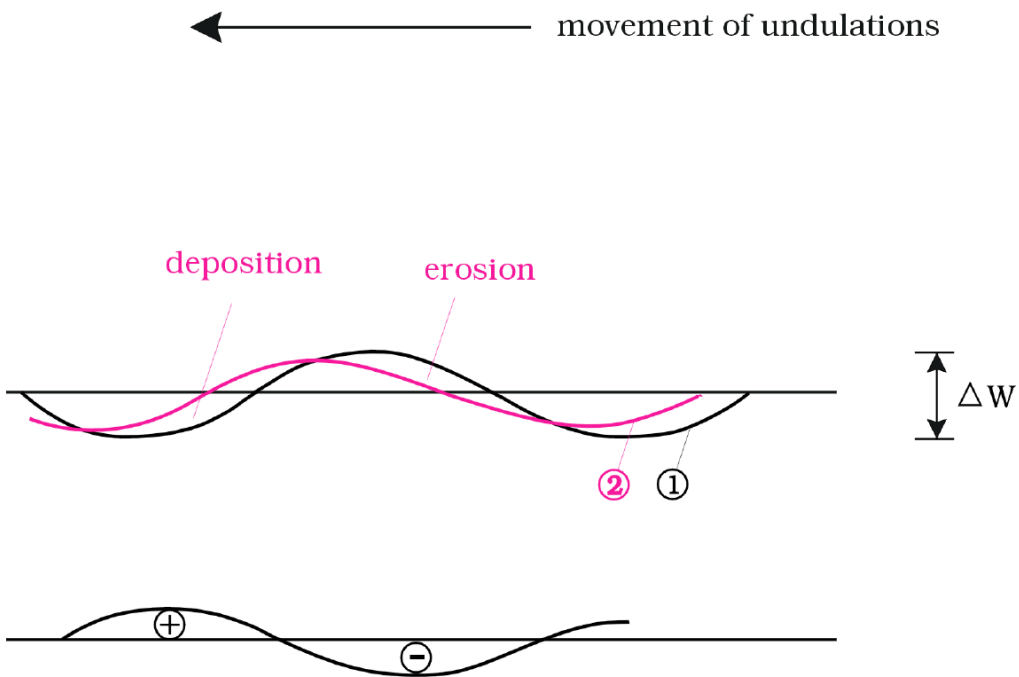


Figure 2c: Erosion and deposition pattern caused by migrating undulations. 2 is the undulation to a later time than 1.

where a is the velocity of the undulation and ΔW the difference in the beach width in between where it is widest and narrowest

As an example, let $a=250$ m/year, $T=2$ m and $\Delta W =80$ m. This gives an average transport equal 20000cbm/year due to the motion of an undulation.

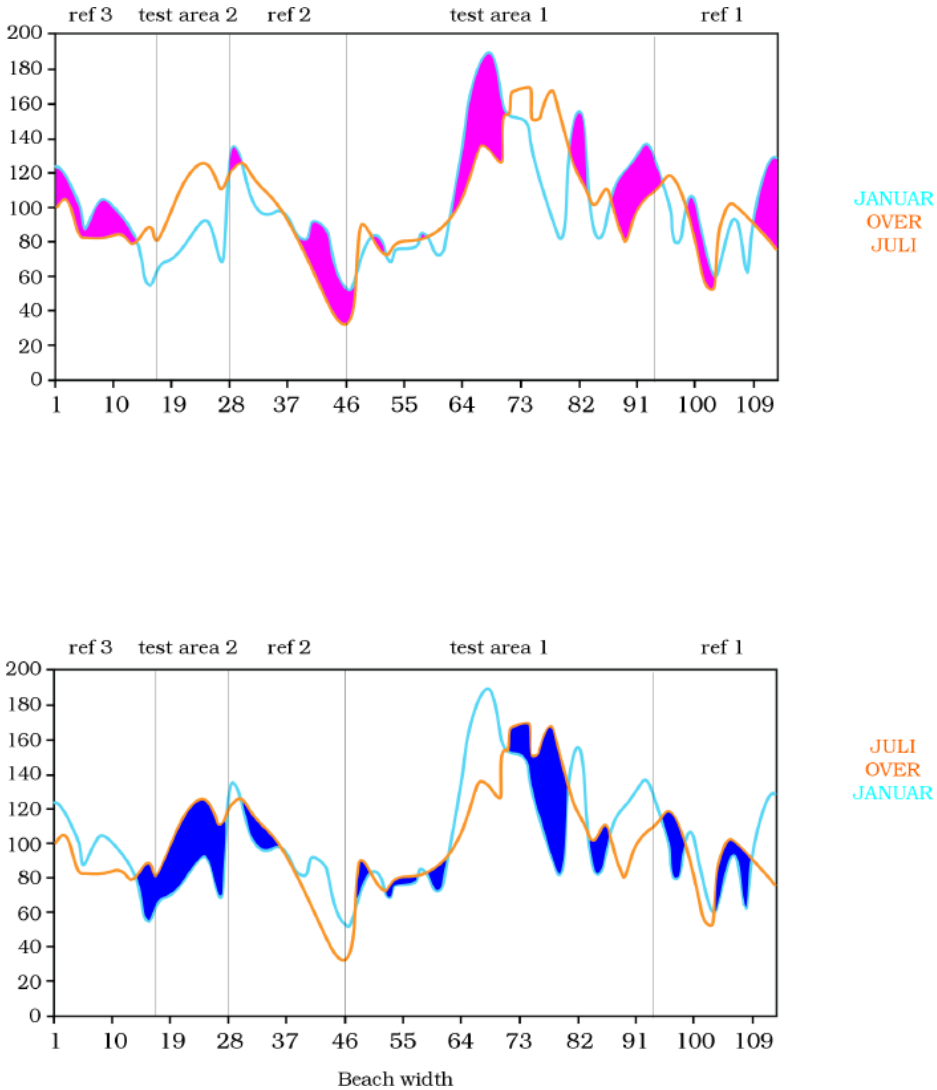


Figure 3A: Variation in beach width from January 2005 to July 2005. Pink: accretion. Blue: erosion.

DIFFERENCES IN BEACH WIDTH

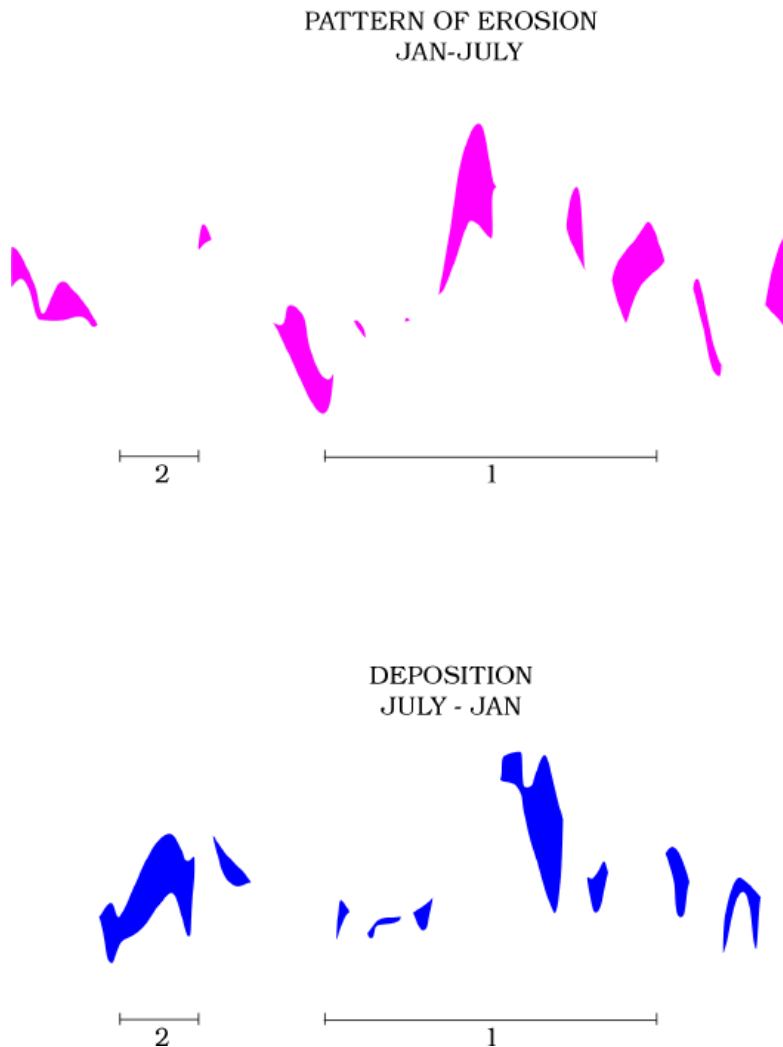


Figure 3B: Like figure 3A, but this picture clearly illustrate that area of erosion is not that different from area of deposition, and everything occur independently of the location of the tubes, at least in the large test area “rør 1”.

A picture like that sketched in figure 2c can to a certain extent be identified in the measurements. Figure 3A and B show the difference in beach width along the site developing during the first 6 months (January to July). The pattern of erosion and deposition is quite patchy due to a variety of different undulations but the tendency is like that sketched in figure 2c.

General observations from satellite-photos June 7 2005 and comparison with measured changes in beach width

Figures 4, 5 and 6 depict the satellite image along the test stretches. From these it is easy to get a visual feeling of the undulations shown in figure 2.

Figures 7 and 8 show the measured changes in the beach width during the first year of the test: Figure 7 shows the changes from January 2005 to April and July 2005 (Second and third “opmåling”), while figure 8 shows the similar change from January 2005 to January 2006.

North of reference 1, figure 4: The beach is quite narrow, and it seems like it has become even narrower during the last 12 months.

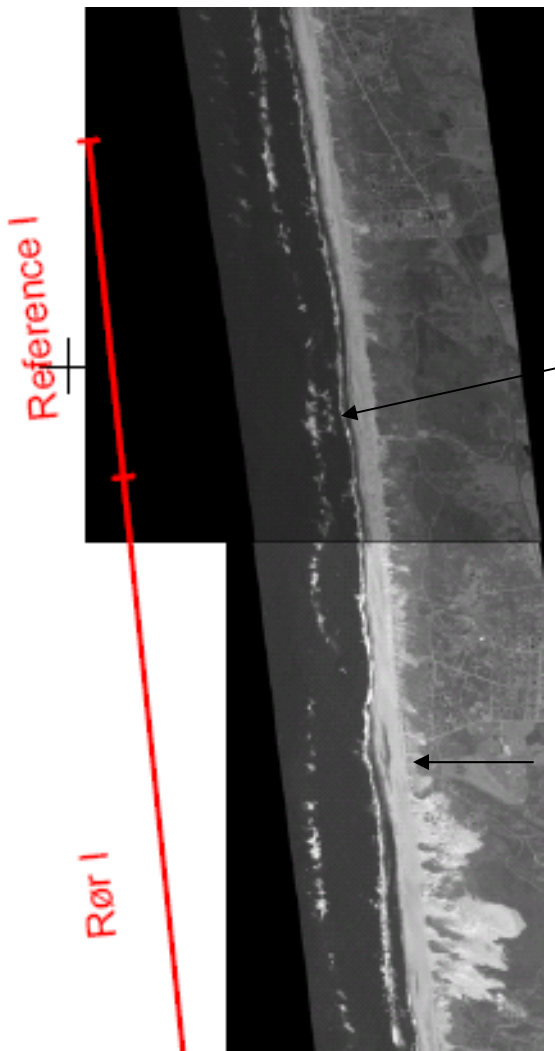


Figure 4: Satellite photo of the Northern part of the test site. The black arrow indicates a pronounced peak in the alongshore undulation.

Reference 1: at least one undulation can be identified in this part of the coast, see figure 4, the upper arrow. The top of this undulation is on its way to move into “Rør-1” during the test period. This will lead to a loss in “ref 1” (see the arrow to the right in figure 8) and a gain in “rør1”. This latter cannot be identified in figure 8.

Rør-1: In addition to the undulation mentioned above, another undulation can be found in this area, see the lower black arrow in figure 4. This undulation does also move, and can be identified at the middle arrow in figure 8. Because it still is contained within the area, only a small flux of sediment is expected to be transferred by the moving undulation from this area to the down drift “reference 2” area.

Reference 2: A very distinct undulation is observed at the border between “reference 2” and “rør-2”, see the white arrow, figures 5 and 8.

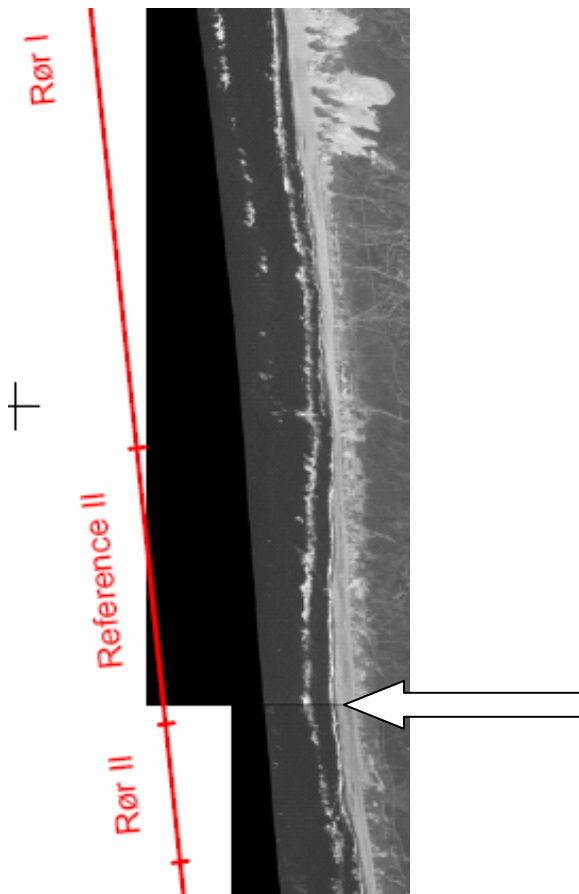


Figure 5: The middle part.

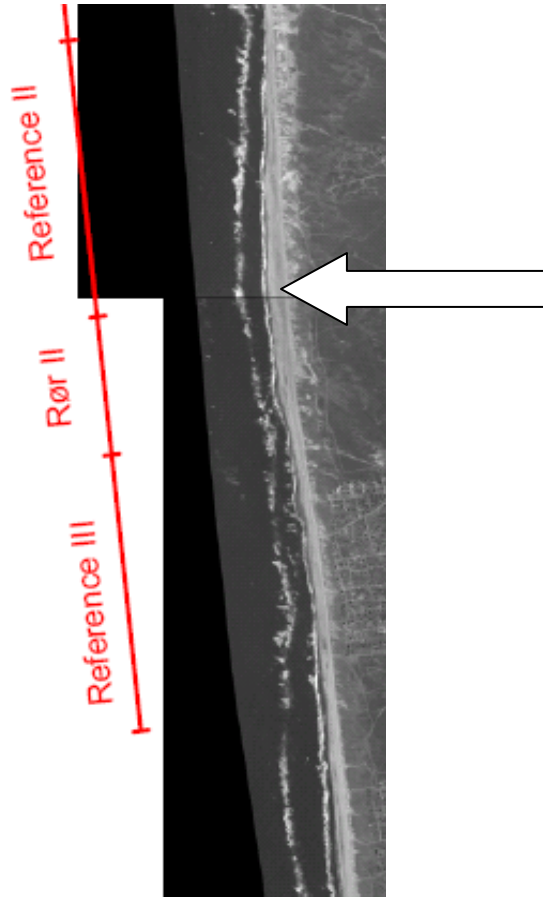


Figure 6: The southern part.

Rør 2 and reference 3: No significant undulations are found here. It seems like the beach widens in the southern direction, indicating the existence of another undulation just south of the test site.

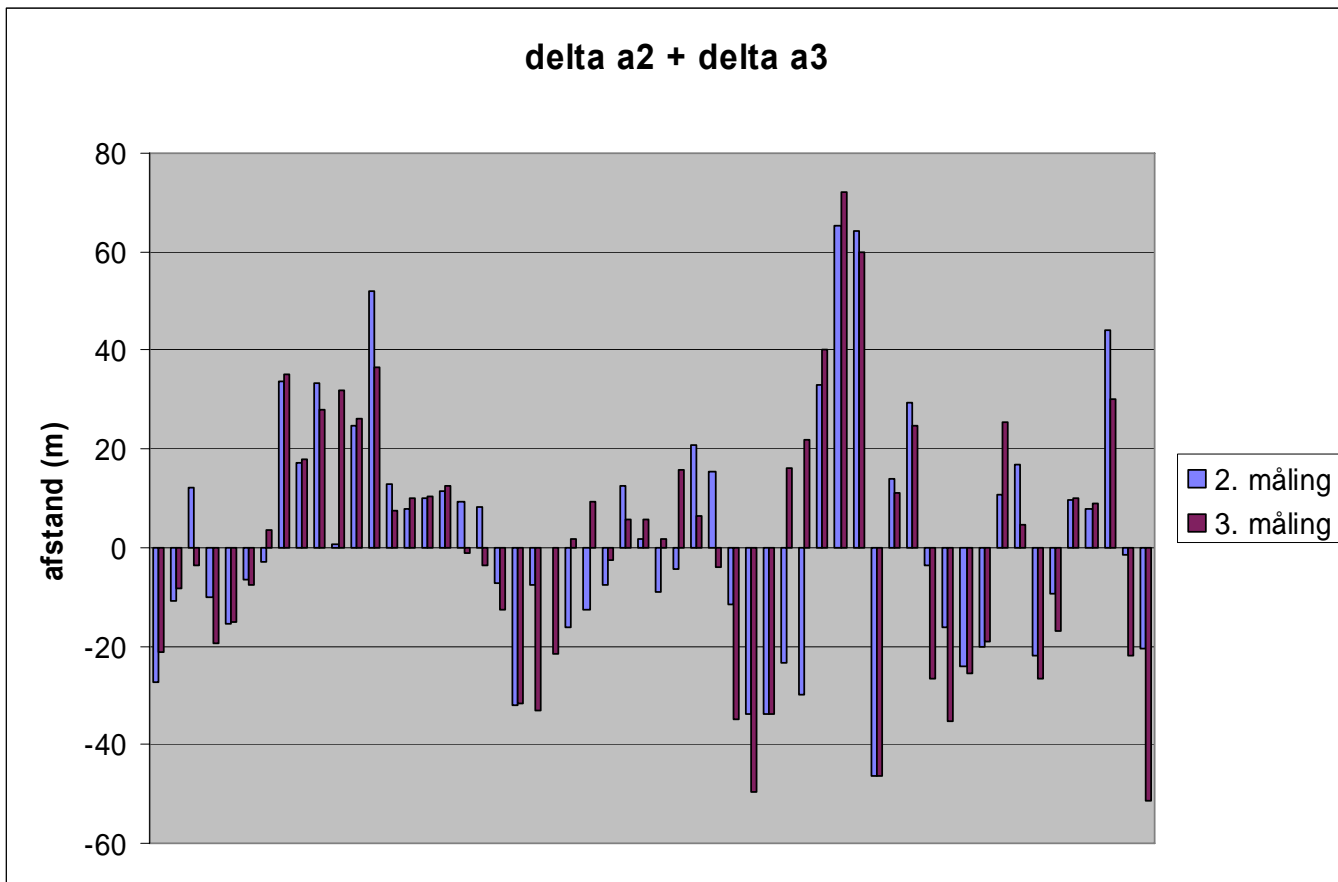


Figure 7 Changes in beach-width from January 2005 to April 2005 (blue) and July 2005 (purple).

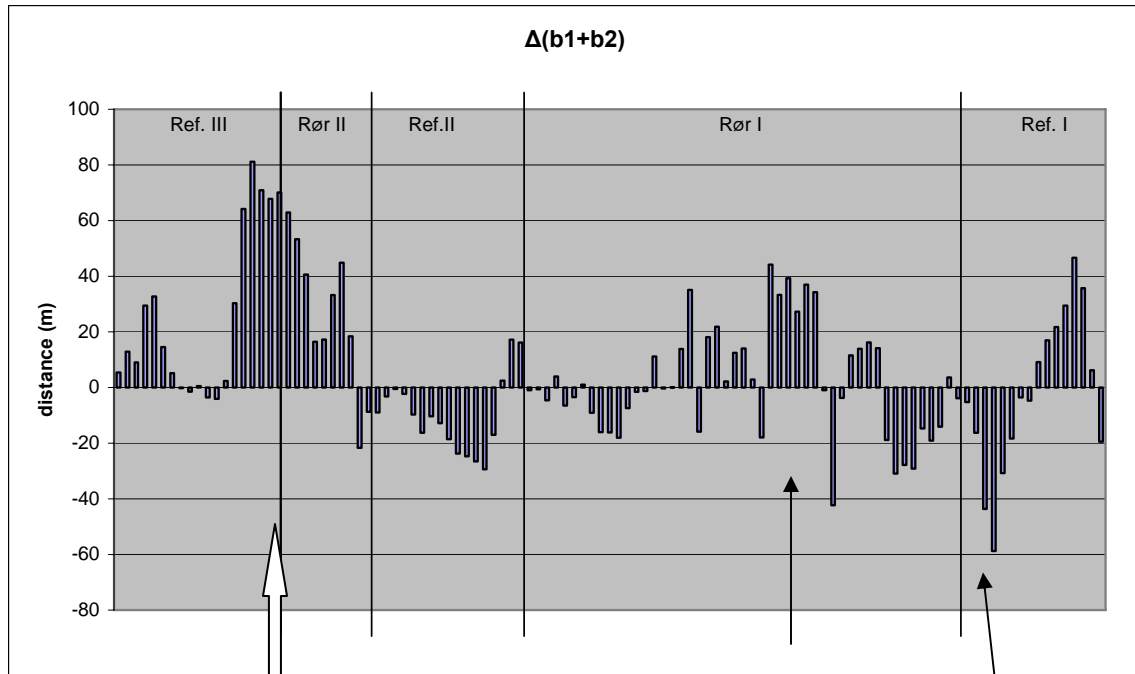


Figure 8. Changes in beach width from January 2005 to January 2006.

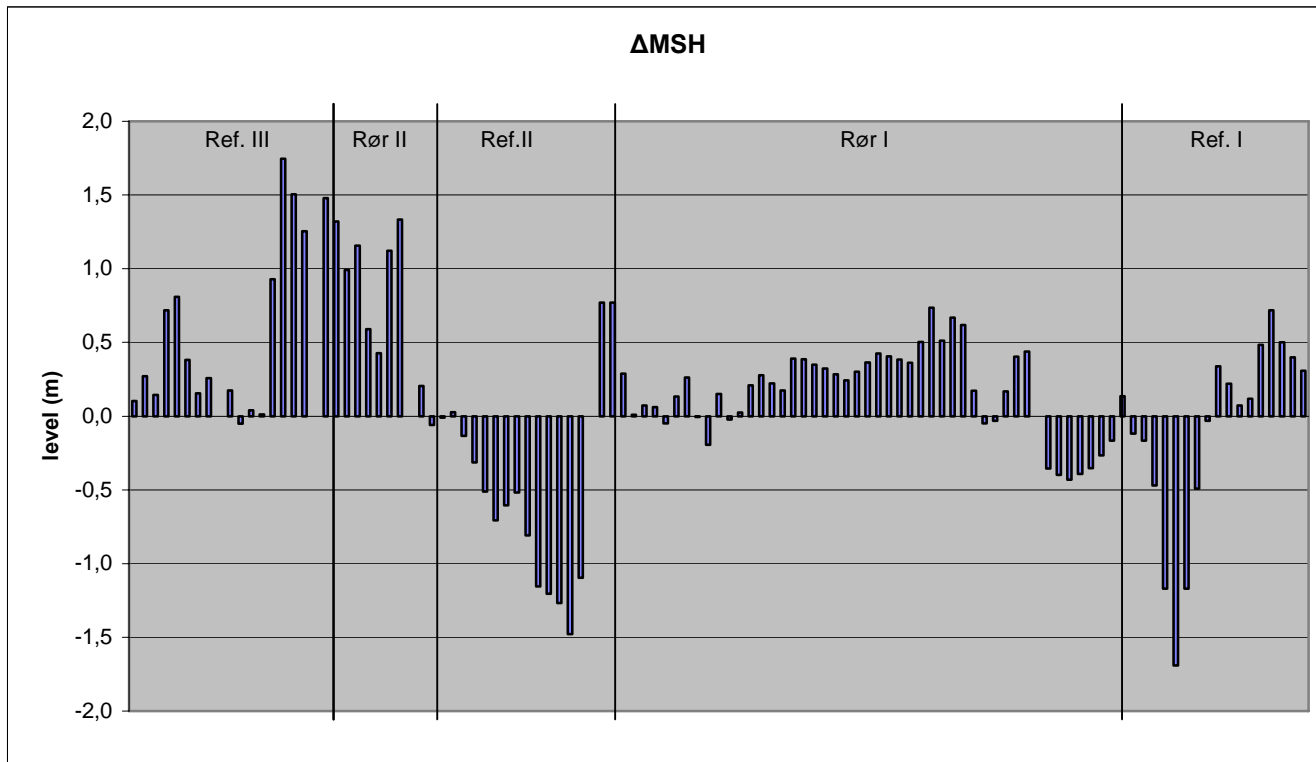


Figure 9: Changes in mean beach level from January 2005 to January 2006. (Volumetric change) The mean level is defined as the average from the dune-foot (level + 4 m) and 100 meter in the seaward direction, independent on whether the actual beach is narrower or wider than 100 meter.